MEDICAL UNIVERSITY OF VIENNA

Novel functions of complement factor H in regulating extracellular vis-à-vis intracellular complement activation during chronic inflammation

Doctoral thesis at the Medical University of Vienna

for obtaining the academic degree

Doctor of Philosophy

Submitted by

Máté Kiss, M.Sc.

Supervisor:

Univ. Prof. Christoph J. Binder, MD, PhD

Department of Laboratory Medicine, Medical University of Vienna

CeMM Research Center for Molecular Medicine

of the Austrian Academy of Sciences

Vienna, 11/2019

Declaration

The following doctoral thesis is presented here in a cumulative format and consists of both published and unpublished results. The work discussed in this thesis was performed by the author in the group of Prof. Dr. Christoph J. Binder at the Department for Laboratory Medicine of the Medical University of Vienna and at CeMM Research Center for Molecular Medicine of the Austrian Academy of Sciences, Vienna. A 6-month internship in the group of Dr. Filip K. Swirski at the Center for Systems Biology, Massachusetts General Hospital and Harvard Medical School, Boston, MA, USA was included in the course of the PhD studies as part of a collaboration leading to a manuscript that is not discussed in this thesis. The author was supported by the PhD scholarship *'Cell Communication in Health and Disease (CCHD)'* granted by the Austrian Science Fund (FWF).

The author of this thesis is first author in both manuscripts presented here. Individual contributions of all other authors are listed in detail in the sections preceding the manuscripts. All additional parts of the thesis were written solely by the author with input and feedback from Prof. Dr. Christoph J. Binder. The manuscripts described in this thesis are:

Manuscript #1, published as:

Complement factor H modulates splenic B cell development and limits autoantibody production

M.G. Kiss, M. Ozsvár-Kozma, F. Porsch, L. Göderle, N. Papac-Miličević, B. Bartolini-Gritti, D. Tsiantoulas, M.C. Pickering, C.J. Binder *Frontiers in Immunology* 2019 Jul 11;10:1607. doi: 10.3389/fimmu.2019.01607.

Manuscript #2, unpublished, presented here as a draft for subsequent submission:

Enhanced cell autonomous complement activation limits atherosclerosis by promoting macrophage efferocytosis

M.G. Kiss, N. Papac-Miličević, D. Tsiantoulas, T. Hendrikx, F. Porsch, M.-S. Narzt, L. Göderle, M. Ozsvár-Kozma, A. Hladik, T. Penz, N. Fortelny, M. Schuster, C. Bock, S. Knapp, F. Gruber, M.C. Pickering, F.K. Swirski, C. Kemper, C.J. Binder

Table of Contents

List of Figures and Tables

Abstract

Atherosclerosis is a lipid-driven chronic inflammatory disease of the arterial wall that gives rise to myocardial infarction and stroke, the leading causes of death and morbidity worldwide. The underlying pathology is characterized by a non-resolving accumulation of apoptotic cells due to defective clearance mechanisms of mainly unknown nature. Given its critical housekeeping function in apoptotic cell removal, the complement system has long been implicated in atherosclerotic lesion formation. Complement consists of a set of inactive soluble precursors that upon stimulation are able to form an amplifying cascade in a self-controlling manner. Although complement activation was thought to be confined to the extracellular space, accumulating evidence suggests that activation of the central complement component C3 occurs also within a wide array of cells and is essential for controlling basic cellular processes, such as cell survival or autophagy. However, if and how intracellular complement activation is regulated remains unexplored.

The findings presented in this thesis derive from the hypothesis, that intracellular complement is actively regulated in immune cells and has a crucial function in modulating inflammatory responses during atherosclerosis. Indeed, we could identify complement factor H (CFH), the master regulator of alternative complement activation as a key player in this context. We found this to be independent of our initial observations that systemic, but not hematopoietic CFH deficiency results in impaired splenic B cell development and autoimmunity. We could demonstrate that CFH displays a unique expression profile among canonical complement repressors that is restricted to monocytes and is upregulated upon inflammatory challenges as well as hypercholesterolemia. Furthermore, CFH has the ability to control the accumulating levels of intracellular C3 in monocyte-derived macrophages during inflammation. In atherosclerosis-prone *Ldlr*$^{-/-}$ mice, hematopoietic deletion of CFH conferred protection against atherosclerosis and necrotic core formation, the primary characteristic of defective efferocytosis. In line with this, transcriptomic analysis of monocyte-derived macrophages revealed that loss of CFH results in a pro-efferocytotic gene expression signature characterized by the upregulation of cell surface receptors involved in a process called LC3-associated phagocytosis, a non-canonical form of autophagy. Accordingly, we found that CFH deficient macrophages exhibit increased autophagic activity as well as heightened efferocytotic capacity both *ex vivo* and within atherosclerotic lesions. Finally, we could demonstrate a dominant role for CFH of monocytic origin in atherosclerosis over the systemic complement-regulatory effects of liver-derived CFH, including its hereby described novel function in calibrating splenic B cell maturation and responsiveness.

Abstract

The work discussed in this thesis offers new insights into the pivotal role of CFH as a repressor of complement activation and moreover, contributes to the dissection of the layers of complement regulation in the extracellular vis-à-vis intracellular space. Our findings highlight the necessity of localized next generation strategies in complement-targeting therapeutics.

Zusammenfassung

Atherosklerose ist eine durch erhöhte Lipide verursachte chronische Entzündungserkrankung der Arterienwand, die in weiterer Folge zu Myokardinfarkt und Schlaganfall, den häufigsten Todesursachen weltweit, führt. Die zugrundeliegende Pathologie charakterisiert sich durch die Akkumulation von apoptotischen Zellen, deren Abtransport aufgrund defekter Clearance-mechanismen verhindert wird. Aufgrund der bedeutenden Funktion bei der Beseitigung von apoptotischen Zellen, ist die Beteiligung des Komplementsystems in die Entstehung von atherosklerotischen Läsionen naheliegend. Das Komplementsystem besteht aus einer Reihe von Proteinen und Proteasen, die nach Stimulierung zur Bildung einer sich selbst kontrollierenden Amplifikationskaskade fähig sind. Obwohl man bisher annahm, dass die Komplementaktivierung nur auf den extrazellulären Raum begrenzt ist, gibt es immer mehr Belege dafür, dass bei einer Reihe von Zelltypen die Aktivierung der zentralen Komplementkomponente C3 auch intrazelluläre erfolgen kann und essentiell für die Kontrolle von grundlegenden zellulären Prozessen, wie Zelltod und Autophagie, ist. Ob und wie die intrazelluläre Komplementaktivierung reguliert wird war bisher unbekannt.

Die Ergebnisse, die in dieser Doktorarbeit präsentiert werden, basieren auf der Hypothese, dass intrazelluläres Komplement in Immunzellen aktiv reguliert wird und eine entscheidende Funktion in der Modulierung der Entzündungsantwort während der Atherosklerose ausübt. Tatsächlich konnte hierbei Komplementfaktor H (CFH), der Hauptregulator der alternativen Komplementaktivierung, als Schlüsselkomponente identifiziert werden. Wir konnten zeigen, dass dies unabhängig von unserer ursprünglichen Erkenntnis, dass systemische, jedoch nicht hämatopoetische CFH Defizienz in einer gestörten Entwicklung von B-Zellen in der Milz und Autoimmunität resultiert. Weiters deuten unsere Ergebnisse darauf hin, dass CFH ein einzigartiges Expressionsprofil unter den kanonischen Komplementrepressoren aufweist, welches auf Monozyten begrenzt ist und durch Entzündungsreize, als auch Hypercholesterinämie hochreguliert wird. Zudem besitzt CFH die Eigenschaft, intrazelluläres C3 in Makrophagen während einer Entzündungsreaktion zu kontrollieren. In atheroskleroseanfälligen *Ldlr*$^{-/-}$ Mäusen verhindert die hämatopoetische Deletion von CFH Atherosklerose und die Bildung von Plaquenekrosen, dem primären Merkmal von fehlerhafter Efferozytose. Damit einhergehend konnten wir durch Transkriptom Analyse von Makrophagen zeigen, dass die Defizienz von CFH die Expression von Efferozytose-begünstigender Gene induziert, wie zum Beispiel Zelloberflächenrezeptoren, die an der LC3-assoziierten Phagozytose, einer nicht-kanonischen Form der Autophagie, involviert sind.

Dementsprechend konnten wir auch zeigen, dass CFH-defiziente Makrophagen erhöhte Autophagie-Aktivität ausüben und eine gesteigerte Efferozytosekapazität *ex vivo* sowie in atherosklerotischen Läsionen besitzen. Zusammenfassend konnten wir daher einerseits neue systemische Effekte von hepatischem CFH in der B-Zellentwicklung und –antwort und andererseits die dominante Rolle von monozytärem CFH in der Atherosklerose beschreiben.

Die in dieser Arbeit diskutierten Studien bieten neue Einblicke in die zentrale Rolle von CFH als Repressor der Komplementaktivierung und tragen überdies zur Aufklärung der Komplementregulierung im extrazellulären und intrazellulären Raum bei. Unsere Erkenntnisse unterstreichen die Notwendigkeit von neuartigen Therapiestrategien die das Komplementsystem lokal anvisieren.

Abbreviations

ABCA1	ATP-Binding Cassette A1
ABCG1	ATP-Binding Cassette G1
ACAT	acetyl-CoA acetyltransferase
ADAM17	ADAM metallopeptidase domain 17
aHUS	atypical hemolytic uremic syndrome
AMD	age-related macular degeneration
AP-1	activator protein 1
APOA1	apolipoprotein A1
ApoB-LP	apolipoprotein B100-containing lipoprotein
APOE	apolipoprotein E
ASC	apoptosis-associated speck-like protein containing a CARD
ATP	adenosine triphosphate
Blimp-1	B lymphocyte-induced maturation protein-1
BMT	bone marrow transplantation
C1INH	C1 inhibitory protein
C1q	complement component 1q
C2	complement component 2
C3	complement component 3
C4	complement component 4
$C3a_{desArg}$	C3a desarginine
C3aR	C3a receptor
C4BP	C4 binding protein
$C5a_{desArg}$	C5a desarginine
C5aR1	C5a receptor 1
C5aR2	C5a receptor 2
C6-9	complement component 6-9

CAD	coronary artery disease
CANTOS	Canakinumab Anti-Inflammatory Thrombosis Outcomes Study
CCP	complement component proteins
CD	cluster of differentiation
CFH	complement factor H
CFHR	complement factor H-related protein
CR	complement receptor
CRP	C-reactive protein
CTSL	cathepsin L
CVD	cardiovascular disease
CX3CL1	chemokine (C-X3-C motif) ligand 1
DAF	decay-accelerating factor
DAMP	damage- or danger-associated molecular pattern
DANN	deoxyribonucleic acid
DRP1	dynamin-1-like protein
ER	endoplasmic reticulum
FHL-1	Factor H-like protein-1
FO B	follicular B cell
FOXP3	forkhead box P3
GAS6	growth arrest-specific 6
GM-CSF	granulocyte-macrophage colony-stimulating factor
HDL	high-density lipoprotein
HMGB1	high mobility group box 1
iC3b	inactivated C3b
IFN-γ	interferon-gamma
IgG	immunoglobulin G
IgM	immunoglobulin M
IL-10	interleukin-10
IL-18	interleukin-18

IL-1β	interleukin-1-beta
IL-3	interleukin-3
IRA B	innate response activator B cell
LAP	LC3-associated phagocytosis
LDL	low-density lipoprotein
LDLR	low-density lipoprotein receptor
LRP1	low-density lipoprotein receptor-related protein 1
LXRα	liver X receptor alpha
LXRβ	liver X receptor beta
Ly6C	leukocyte antigen-6C
MAC	membrane attack complex
MARCO	macrophage receptor with collagenous structure
MASP	mannose-binding lectin serine protease
MAVS	mitochondrial antiviral signaling
MBL	mannose-binding lectin
MCP	membrane cofactor protein
M-CSF	macrophage colony-stimulating factor
MDA	malondialdehyde
MerTK	proto-oncogene tyrosine-protein kinase MER
MFG-E8	milk fat globule-EGF factor 8 protein
MHCII	major histocompatibility complex II
MPGN	membranoproliferative glomerulonephritis
mRNA	messenger ribonucleic acid
MSR	macrophage scavenger receptor 1
mTOR	mammalian target of rapamycin
MZB	marginal zone B cell
NET	neutrophil extracellular trap
NF-κB	nuclear factor-kappa B
NK	natural killer cell

NLRP3	NACHT, LRR and PYD domains-containing protein 3
OSE	oxidation-specific epitope
oxLDL	oxidized LDL
PLA_2	phospholipase A2
PNH	paroxysmal nocturnal hemoglobinuria
PRR	pattern recognition receptor
PtdSer	phosphatidylserine
PTX3	pentraxin 3
PUFA	polyunsaturated fatty acid
RCA	regulators of complement activation
ROS	reactive oxygen species
SCR	short consensus repeat
SIGNR1	specific ICAM-3 grabbing nonintegrin-related 1
SPM	specialized pro-resolving mediators
SR-A1	scavenger receptor A1
SR-A2	scavenger receptor A2
SR-B1	scavenger receptor B1
T-Bet	T-box transcription factor TBX21
TCR	T cell receptor
TG2	transglutaminase 2
TGFβ	transforming growth factor beta
TIM4	T-cell immunoglobulin and mucin domain containing 4
TLR	Toll-like receptor
Treg	regulatory T cell
UTP	uridine triphosphate
VLDL	very low-density lipoprotein
VSIG4	V-set immunoglobulin domain containing 4
XBP1	X box binding protein 1

Acknowledgements

The completion of this thesis would have not been feasible without the kind contribution and constant support of many people whom I would like to acknowledge.

First and foremost, I would like to express my gratitude to my supervisor *Christoph* for putting his trust in me and for being an exceptional '*Doktorvater'* in mentoring me in a both scientific as well as personal way. I highly appreciate his enthusiasm for science and his sincere and caring guidance in breaking fresh grounds together; I hope we keep discussing science (and beyond) for many years to come.

I am truly honored for being part of such an inspiring community here, in Vienna. Therefore, I would like to thank *all past and current members of the Binder group* for their kindness, support and scientific professionality and for creating an atmosphere that made me thrive more than I had ever imagined. I am particularly grateful to *Mária, Nikolina, Laura, Vesna* and *Tim* who have always been with me along these six years and to *Florentina* for being the ideal partner in crime during long experiments and conferences. Special thanks go to *Vesna* for her contribution to this thesis with beautiful figures as well as with the German translation of the abstract. Moreover, I also wish to acknowledge *every single member of CeMM* for making this institute a truly unique research environment.

I would like to acknowledge all my co-authors for their important contribution in publishing the work discussed in this thesis. In particular, I would like to thank *Fil* for giving me the chance to spend half a year in his lab, which was a truly educative and inspiring experience. I am also grateful to all the *Swirski lab members*, especially *Cameron* and *John* for their welcoming and friendly attitude.

I would also take the opportunity to thank everyone who was involved in my former education in Pécs for paving my way to such top-notch scientific institutions.

I consider myself extremely fortunate that I started my career at CeMM together with a remarkable group of people who became true friends of mine during the past years. Therefore, profound gratitude goes to the 2013 PhD generation including *Adrián, Thea, Michel, Anikó, Juliane, Paul, Bianca* and *Anna*, but also to *Cecilia, Ferran, Yi-Jang*, *Camilla* and *all my friends in CCHD* for all the unforgettable experiences, journeys and fun we have had together.

Last but definitely not least, I would like to thank all my friends, especially *Ricsi, Tomi* and *Dávid*, *my beloved family* and my partner *Anne* for all the love, joy, empathy and encouragement that they bring to my life on a daily basis.

1 Introduction

The introduction of this thesis offers a detailed overview of the main topics discussed in the two manuscripts presented in the *Results* section and is divided into four distinct parts summarizing:

I) the current scientific consensus on the underlying pathology of atherosclerosis with special emphasis on the role of macrophages in plaque formation.

II) the homeostatic functions of the complement system and in particular, its plethora of regulatory proteins and receptor molecules. This chapter also introduces the recently discovered field of intracellular complement activation.

III) the present knowledge on the involvement of complement activation in atherosclerosis development discussing all the to-date available complement-related literature in experimental atherosclerosis.

IV) the mechanisms by which complement factor H (CFH) exerts its complement-regulatory effects.

1.1 Atherosclerosis

The complications arising from atherosclerosis including myocardial infarction and stroke are the major causes of death and morbidity worldwide (**Figure 1**). The underlying pathology involves a decades-long chronic inflammatory process of the arterial wall, primarily occurring at branch points and bifurcations with disturbed laminal flow and low shear stress. Atherosclerosis is initiated by the subendothelial accumulation of lipids and infiltrating cells, which results in plaque formation and the subsequent expansion of the arterial intima leading to the progressive narrowing of the arterial lumen. As early as the age of 40, 95% of the population develops well distinguishable atherosclerotic lesions (Swirski and Nahrendorf, 2013). Although most of these lesions are well preserved by fibrous thickening, problem occurs when vulnerable plaques undergo necrotic breakdown culminating in plaque rupture, which results in occlusive luminal thrombosis (Virmani et al., 2002). As a direct consequence, the oxygenation of heart and brain becomes perturbed leading to the manifestation of acute conditions such as coronary artery disease including myocardial infarction, unstable angina and sudden cardiac death as well as cerebrovascular diseases, such as stroke.

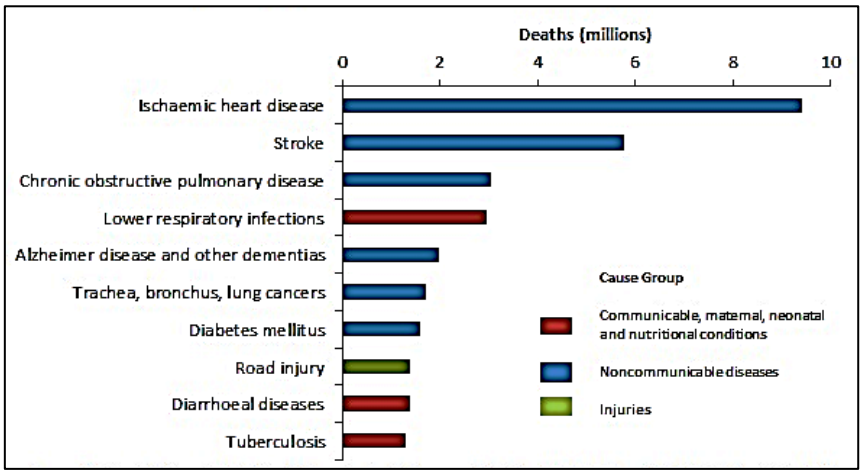

Figure 1 – Top 10 global causes of death in 2016 – The complications of atherosclerosis, such as ischaemic heart disease and stroke are the leading causes of death worldwide. *Source: Global Health Estimates 2016 Geneva, World Health Organization; 2018 (www.who.int)*

1.1.1 Early plaque formation: a lipid-driven disease

The key initiating step of atherosclerosis is the retention of apolipoprotein B100-containing lipoproteins (ApoB-LPs) in the subendothelial space of the arterial wall. ApoB-LPs are

derived mainly from the liver and their role is to transfer lipids all around the body. Secreted as very low density lipoproteins (VLDL), they are further converted into low density lipoproteins (LDL) in the bloodstream. Increased levels of plasma cholesterol transported by apoB-containing LDL are a major risk factor of atherosclerosis and promote cardiovascular events (Moore and Tabas, 2011). When ApoB-LDL enter the intima, the binding of negatively charged proteoglycans by ApoB100 leads to the entrapment of LDL under the endothelial layer, where they are susceptible to undergo oxidative modifications due to increased oxidative stress e.g. by reactive oxygen species (such as superoxide or hydrogen peroxide) or enzymatically via myeloperoxidase (Weber and Noels, 2011). Oxidation-specific epitopes (OSE) appearing on the surface of lipoproteins are immunogenic danger-associated molecular patterns (DAMP) that are able to activate neighboring endothelial cells (Chou et al., 2008; Miller et al., 2011). Subsequently, they secrete chemokines and express adhesion molecule thereby inciting the recruitment and infiltration of blood-derived monocytes that is the key early inflammatory event in atherosclerotic lesion development.

1.1.2 Monocyte-derived macrophages as protagonists in lesion progression

Hypercholesterolemia triggers heightened medullary hematopoiesis, which is characterized by the rapid proliferation of progenitor cells of myeloid fate in the bone marrow (Moore et al., 2013; Nahrendorf and Swirski, 2015). This leads to an increased numbers of monocytes in the blood i.e. monocytosis and the excessive passage of circulating monocytes across the endothelial layer of the arterial wall (**Figure 2**). There has been a lot of emphasis on investigating the role of different monocyte subsets in atherosclerosis. Both in humans and mice, two main types of circulating monocytes exist that can be distinguished by the expression profile of certain cell-specific surface markers. While Ly6C^{lo} monocytes (similar to CD16^{+}CD14^{dim} monocytes in humans) possess a patrolling function and enter the lesions less readily, inflammatory Ly6C^{hi} monocytes, which share numerous properties with human CD16^{-}CD14^{+} monocytes accumulate preferentially in the lesions and differentiate into macrophages when exposed to certain differentiation and growth factors, such as macrophage colony stimulating factor (M-CSF) (Hilgendorf and Swirski, 2012). Macrophages are the hallmark cells of atherosclerosis and they are involved in a myriad of functions, including lipid uptake and the clearance of dying cells i.e. efferocytosis. Hypothetically, macrophages can prevent atherosclerosis by scavenging and clearing excess oxLDL from the lesions without mounting inflammation. However, due to the chronic nature of the disease, macrophages become overloaded by cholesterol and they eventually die, which initiates a vicious circle of further monocyte infiltration and cell death. The accumulation of oxLDL and dying cells contributes to the formation of a lipid-filled necrotic core, which reduces plaque stability and makes the plaque vulnerable to rupture (Weber and Noels,

2011). Therefore, the efficient clearance of excessive lipids and dying cells by phagocytic macrophages is essential for the protection against atherosclerosis and provides a promising target for clinical interventions.

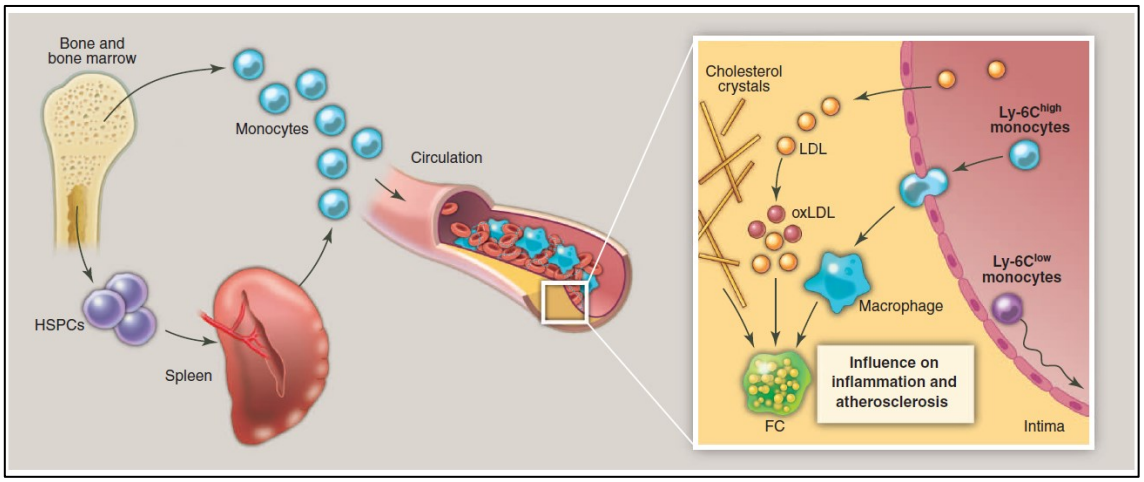

Figure 2 – Initiating stages of atherosclerosis development – The retention of oxLDL in the arterial intima triggers heightened hematopoiesis in the bone marrow, but also in the spleen, which results in monocytosis. While Ly6C^{lo} monocytes patrol the vasculature, Ly6C^{hi} monocytes infiltrate the lesion and differentiate into macrophages, which become lipid-laden foam cells upon the ingestion of lipids and cholesterol crystals. *Adapted from (Swirski and Nahrendorf, 2013).*

Lipid uptake and foam cell formation

The excessive uptake of apoB-LDL by macrophages is considered the primary pathogenic event in nascent plaques. As a consequence, the cytoplasm of these macrophages becomes enriched in membrane-bound lipid droplets giving them a 'foamy' appearance; therefore referred as foam cells **(Figure 3)**. Although other mechanisms are also operational, the uptake of modified lipids by foam cells is mediated predominantly via scavenger receptors that are a type of pattern recognition receptors (PRR) on the surface of macrophages and bind OSEs (Binder et al., 2016). Scavenger receptors are divided into two major classes: while *Class A* includes scavenger receptor A1 (SR-A1 or MSR), macrophage receptor with collagenous structure (MARCO or SR-A2) and many others; CD36 and scavenger receptor B1 (SR-B1) belongs to the *Class B* family (Yan and Hansson, 2007). Upon internalization, the cholesteryl esters of oxLDL are hydrolyzed to free cholesterol in endolysosomal compartments. The free cholesterol then undergoes re-esterification in the endoplasmic reticulum (ER) by the enzyme acetyl-CoA acetyltransferase (ACAT). These cholesteryl fatty acid esters provide the 'foam' of foamy macrophages (Brown et al., 1980). Excess

cholesterol is disposed by macrophages via reverse cholesterol transport, which requires ABCA1- and ABCG1-mediated trafficking of cholesterol to lipid-poor apolipoprotein A1 (APOA1) and high density lipoprotein (HDL), the major extracellular acceptors (Rothblat and Phillips, 2010; Tall et al., 2008; Yvan-Charvet et al., 2010b). The cholesterol efflux machinery via ABCA1 and ABCG1 is transcriptionally induced by the sterol sensing transcription factors liver X receptor alpha (LXRα) and beta (LXRβ) (Zelcer and Tontonoz, 2006) and is considered to be the dominant mechanism involved in lesion regression upon normalizing systemic cholesterol levels. In line with this, combined ABCA1 and ABCG1 deficiency exacerbate experimental atherosclerosis (Yvan-Charvet et al., 2007) and HDL cholesterol levels inversely correlate with CAD risk (Libby et al., 2011). Therefore, several clinical trials have attempted to increase systemic HDL levels to promote macrophage cholesterol efflux; however, to date no drug has been proven to significantly affect cardiovascular health.

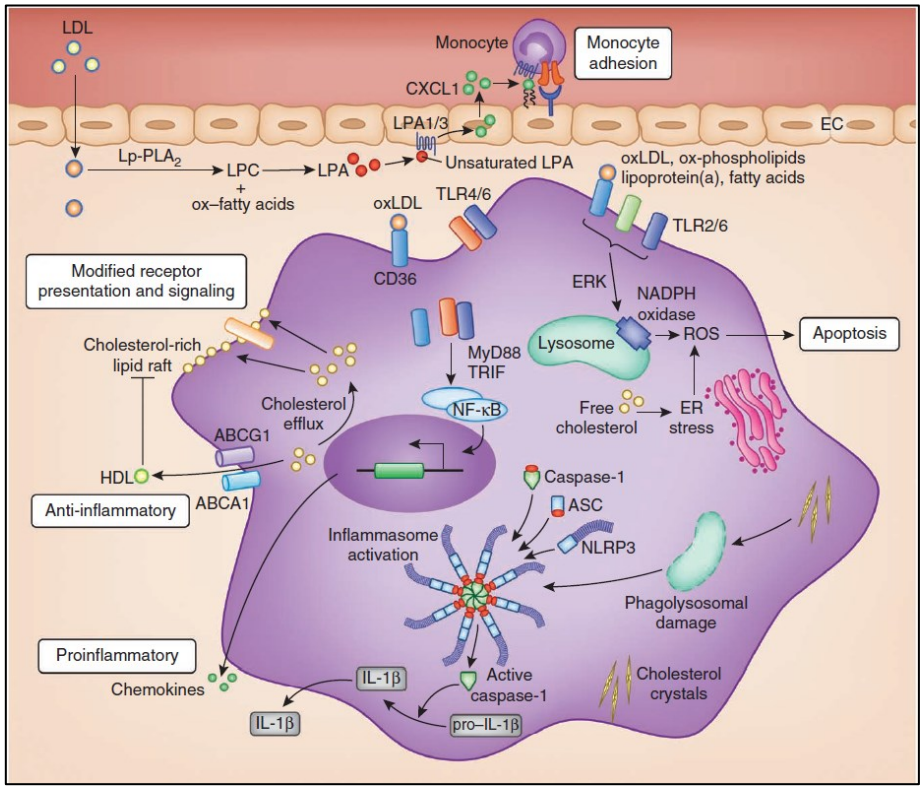

Figure 3 – The effect of lipid sensing on lesional macrophages – Numerous pro-inflammatory and anti-inflammatory signaling pathways become activated in macrophages of atherosclerotic plaques upon engulfing lipids. These include cooperative pathways between scavenger receptors and toll-like receptors (TLRs), the inflammasome, endoplasmic reticulum (ER) stress and reverse cholesterol transport through ABCA1 and ABCG1. *Adapted from (Weber and Noels, 2011).*

The effects of excessive cholesterol loading

Cholesterol is rather inert when it is present in the form of cholesteryl ester within cells. However, elevated amount of free cholesterol e.g. due to disturbances in ACAT function can lead to the dysregulation of lipid metabolism by perturbing the efflux machinery, resulting in sustained oxidative burst and increased ER stress (Moore et al., 2013). Furthermore, it can promote lipid raft formation, which on the one hand, induces inflammatory signals due to enhanced toll-like receptor (TLR) and nuclear factor-kappa B (NF-κB) activation (Yvan-Charvet et al., 2008; Zhu et al., 2010) and on the other hand, triggers myeloproliferation via increased interleukin-3 (IL-3) and granulocyte-macrophage colony-stimulating factor (GM-CSF) signaling (Yvan-Charvet et al., 2010a). Importantly, the accumulation of free cholesterol can also lead to cholesterol crystal build up within macrophages, which promotes lysosome destabilization and inflammasome activation, a complex that involves multiple proteins, such as NACHT, LRR and PYD domains-containing protein 3 (NLRP3), ASC and caspase-1 (Duewell et al., 2010). The assembly of the inflammasome complex induces the proteolytic cleavage and secretion of pro-inflammatory cytokines interleukin-1 beta (IL-1β) and interleukin-18 (IL-18). Ultimately, the combination of all these insults can render macrophages to succumb to types of programmed cell death, mainly apoptosis.

The implication of inflammasome activation in atherosclerosis has been widely studied in the past decade. Hematopoietic deletion of NLRP3, ASC or IL-1β has been shown to reduce IL-18 levels and lesion size in experimental atherosclerosis (Duewell et al., 2010). Moreover, the potential efficacy of IL-1β targeting in reducing cardiovascular disease risk was recently evaluated in a randomized, double-blind and event-driven phase III study, called the Canakinumab Anti-Inflammatory Thrombosis Outcomes Study (CANTOS). Subcutaneous administration of canakinumab, a selective, high-affinity human monoclonal antibody against IL-1β could significantly reduce cardiovascular events in patients with previous myocardial infarction providing evidence for the first time that targeting inflammation independently of lipid levels holds promise for lowering the risk of atherosclerotic vascular diseases (Ridker et al., 2017).

Macrophage death and lesion progression

Apoptotic macrophage death due to lipid misbalance requires constant monocyte infiltration to the plaques that contributes to a non-resolving inflammatory condition and leads to qualitative changes in lesion morphology, advancing plaque progression (**Figure 4**). The main characteristic of advanced atherosclerosis is the formation of a necrotic core as a consequence of secondary necrosis. Necrosis promotes inflammation, thrombosis and the proteolytic breakdown of plaques as well as weakens the fibrous cap, a protective scar

covering the inflamed lesion (Glass and Witztum, 2001). Importantly, plaque necrosis does not occur upon macrophage apoptosis itself, but rather results from the defective clearance of dying macrophages by newly recruited phagocytes i.e. efferocytosis (Tabas, 2010). Efficient efferocytosis critically controls normal plaque homeostasis by multiple processes. It mediates the removal of dying cells before membrane leakage of cytokines, proteases and prothrombotic factors, and tempers inflammation by triggering an anti-inflammatory response in the engulfing cells via the secretion of interleukin-10 (IL-10), transforming growth factor beta (TGF-β) and pro-resolving lipid mediators. Moreover, it also promotes the survival of the

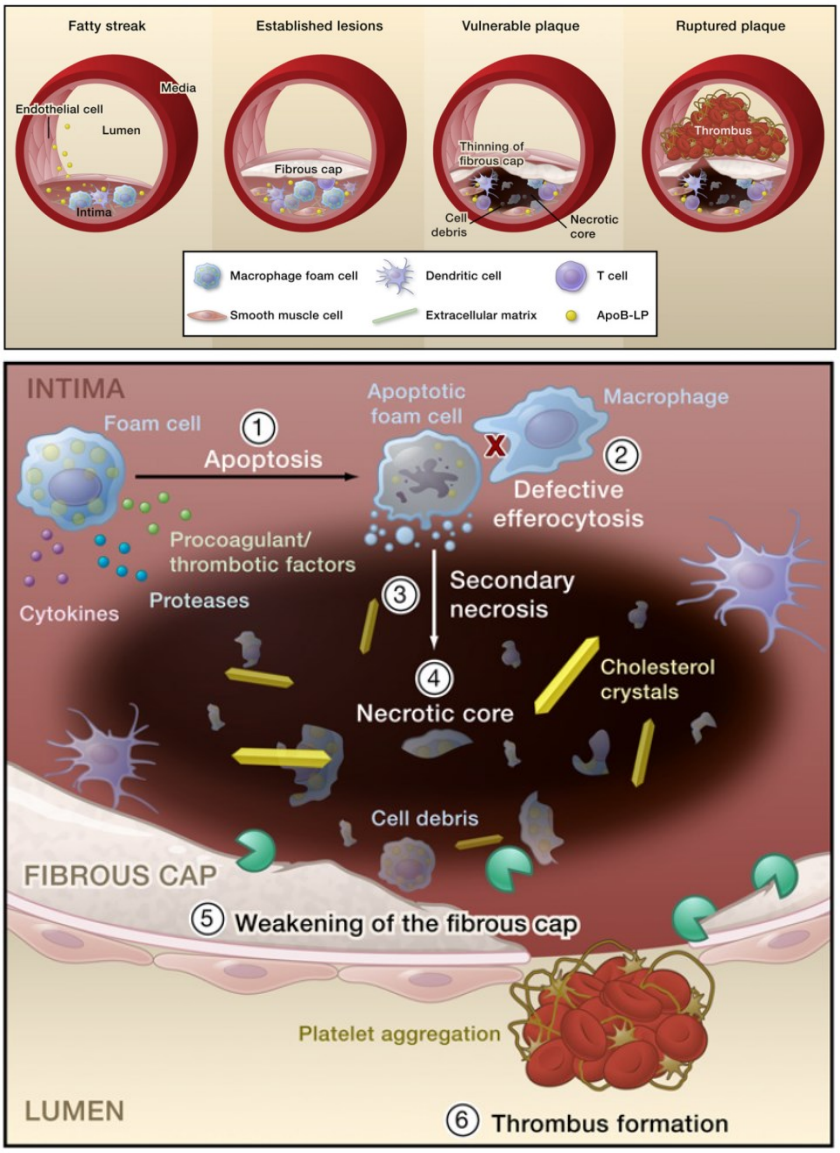

Figure 4 – Progression of atherosclerosis – The main steps involved in plaque progression and rupture are shown (1-6). *Adapted from (Moore and Tabas, 2011).*

efferocytes from the cytotoxic content of engulfed cells (Moore and Tabas, 2011). However, as the plaques progress, cellular reprogramming takes place in macrophages and the efferocytotic machinery becomes defective leading to the accumulation of uncleared dying cells that undergo post-apoptotic necrosis (Tabas and Lichtman, 2017). Defective efferocytosis is the major driver of the formation of the necrotic core that is always in close proximity to the sites of acute vascular events, so called culprit lesions (Tabas, 2011). Therefore, therapeutic strategies to enhance macrophage efferocytosis would play a leading role in preventing the progression of clinically relevant plaques.

Mechanisms of effective efferocytosis

When lesional macrophages succumb to apoptotic cell death, they secrete so called 'find-me' signals that navigate efferocytes to apoptosis-rich areas. These signals include CX3CL1, sphingosine-1-phosphate and nucleotides, such as ATP and UTP (Van Vre et al., 2012). Upon arrival, the engulfing macrophages employ an array of receptors that are able to recognize – either directly or through bridging molecules - 'eat-me' signals, such as phosphatidylserine (PtdSer), which decorate the surface of apoptotic cells (Li, 2012). Several of these interactions have been described with relevance to atherosclerosis development (**Table 1**). The binding of externalized 'eat me' signals together with coupling with additional receptors triggers dynamic cytoskeletal reorganization around the dying cell and mediates tethering and internalization (Yurdagul et al., 2017). Notably, viable cells that may express PtdSer on their surface are protected from this process due to the presentation of 'don't eat me' molecules including CD31 and CD47 that actively hinder efferocytosis (Brown et al., 2002; Tsai and Discher, 2008). The assembly of a phagocytic cup by enhanced F-actin formation and polymerization around the apoptotic cell triggers phagosome retraction into the cells (Castellano et al., 2000).

During efferocytosis, engulfing cells internalize around 50% of their entire surface, yet the plasma membrane surface area is not affected upon full internalization (Yurdagul et al., 2017). Therefore, it seems evident that vesicular trafficking events have a crucial role in contributing to efficient efferocytosis. As an example, Drp1-dependent mitochondrial fission promotes the release of ER calcium into the cytosol thus mediating the fast recruitment of vesicles to the site of apoptotic cell docking in order to orchestrate phagosome sealing (Wang et al., 2017). Furthermore, autophagy-related proteins are also mobilized upon engulfment to conjugate lipids to LC3-bound phagosomal membranes, a process referred as LC3-associated phagocytosis (LAP) (Martinez et al., 2015). LAP is triggered by the engagement of PtdSer receptor TIM4 and it promotes phagolysosomal fusion and the degradation of apoptotic material (Martinez et al., 2011). Accordingly, LAP-deficient mice that

bear uncompromised canonical autophagy still accumulate apoptotic bodies and develop autoimmunity upon aging (Martinez et al., 2016). Therefore, LAP is obligatory for immune-silent efferocytosis. Following efficient LAP, the surplus macromolecular components derived from the engulfed cell including amino acids, sugars, lipids and nucleotides can be recycled as energy supplies or be utilized for efflux, such as excess cholesterol.

Molecule	Action	Ligand	Reported effect in atherosclerosis	References
MerTK	Receptor	PtdSer	promotes efferocytosis, blocks necrotic core formation	(Ait-Oufella et al., 2008; Cai et al., 2017; Thorp et al., 2008)
Tim-1/Tim-4	Receptor	PtdSer	promotes efferocytosis	(Foks et al., 2016)
Axl	Receptor	PtdSer	no effect	(Subramanian et al., 2016)
LRP1	Receptor	calreticulin	promotes efferocytosis, blocks necrotic core formation	(Overton et al., 2007; Yancey et al., 2010; Yancey et al., 2011)
SR-B1	Receptor	oxPL	promotes efferocytosis, blocks necrotic core formation	(Tao et al., 2015)
CD36	Receptor	oxPL	conflicting, but mainly pro-atherogenic	(Park, 2014)
Gas6	Bridging molecule	PtdSer	reduces plaque stability	(Lutgens et al., 2008)
C1q	Bridging molecule	calreticulin	promotes efferocytosis	(Bhatia et al., 2007; Lewis et al., 2009; Pulanco et al., 2017)
MFG-E8	Bridging molecule	oxPL	blocks necrotic core formation	(Ait-Oufella et al., 2007)
TG2	Bridging molecule	several	Promotes efferocytosis	(Boisvert et al., 2006)
Calreticulin	Eat-me signal	-	promotes efferocytosis, blocks necrotic core formation	(Kojima et al., 2014)
CX3CL1	Find-me signal	-	reduces plaque complexity, less lesional macrophages	(Teupser et al., 2004)
Fas/Fas ligand	Find-me signaling	-	blocks efferocytosis	(Aprahamian et al., 2004; Feng et al., 2007)
CD47	Don't-eat me signal	-	blocks efferocytosis, promotes necrotic core formation	(Kojima et al., 2016)

Table 1 – Efferocytosis-related molecules studied in experimental atherosclerosis – *Adapted and modified from (Yurdagul et al., 2017).*

Efferocytosis and the resolution of inflammation

Besides the clearance of apoptotic cells and the prevention of secondary necrosis, efferocytosis plays a crucial role in the resolution of inflammation by inducing the production of several endogenous molecules that mitigate inflammation. These include the phospholipid-binding protein Annexin A1 that suppresses phospholipase A2 (PLA_2) activity; anti-inflammatory cytokines, such as IL-10 and TGF-β that downregulate the secretion of pro-

inflammatory cytokines; gasses, such as hydrogen sulfide that suppresses NF-κB activation and promotes tissue repair (Back et al., 2019); as well as specialized pro-resolving mediators (SPM) that are bioactive polyunsaturated fatty acid (PUFA) metabolites secreted in great amounts upon the uptake of dead cells (Serhan, 2014). Resolvins, maresins, lipoxins and protectins all belong to SPM family and can limit monocyte infiltration, inhibit the release of pro-inflammatory mediators and promote macrophage egress. Numerous atherosclerosis studies have documented reduced plaque necrosis upon treating mice with various pro-resolving molecules including IL-10, maresin, resolvin D1, resolvin D2 and annexin A1 (Kasikara et al., 2018; Yurdagul et al., 2017). Thus, enhancing efferocytosis in combination with restoring resolution mediators might be a promising approach to combat cardiovascular diseases.

Defective efferocytosis in atherosclerosis

The mechanisms of impaired efferocytosis in advanced atherosclerosis remains largely unknown. As efferocytosis is a high-capacity process, overwhelming apoptotic death of lesional macrophages is unlikely to act as the primary force (Henson et al., 2001). In line with this, when apoptosis is genetically increased in efferocytosis-competent early plaques, dying cells are removed efficiently (Tabas, 2010). Therefore, it is more plausible that either efferocytosis itself becomes defective or the quality of lesional apoptotic cells worsens for efficient uptake (**Figure 5**). The latter view is supported by findings that in advanced plaques, apoptotic cells display reduced levels of surface calreticulin (Kojima et al., 2014) as well as increased CD47 expression (Kojima et al., 2016), both rendering them poorly recognizable by lesional efferocytes. In addition, PtdSer can be either hydrolyzed or masked on apoptotic surfaces by PLA_2 (Wilensky and Macphee, 2009) or the pro-inflammatory molecule high-mobility group box 1 (HMGB1) (Weber and Noels, 2011), respectively. The accumulating amount of lipids and reactive oxygen species may also compete for apoptotic cell binding over disease progression.

Growing evidence suggests that the pro-inflammatory environment impacts the expression and function of key efferocytosis molecules in advanced atherosclerotic lesions. As such examples, the surface levels of MerTK and LRP1 on macrophages gradually decrease over plaque progression and this decline is accompanied by an enhanced proteolytic cleavage by the metalloproteinase ADAM17 (Cai et al., 2017; Costales et al., 2013; Gorovoy et al., 2010). Furthermore, reduced availability of bridging molecules, such as MFG-E8 and C1q has been demonstrated to promote necrotic core formation and to exacerbate experimental atherosclerosis (**Table 1**). Finally, defects in mitochondrial fission and calcium-dependent vesicular trafficking as well as impaired LAP can contribute to the inefficient internalization

and degradation of dying cells (Martinez et al., 2016; Wang et al., 2017). As a result, the combination of these processes manifests in defective efferocytosis and transform stable atherosclerotic plaques into highly inflammatory, necrotic and non-resolving culprit lesions.

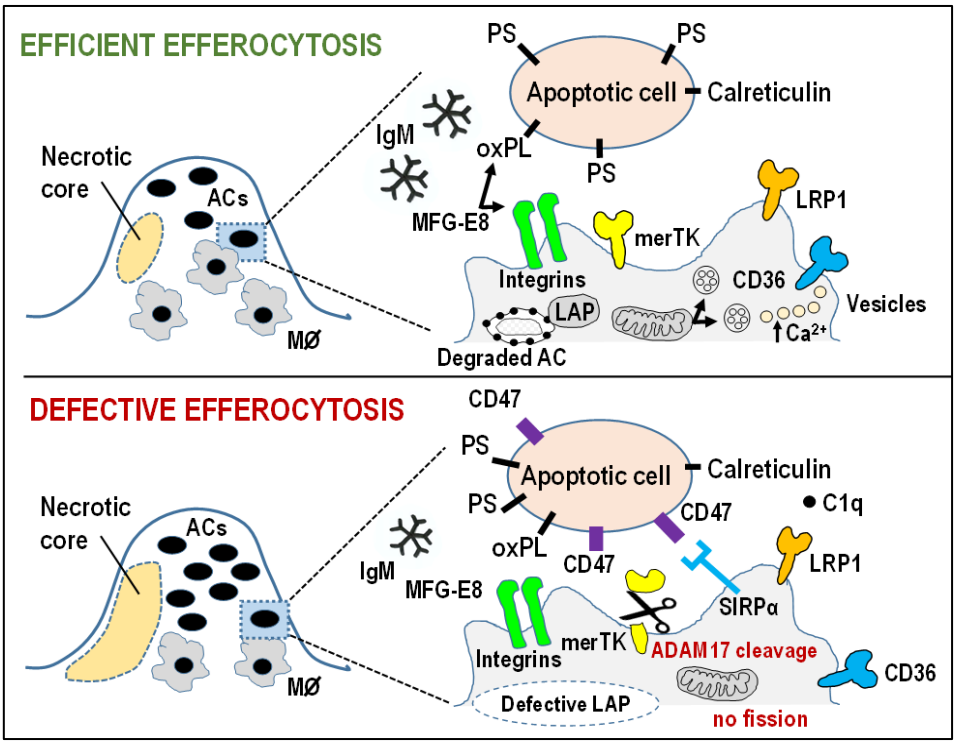

Figure 5 – Processes involved in lesional efferocytosis – ***Efficient efferocytosis (above)*** - externalized "eat me" signals including phosphatidylserine (PtSer), calreticulin and oxidized phospholipids (OxPL) are recognized by their respective receptors Mer tyrosine kinase (MerTK), LDL-receptor related protein 1 (LRP1) as well as integrin αvβ3 and CD36 on macrophages either directly or mediated by bridging molecules such as growth arrest-specific 6 (Gas6) for PtSer, complement protein C1q for calreticulin and milk fat globule-epidermal growth factor 8 (MFG-E8) for OxPL. Calcium-dependent vesicular trafficking events driven by mitochondrial fission and LC3-associated phagocytosis (LAP) promote phagolysosomal fusion and the hydrolytic degradation of apoptotic material. Simultaneously, natural IgM antibodies with reactivity towards oxidation-specific epitopes (OSE) further enhance the efficient clearance of dying cells via complement receptors. ***Defective efferocytosis (below***) - In advanced atherosclerosis, one or more of these mechanisms are dysfunctional and can lead to defective efferocytosis propagating non-resolving inflammation and plaque necrosis. Additional processes contributing to impaired efferocytosis include ADAM-17-mediated cleavage of MerTK as well as the inappropriate expression of the "don't eat me" signal CD47 on apoptotic cell surfaces.

1.1.3 Additional components of cellular and humoral immunity in atherosclerosis

Although monocyte-derived macrophages are undoubtedly the hallmark cells of atherosclerosis, they are only one of the many members of the vertebrate immune system all involved in atherosclerotic lesion formation. In principal, the vertebrate immune system is divided in two separate branches: the innate immunity (including macrophages) and the adaptive or acquired immunity (**Figure 6**). While innate immunity acts as the first line of self-defense and is specialized to recognize well-conserved structures on pathogens and modified host cells, adaptive immunity had developed later during evolution and is responsible for generating highly specific immune responses as well as immunological memory. Both innate and adaptive immunity comprise cellular as well as humoral (molecular) components (Delves and Roitt, 2000a, b). Studies investigating the single-cell immune landscape of murine as well as human plaques confirmed that all sorts of immune cell populations are present in atherosclerotic lesions and the adventitia (Cochain et al., 2018; Fernandez et al., 2019; Kim et al., 2018; Winkels et al., 2018). Among them, different subsets of T lymphocytes are the most abundant, followed by B lymphocytes, dendritic cells, natural killer (NK) cells and neutrophils. Moreover, each of them - along with other cell types including endothelial cells, epithelial cells and hepatocytes – has the ability to secrete and respond to the humoral components of immunity, which consists of a myriad of molecules with important effector and mediator functions.

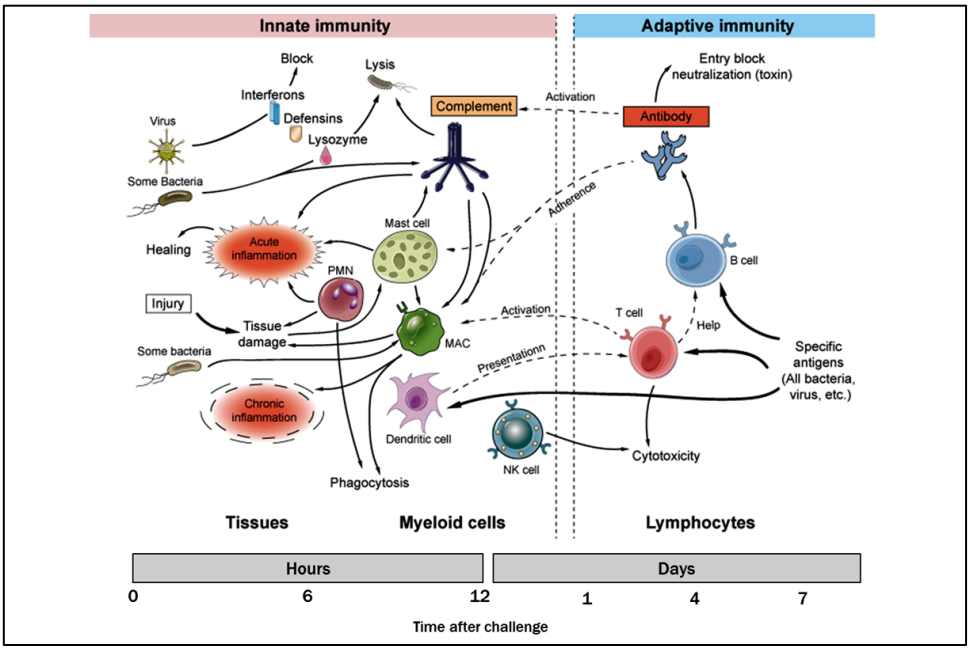

Figure 6 – The immune system of vertebrates – *Adapted and modified from Creative Diagnostics (www.creative-diagnostics.com).*

Neutrophils and dendritic cells in atherosclerosis

Similar to monocytes and macrophages, both neutrophils and dendritic cells belong to the innate arm of immunity. Neutrophils are short-lived effectors of the innate immune response and the very first cells to arrive to the site of inflammation. Therefore, they play an important role in the initial phase of atherosclerosis development mainly by triggering the intimal recruitment of monocytes via releasing 'find me' and 'eat me' signals (Weber and Noels, 2011). In line with this, neutrophil depletion results in decreased monocyte infiltration and reduction in early plaque size in experimental atherosclerosis (Drechsler et al., 2010; Zernecke et al., 2008). However, recent evidence suggests a role for neutrophils in chronic atherogenesis. Upon TLR or Fc receptor activation, neutrophils can release their nuclear content including DNA fibers and chromatins. This leads to the formation of a scaffold to which various antimicrobial proteins can adhere, termed neutrophil extracellular traps (NET). NETs can prime macrophages and T cells for pro-inflammatory cytokine release and promote thrombus growth (Papayannopoulos and Zychlinsky, 2009; Warnatsch et al., 2015). Therefore, the continuous presence of neutrophils in advanced atherosclerotic lesions can act as a trigger for luminal thrombosis.

Dendritic cells are well positioned at the crossroad of innate and adaptive immunity and are a rather versatile population that includes resident, migratory and inflammatory subtypes (Libby et al., 2013). They are considered to be mainly of Ly6C^{lo} monocyte origin and have high proliferative capacity in the intima via a GM-CSF dependent mechanism. Although they share functional and phenotypic similarities with macrophages, they are bona fide antigen-presenting cells and are instrumental to activate or suppress the activation of adaptive immunity, especially of T cell responses. In early lesions dendritic cells secrete pro-inflammatory cytokines, break T cell tolerance and license them to atherogenic responses. In advanced plaques, they limit regulatory T cell expansion and sustain atherosclerosis (Weber and Noels, 2011). Thus, dendritic cells exert pro-atherogenic effects by translating innate danger signals into a corroborating adaptive immune response.

Adaptive immunity in atherosclerosis

Adaptive immunity uses antigen specificity to provoke potent defense and long-lasting memory against pathogens or danger signals. The cellular components are composed predominantly of lymphocytes, including T cells and B cells. The high specificity of the antigen response is generated by V(D)J recombination and somatic hypermutation, which lead to a remarkable diversity in T cell receptor (TCR) of T cells and antibody repertoire of B-cell derived, antibody-producing plasma cells (Janeway, 2011). Advanced plaques are characterized by a clonal expansion of effector T cells following antigen presentation by

dendritic cells. T cells can be divided into two main subgroups: $CD4^+$ T cells that are able to differentiate into multiple types of helper T cells and cytotoxic $CD8^+$ cells. While to date, the role of $CD8^+$ T cells in atherosclerosis is rather unexplored, the ratio of various types of helper T cells (T_h) has been shown to define disease progression. Interferon gamma (IFN-y)-producing effector T_h1 cells exacerbate plaque formation mainly by influencing macrophage polarization (Tse et al., 2013). In line with this, hypercholesterolemic mice deficient in the signature T_h1-differentiating transcription factor Tbet develop decreased atherosclerosis (Buono et al., 2005) and plaques of symptomatic patients are characterized by a distinct subset of activated and differentiated $CD4^+$ T cells (Fernandez et al., 2019). Conversely, $CD4^+CD25^+FoxP3^+$ regulatory T cells (Tregs) are negative regulators of pro-inflammatory effector cells and are believed to be atheroprotective. Their commitment is driven by IL-10 and TGF-β exposure and therefore, their numbers gradually decline during disease progression. In summary, a misbalance in T_h1 and Treg numbers can reflect phenotypic plasticity and metabolic conditions in the plaque and greatly affect macrophage polarization and lesion progression/regression (Tabas and Lichtman, 2017).

A recent network-based integrative approach revealed that B cell-related genes are causative in coronary heart disease (Huan et al., 2013). Compared to T lymphocytes, B cells are fewer in lesions, but more prevalent in the adventitia. B cells come in many different subtypes, but can be classified into two main subsets according to their developmental origin: B1 and B2 cells. While B1 cells develop during fetal liver hematopoiesis and reside mainly in the peritoneum and pleural cavity, B2 cells are bone marrow-derived and their terminal differentiation towards follicular B (FO B) cells or marginal zone B (MZB) cells takes place in the spleen (Tsiantoulas et al., 2015). B1 cells exert atheroprotective effects mainly due to the secretion of germline-encoded natural immunoglobulin M (IgM) antibodies with high specificity against danger-associated signals (Tsiantoulas et al., 2014). Upon binding OSEs, natural IgM can neutralize the proinflammatory effects of oxLDL, temper foam cell formation and mediate the anti-inflammatory clearance of apoptotic cells (Binder, 2010; Chou et al., 2009). In line with this, adoptive transfer of wildtype, but not secreted IgM-deficient B1 cells can dampen lesion formation in splenectomized mice (Kyaw et al., 2011).

The effect of B2 cells on atherosclerosis is less evident. While both FO B cells and MZB cells were considered to induce plaque formation via the production of proatherogenic IgG and IgE antibodies, a recent study has identified a protective role for MZBs in modulating the response of follicular helper T cells to hypercholesterolemia (Nus et al., 2017). Moreover, X-Box binding protein-1 (XBP1)-mediated plasma cell responses were also found to attenuate atherosclerosis development (Sage et al., 2017). However, two recent studies confirmed that FO B cell-derived plasma cells promote atherosclerotic lesion formation by producing

pathogenic IgG antibodies via a mechanism that involves Blimp-1, MHCII and CD40 (Tay et al., 2018) as well as T cell-dependent germinal center formation (Centa et al., 2019). Although of note, IgG antibodies may also limit plaque vulnerability by enhancing smooth muscle cell proliferation (Centa et al., 2019). Finally, a small subset of splenic B cells, called innate response activator (IRA) B cells characterized by GM-CSF secretion has been shown to aggravate atherosclerosis by expanding oxLDL-specific IgG2c antibodies (Hilgendorf et al., 2014). Thus, B cells – predominantly via the antibody-mediated humoral immune response – play an important role in atherosclerosis (**Figure 7**) and represent a plausible target for future therapeutic approaches to combat cardiovascular disease.

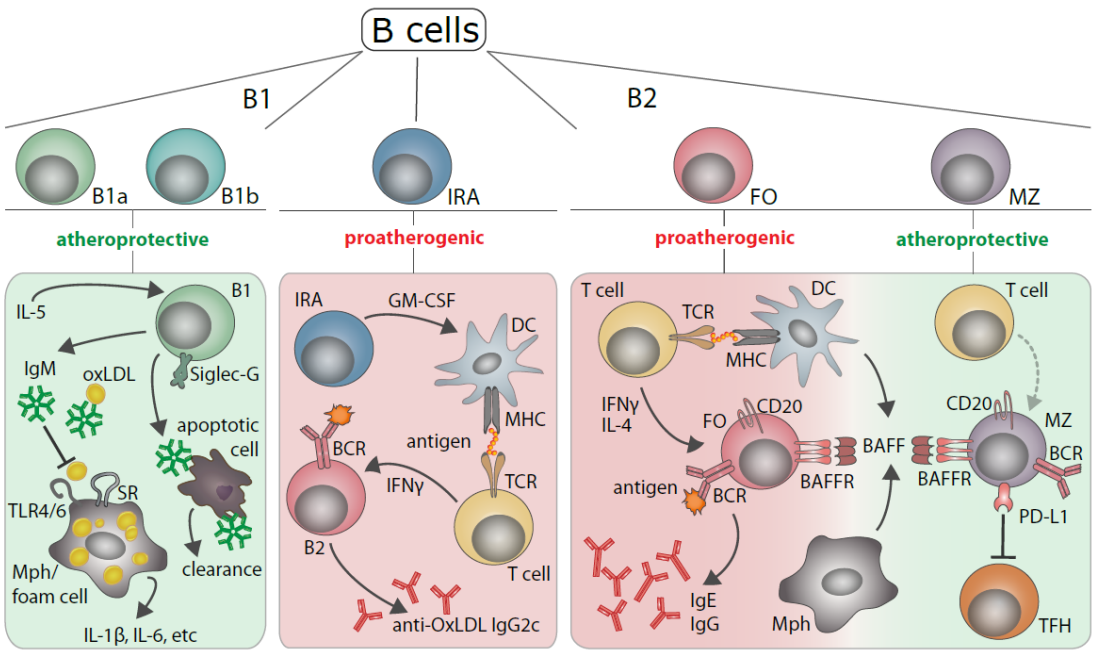

Figure 7 – The role of B cells in atherosclerosis – Fetal liver-derived B1 cells protect from atherosclerosis predominantly by the secretion of natural IgM antibodies against danger-associated molecular patterns. Innate-like MZ B cells also mitigate lesion formation via modulating follicular helper T cell responses. On the contrary, FO B and IRA B cells exaggerate atherosclerosis due to the secretion of pro-atherogenic class-switched IgG and IgE antibodies.

Humoral components of innate immunity in atherosclerosis

The humoral innate immune response is composed of conserved, soluble serum components, such as antitoxins, bacteriolysins, opsonins, collectins, pentraxins as well as the components of the complement system (Shishido et al., 2012). While these molecules have key functions in controlling viral and bacterial infections, they are often pathogenic in

chronic inflammatory diseases including atherosclerosis. Accordingly, C-reactive protein (CRP), an acute phase protein belonging to the pentraxin family, is used as an important predictor of myocardial infarction and stroke, as its levels are strongly associated with cardiovascular diseases; although no casual effect of CRP on atherosclerosis exists (Paffen and DeMaat, 2006). The physiological role of CRP is to bind to dying cells or bacteria and activate the central element of innate humoral immunity, the complement system.

1.2 The complement system

Complement is one of the cornerstones of innate immunity and is comprised of a number of evolutionarily conserved, soluble peptides that are present in the circulation as inactive precursors (**Figure 8**). Upon stimulation, these components are able to form an amplifying cascade that leads to complement activation in a self-controlling manner (Walport, 2001a). Complement was discovered more than 100 years ago (Ehrlich & Morgenroth, 1899) and was named after its 'complementary' bactericidal activity that enhances the function of antibodies and phagocytic cells in the clearance of invading pathogens and damaged host cells (Walport, 2001b). Moreover, it also participates in modulating B cell responses (Carroll, 2004; Carroll and Isenman, 2012). Thus, complement has a crucial role in maintaining cellular integrity and tissue homeostasis as well as in regulating adaptive immunity (**Figure 9**).

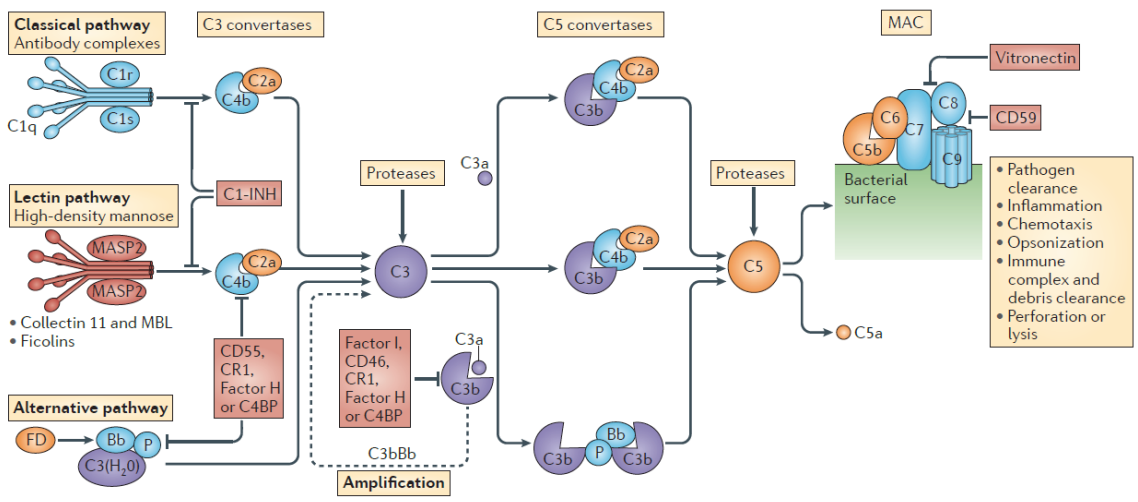

Figure 8 – Systemic complement activation – Liver-derived systemic complement activation is the first line of immune response against invading microorganisms. The complement cascade can be initiated by three major pathways: the classical, the lectin and the alternative pathway and they all converge at the step of C3 cleavage, followed by C5 activation and membrane attack complex (MAC) assembly. Host cells are protected from extensive complement activation via a wide array of complement regulators (*in red*). *Adapted from (Kolev et al., 2014)*.

1.2.1 Initiation of complement activation

Upon encountering biological surfaces, the inactive components of complement undergo structural modifications, which allow them to assemble with other complement molecules.

This results in the generation of effector compounds and active proteases that further perpetuate cascade progression. Importantly, different complement activators can trigger separate pathways of complement activation. In general, complement can be divided into three main pathways: the classical, the lectin and the alternative pathway. All three pathways revolve around the proteolytic cleavage of the central complement component C3 which is a convergence point in further downstream complement activation (Reis et al., 2019).

The classical pathway

The classical pathway is initiated by the engagement of the C1-complex ($C1qr^2s^2$). As C1q preferentially binds immune complexes consisting of antibody-bound antigens, antibodies are considered as the most potent activators of the classical pathway. Due to their pentameric structure, IgMs have the highest complement-fixing potential, while IgG-mediated complement activation requires the interaction of C1q with 2-6 IgG molecules at the same time (Ugurlar et al., 2018). Notably, the classical pathway can also be triggered in an antibody-independent manner via antigens that directly bind C1q, such as mitochondrial products, beta-amyloid fibrils as well as viruses and certain bacteria (Holers, 2014). Upon binding, a conformational change occurs in the C1q molecule, which promotes the autocatalytic activation of the serine protease C1r molecule and the subsequent transactivation of C1s. As a consequence, C1s cleaves complement components C4 and C2 into C4a, C2a, C4b and C2b. Ultimately, C4b and C2b bind to assemble into the classical pathway C3 convertase (C4bC2b complex) with C3-cleaving ability (Mortensen et al., 2018).

The lectin pathway

The initiation of the lectin pathway is homologous to the classical pathway, but the target recognition involves different opsonins, such as mannose binding lectin (MBL) or ficolins, instead of C1q. These proteins belong to the collectin family and recognize repeated simple sugar moieties (such as mannose residues) on the surface of microorganisms leading to the activation of MBL-associated proteases mannose-binding lectin serine protease 1 (MASP1) and MASP2, which subsequently cleave C2 and C4 to form the classical pathway C3 convertase (Fujita, 2002; Gal et al., 2007). Therefore, the lectin pathway has a prominent function in the removal of foreign invaders.

The alternative pathway

The alternative pathway does not demand any specific trigger as it is continuously activated to a low extent in the fluid phase. Due to its unstable nature, C3 undergoes a conformational change as a consequence of spontaneous hydrolysis derived from the breakdown of its internal thioester bond (Zipfel et al., 2007). This process is also referred as a ‘tick-over’

mechanism and results in a 'C3b-like' C3, termed $C3_{H2O}$. Surface-bound $C3_{H20}$ can interact with factor B and in the presence of factor D they form the alternative pathway C3 convertase C3bBb. This convertase is stabilized by the complement activator properdin and the C3bBbP complex then acts as the trigger for additional C3 cleavage, which can also deposit on the same biological surface as C3b and recruit additional factor B, factor D and properdin molecules to greatly amplify local complement activation (Walport, 2001a).

1.2.2 C3 cleavage and amplification

Both the classical pathway (C4bC2b) and the alternative C3 convertases (C3bBb) cleave C3 to C3a and C3b. C3a has anaphylactic and antimicrobial ability and it serves to recruit innate effector cells to the site of inflammation by engaging the C3a receptor (Nordahl et al., 2004). Meanwhile, C3b gets deposited on nearby surfaces and can trigger an amplifying reaction by forming surface-bound C3 convertases. Deposition of C3b on microbial or apoptotic surfaces leads to opsonization, which mediates the anti-inflammatory phagocytosis of these particles. When inflammation progresses, C3 convertases may additionally bind another C3b that results in the formation of a C5 convertase (C4bC2bC3b or C3bBbC3b). These complexes cleave C5 into the anaphylactic peptide C5a and C5b. C5b then initiates the terminal pathway by recruiting C6, C7, C8 and C9 to form the membrane attack complex (MAC, also known as terminal complement complex) (Ricklin et al., 2016). Ultimately, this assembly results in pore formation and the lysis of the bacteria or cells.

1.2.3 Complement regulation

Although complement has a crucial housekeeping function in clearing microorganisms and dying cells, it can also act as a double-edged sword when it attacks host bystander cells during infection or inflammation. To prevent this scenario, a wide array of complement regulators is available to ensure maximal protection on uncompromised host cell surfaces to block complement activation thereby sustaining a delicate balance between amplification and inhibition (Holers, 2014). Furthermore, complement repressors secure that complement activation only proceeds until C3b opsonization on damaged host cell surfaces, thus mediating their non-inflammatory removal. Inappropriate function of regulators can therefore lead to host cell damage, the accumulation of apoptotic cells, secondary necrosis and the development of immunopathologies and autoimmune diseases (**Figure 10**). The relevance of complement inhibition is well emphasized by the high numbers of regulators that act at all levels of the pathway. In fact, they exceed the number of complement components (C1 to C9) and can be categorized in three distinct classes based on their site of actions.

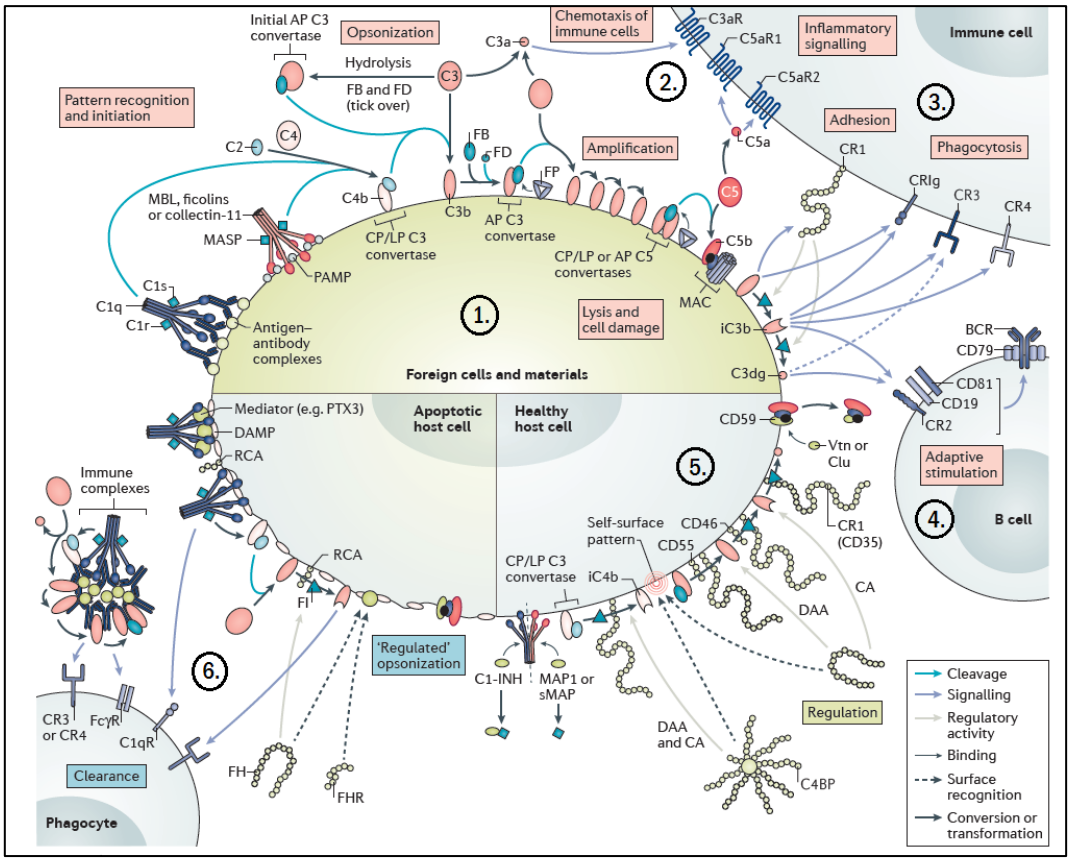

Figure 9 – Main mechanisms of differential complement activation – **(1)** On the surface of foreign cells and materials, all complement pathways (CP – classical pathway, LP – lectin pathway, AP – alternative pathway) become activated leading to MAC-dependent lysis and cell damage. **(2)** The released C3a and C5a recruit and prime immune cells via C3aR1 and C5aR1, while the **(3)** interaction of C3b with membrane-integral complement receptors (CR) facilitates cell adhesion and phagocytic engulfment. Furthermore, complement modulates adaptive immunity **(4)** via the engagement of the B-cell co-receptor CR2 (CD21) by inactivated C3b products iC3b and C3dg that lowers the threshold for B cell receptor activation. **(5)** Unmodified host cell surfaces are protected from exaggerated complement activation by a myriad of complement regulators including C1-INH, MAP1 and the repressors of complement activation (RCA) family (*see **Figure 13***). Lastly, **(6)** the non-inflammatory removal of apoptotic cells, immune complexes and cell debris is mediated by direct sensing of DAMPs or through complement activators, such as pentraxins (e.g. PTX3) and antigen-bound IgM leading to controlled C3b-associated phagocytosis. *Adapted and modified from (Ricklin et al., 2016).*

Membrane-integral complement receptors

Membrane-integral clearance receptors convey the signal derived from bioactive complement cleavage products including C3a, C3b, C4b and C5a to modulate inflammatory responses, such as phagocytosis (Ricklin et al., 2016). Five major effector receptors are

involved in driving effector functions via C3b and C4b deposited on target surfaces: CR1 (or CD35), CR2 (or CD21), CR3 (CD11b-CD18), CR4 (CD11c-CD18) and CRIg (also known as VSIG4). The distribution and the expression profile of these regulators highly vary between distinct cell types. The anaphylactic peptides C3a and C5a activate transmembrane spanning receptors C3aR as well as C5aR1 (CD88) and C5aR2 (C5L2), respectively. These receptors are highly abundant on innate immune cells, such as neutrophils, monocytes and macrophages. While C3a appears to display less biological effects, C5a exerts multiple pro-inflammatory properties including leukocyte recruitment, neutrophil aggregation and inflammasome activation, mainly via engaging C5aR1. Although structurally similar, the exact role of C5aR2 is not well described as has been believed to act as a decay receptor to attenuate the actions of C5a. Finally, receptors for direct C1q binding have been recently identified including C1qR and SIGNR1 (CD209) (Reis et al., 2019; Zipfel and Skerka, 2009).

Membrane zone complement regulators

Membrane zone repressors include CD46 (also known as MCP), CD55 (also known as decay accelerating factor; DAF) and CD59 (or protectin). CD46 is present on every cell except for erythrocytes and it blocks the effects of C4b and C3b. CD55 and CD59 are both expressed by most cells and inhibit the decay of the classical and alternative C3 convertases or MAC formation, respectively. These regulators control all three pathways of complement activation and act in a homologous manner on every cell surface (Kim and Song, 2006).

Fluid phase regulators

Fluid phase regulators are abundant in plasma and other body fluids and thus, largely affect systemic complement activation. They are more specific in function compared to membrane zone repressors, as they control either the alternative or the classical/lectin pathways and act essentially on either C3 or C4 (Noris and Remuzzi, 2013). The fluid phase repressors of the classical and lectin pathway include C1 inhibitory protein (C1INH), C4-binding protein (C4BP) and carboxypeptidase N, while the alternative pathway C3 activation is regulated by properdin, complement factor H (CFH) and its alternative splice variant, FHL-1. In addition, CFH-related protein 1 (CFHR1), clusterin and vitronectin can control the terminal stages of the complement cascade (Zipfel and Skerka, 2009). It is now evident that several fluid phase regulators can attach to cell surfaces or bio-membranes and provide an additional layer of protection for host cells (Borras et al., 2019; Clark et al., 2013). Moreover, they can also bind to modified host cells, such as apoptotic cells and bodies to prevent terminal pathway activation on their surface and mediate their anti-inflammatory clearance (Mihlan et al., 2009; Trouw et al., 2005). In this aspect, the two main soluble complement repressors C4BP and CFH have been shown to play the major role.

Molecule	Pathway	Ligand	Expression pattern	Function
Membrane-integral complement receptors				
CR1/CD35	C3	C3b, iC3b, C4b, C1q	ubiquitous	immune complex clearance, enhancement of phagocytosis
CR2/CD21	C3	C3dg, C3d, iC3b	mainly B cells, follicular DCs	B cell co-stimulation, immune complex clearance
CR3/MAC1	C3	iC3b	among immune cells, mainly myeloid cells	iC3b-mediated phagocytosis
CR4	C3	iC3b	monocytes, macrophages, DCs	iC3b-mediated phagocytosis
VSIG4/CRIg	C3	C3b, iC3b, C3c	macrophages	iC3b-mediated phagocytosis
C3aR	C3	C3a	myeloid cells, APCs, T cells, astrocytes, neurons	immune cell recruitment, inflammation
C5aR1/CD88	C5	C5a	mainly myeloid cells, APCs, T cells,	immune cell recruitment, inflammation
C5aR2/C5L2	C5	C5a	macrophages and neutrophils	immune cell recruitment, inflammation
C1qR/CD93	Classical	C1q	monocytes, macrophages, B cells	phagocytosis, cell adhesion
SIGNR1/CD209	Classical	C1q	DCs, macrophages	enhancement of phagocytosis
Membrane zone complement regulators				
CD46/MCP	C3	C3b, C4b	all cells except erythrocytes	C3 degradation, co-factor activity for factor I and CFH
CD55/DAF	C3	Convertases	Ubiquitous	acceleration of C3 convertase decay
CD59/protectin	Terminal	C8 & MAC	Ubiquitous	inhibition of MAC assembly
Fluid-phase complement regulators				
C1q	Classical	Immune complexes	binds to apoptotic cell surfaces	activation of the classical pathway
C1INH	Classical and lectin	C1r, C1s, MASP2	NA	blocks classical and lectin pathway activation
C4BP	Classical and lectin	C4	acquired to the surface	co-factor activity for factor I, acceleration of C4bC2b decay
Carboxy-peptidase N	Classical and lectin	C3a, C4a, C5a	NA	inactivation of anaphylatoxins
Properdin	Alternative	C3	binds to apoptotic cell surfaces	stabilization of C3bBb
CFH	Alternative	C3b, C3d	acquired to the surface	co-factor activity for factor I, acceleration of C3bBb decay
FHL-1	Alternative	C3b	acquired to the surface	co-factor activity for factor I, acceleration of C3bBb decay
CFHR1	Terminal	C5 con-vertase, MAC	acquired to the surface	inhibition of C5 convertase and MAC assembly
Clusterin	Terminal	C7, C8, C9, MAC	NA	inhibition of MAC assembly
Vitronectin	Terminal	C5b-7, MAC	NA	inhibition of MAC assembly

Table legend on next page

Table 2 – Complement regulators and receptors - *Adapted and modified from (Zipfel and Skerka, 2009).*

1.2.4 Sites of complement synthesis

It has been long acknowledged that the liver is the primary source of complement secretion. However, it is now evident that almost every cell - including immune cells, epithelial cells, endothelial cells and fibroblasts - can produce complement proteins and in certain immune-sequestered organs, such as the eye, local production by resident cells outweighs the contribution of hepatic, systemically circulating complement (Kolev et al., 2014). The significance of local complement production is well underlined by studies showing that macrophage-derived C4 can restore the defective humoral immune response in serum C4 deficient mice (Gadjeva et al., 2002) and C3 of epithelial origin regulates acute renal transplant rejection (Pratt et al., 2002). Moreover, dysregulated synthesis of complement factors by adipocytes has been associated with partial lipodystrophy (Rosen et al., 1989).

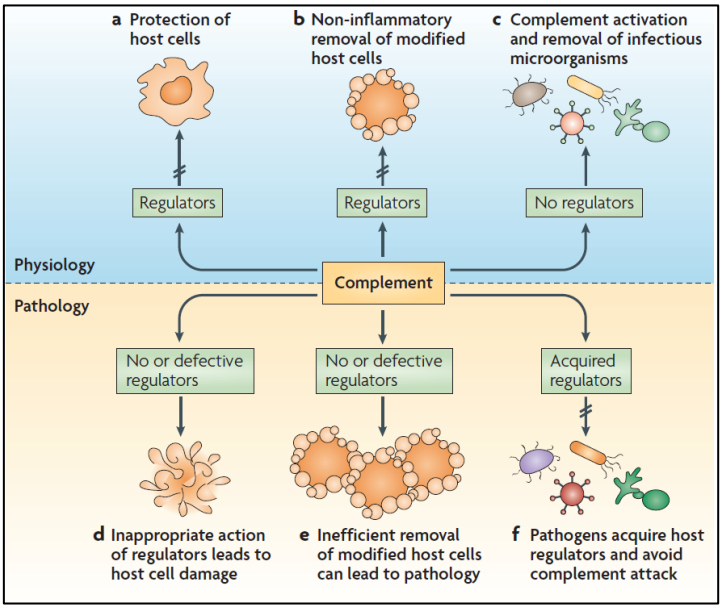

Figure 10 – Complement in pathology – While complement can largely benefit the host **(a-c)** by recognizing and lysing invading pathogens and mediating the non-inflammatory removal of apoptotic cells, uncontrolled complement activation **(d-e)** due to the lack of proper complement regulation results in host tissue damage and an impaired clearance of dead cells that can culminate in autoimmune diseases. Acquisition of complement regulators **(f)** is used as a common immune evasion strategy by microorganisms or tumor cells to enhance the control over complement in their microenvironment thereby escaping elimination. This can lead to severe infections and increased tumor growth. *Adapted from (Zipfel and Skerka, 2009).*

The site of synthesis dictates the function of complement activation. While systemic C3 and C5 have crucial sentinel role in protecting against invading microorganisms and accordingly, patients with C3 or C5 deficiency develop recurrent infections, local synthesis of complement appears to have a key role in the activation and modulation of immune cell functions (Kolev et al., 2014). Consistently, the presence of a wide array of complement receptors on immune cells allows both rapid autocrine and paracrine complement signaling. For example, T cell receptor stimulation leads to the generation of C3 and C5 by $CD4^+$ T cells as well as the formation of C3 and C5 convertases in the extracellular space (Strainic et al., 2008). This ultimately results in C3a and C5a generation, which can engage their respective receptors on the surface of T cells and promote cellular responses in an autocrine manner. Furthermore, anaphylatoxins secreted by antigen presenting cells can drive T cell expansion and differentiation in a paracrine fashion (Lalli et al., 2008). Therefore, extrahepatic complement production might have evolved to respond to nearby environmental cues which require the induction, differentiation or effector function of local immune cells.

1.2.5 New paradigm in complement research – the intracellular complement

Traditionally, both systemic and local complement activation were considered to be confined to the extracellular space. However, growing evidence suggests that complement activation fragments are generated also within cells, which led to a novel paradigm in complement research: the concept of intracellular complement activation **(Figure 11)**. Specifically, recent work using human T cells showed that $CD4^+$ T cells are equipped with intracellular C3 stores where the cleavage of C3 continuously occurs via cathepsin L (CTSL) into functionally active C3a and C3b (Liszewski et al., 2013). C3a then activates C3aR located on lysosomes thereby promoting the homeostatic survival of T cells via mammalian target of rapamycin (mTOR) signaling. This whole intracellular system is able to translocate to the cell surface upon T cell activation where membrane-bound C3aR and CD46 further mediate IFN-γ production and T_h1 induction in an autocrine fashion. The dysregulation of this intracellular complement machinery has disease relevance, as T cells isolated from patients with juvenile idiopathic arthritis display hyperactive intracellular C3 activation and exacerbated T_h1 responses, which can be rescued with a cell permeable inhibitor against CTSL. Interestingly, individuals with serum C3 deficiency, whose T_h1 responses are severely impaired, can still produce sufficient levels of intracellular C3a to maintain cell survival (Liszewski et al., 2013). Thus, the cellular location of complement receptors highly defines their function in cell homeostasis.

Importantly, intracellular C3 activation is not limited to T cells and has been observed in many other cell types (Liszewski et al., 2013). Moreover, intracellular C5 stores have also been reported and C5 is also cleaved within cells by a yet unknown protease to mediate C5a-driven T cell activation (Arbore et al., 2016). These findings suggest that the intracellular complement machinery may be of wide physiological significance. Indeed, intracellular C3 has been reported to regulate nutrient influx and metabolic reprogramming (Kolev et al., 2015) as well as pancreatic beta cell survival (King et al., 2019).

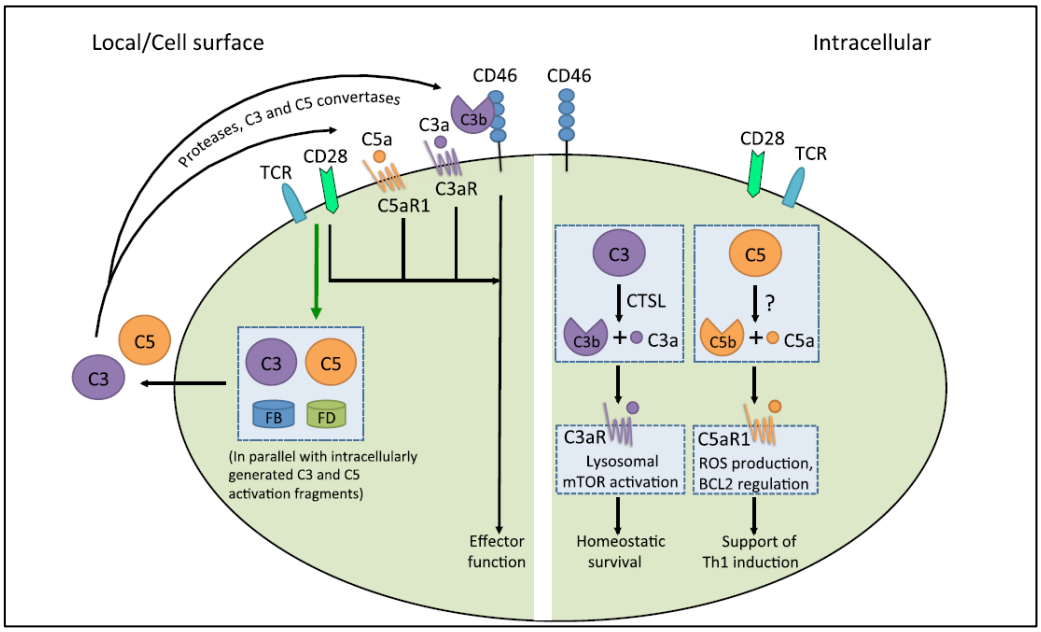

Figure 11 – Local and intracellular complement activation – ***Local activation (left)*** of complement occurs, when cell-activating signals induce the secretion of C3 and C5 followed by convertase formation either on the cell surface or in the extracellular space. Ultimately, this results in the generation of bioactive complement fragments (C3a, C3b, C5a and C5b), which bind to their respective cell surface receptors and trigger cellular responses in an autocrine manner***. Intracellular complement activation (right)*** is mediated by cell-specific proteases, which have the ability to cleave intracellular C3 and C5 into their bioactive fragments. C3a and C5a generated by this pathway then can engage their respective intracellular receptors and exert effector functions or promote cell survival. *Adapted from (Hess and Kemper, 2016).*

In addition, intracellular C3 stores can also act as a cytosolic surveillance system against local environmental danger signals (Arbore et al., 2017). In line with this, intracellular C3 aids the protection against microorganisms by driving autophagy-mediated growth restriction of cyto-invasive bacteria (Sorbara et al., 2018) and VSIG4-dependent degradation of C3-

opsonized *Listeria* (Kim et al., 2016). Furthermore, the intracellular presence of C3-opsonized viruses induces NF-kB and AP-1 expression through mitochondrial antiviral signaling (MAVS), resulting in a strong pro-inflammatory response (Tam et al., 2014). Besides pathogen recognition, intracellular complement may be a major danger sensing machinery during sterile inflammation. Intracellular C3 fragments control lysosomal fusion and promote the processing of the apoptotic cargo in murine dendritic cells (Baudino et al., 2014). Furthermore, intracellular C5a has been shown to regulate inflammasome activation upon the accumulation of reactive oxygen species (ROS) (Arbore et al., 2016). Thus, intracellular complement activation may have a fundamental role in orchestrating cellular immunity during inflammatory processes.

Open questions in intracellular complement research

The discovery of intracellular complement activation aids to explain the wide range of effects of complement in immunity and beyond. Nevertheless, it also poses a lot of pressing questions that still need to be answered including: How does extracellular, autocrine and intracellular complement co-operate? Are metabolic changes in the extracellular space integrated by complement at the cellular level? How does intracellular complement interact with the microbiome? Are there additional complement components that actively operate inside the cell? And probably the most fundamental of all: How is intracellular complement activation regulated? Given the wide array of repressors involved in systemic complement regulation, it is expected that certain canonical regulators are also functionally active within cells. However, whether these regulators are ubiquitously expressed among cells or display a compartmentalized expression pattern or whether intracellular complement regulation also occurs beyond canonical repressors as well as their potential influence on inflammatory responses remain all elusive. Nevertheless, active regulation of cell autonomous complement could let us envision the existence of an intracellular *complosome* that has a pivotal function in maintaining cellular integrity and homeostasis (Hess and Kemper, 2016; Kolev et al., 2014).

1.3 Complement in atherosclerosis

Due to its crucial homeostatic functions, the involvement of complement has long been implicated in the pathogenesis of atherosclerosis (**Figure 12**). In the arterial intima, activated complement occurs simultaneously with the formation of early fatty streaks in cholesterol-fed animals and is especially active in vulnerable plaques (Seifert et al., 1989). Although complement components in the intima can be retained from plasma, mRNA levels of C1rs, C1s, C4 etc. are present in human aortic atherosclerotic plaques, which suggests local production of complement inside the vessel wall (Yasojima et al., 2001). In general, hyperactive complement is considered pro-atherogenic, which is supported by findings that C5b-9 deposition correlates with the severity of lesion vulnerability (Seifert et al., 1989) and that C5a is associated with necrotic cell debris in lipid-rich unstable plaques, while absent in stable lesions (Speidl et al., 2011a).

1.3.1 Complement activation in atherosclerosis

Complement can be activated by all three separate pathways during atherogenesis. One of the main activator of the classical pathway is CRP, which has been found to co-localize with MAC (Torzewski et al., 1998) and is strongly associated with cardiovascular events (Paffen and DeMaat, 2006). Moreover, OSE-specific natural antibodies can also trigger classical pathway activation via C1q (Tsiantoulas et al., 2014). In addition, numerous studies have reported a potential role for *Chlamydia pneumoniae* in atherosclerosis by activating the lectin pathway (Campbell and Kuo, 2003). However, due to its self-amplifying property, alternative complement appears to be the major pathway implicated in atherosclerosis development. This is especially true for advanced lesions, in which accumulating apoptotic cells and free cholesterol crystals are both known to potentiate alternative pathway activation (Seifert et al., 1989; Seifert et al., 1990). As an opsonin, C3b generated through this amplification loop is essential for promoting the non-infammatory clearance of apoptotic cells by professional phagocytes.

While the outer layers of the intima, which are in contact with smooth muscle cells and extracellular lipids show signs of terminal pathway activation including extensive MAC staining, in deeper layers of the intima complement activation does not seem to proceed beyond C3 or C5 convertase activation, which can be due to the local production of complement regulators (Oksjoki et al., 2003). Nevertheless, the constant production of C3a and C5a promotes the infiltration of myeloid cells into the lesions and may also have additional metabolic effects when they are degraded into $C3a_{desArg}$ and $C5a_{desArg}$ by carboxypeptidase N (Speidl et al., 2011a). C5a has been also shown to induce MMP-1 and MMP-9 expression in human macrophages (Speidl et al., 2011b). Furthermore, increasing

evidence supports that C5a is a potent trigger of inflammasome-mediated IL-1β secretion (Arbore et al., 2016; Samstad et al., 2014), which may explain why overexpression or administration of C5a results in accelerated atherosclerosis (An et al., 2016) and induces plaque disruptions (Wezel et al., 2014), while C5a inhibition leads to decreased atherosclerotic lesion formation in experimental atherosclerosis (Manthey et al., 2011). In line with these findings, both C3aR and C5aR2 deficiency mitigates atherosclerosis (Selle et al., 2015; Yang et al., 2010) and C5aR1 targeting protects from neointima formation during hypercholesterolemia (Shagdarsuren et al., 2010).

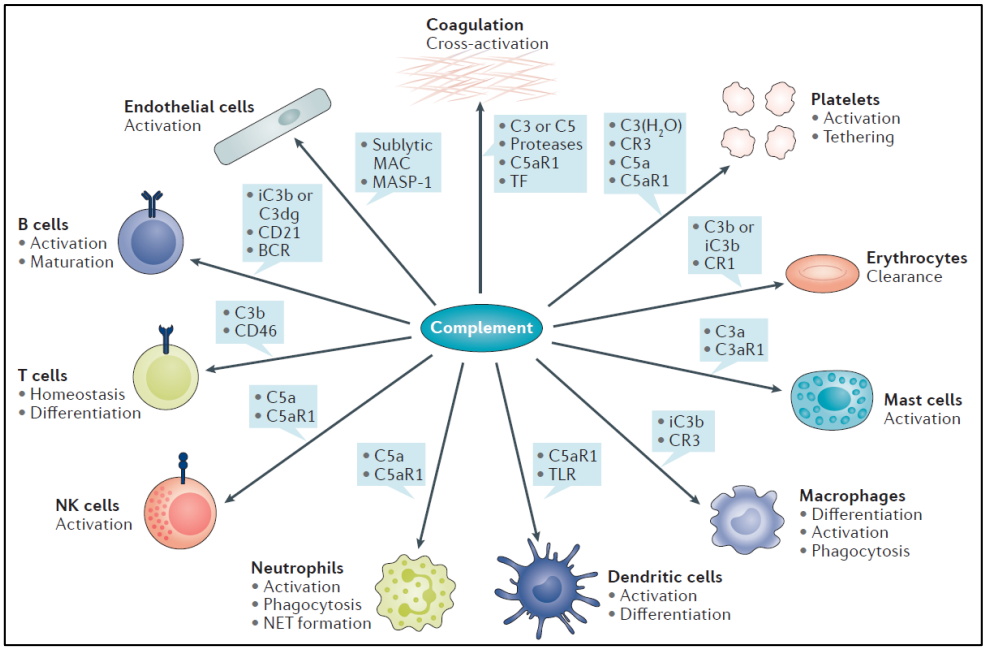

Figure 12 – Complement in orchestrating the immune response during atherogenesis – The generation of bioactive complement fragments can trigger a large variety of downstream responses via different cellular effectors. These include the activation of endothelial cells, the priming of both innate and adaptive immunity as well as pro-coagulative responses through cross-activation with the coagulation system. *Adapted from (Ricklin et al., 2016).*

1.3.2 Modulation of complement activation in experimental atherosclerosis

First and foremost, global C3 deficiency in mice results in increased aortic plaque size in multiple studies. On an Ldlr deficient background, lack of C3 is associated with unstable lesions with high macrophage content and decreased collagen staining (Buono et al., 2002), which might be due to defective efferocytosis. In *Apoe*$^{-/-}$ *Ldlr*$^{-/-}$ mice, the absence of C3 also leads to increased triglyceride levels and a pro-atherogenic lipid phenotype that complicate

the dissection of potential inflammatory effects (Persson et al., 2004). Although C5 deficiency did not affect aortic root plaque size in *Apoe*$^{-/-}$ mice (Patel et al., 2001), the pro-atherogenic effect of C6 and the terminal pathway has been confirmed in several studies (Geertinger and Sorensen, 1970; Lewis et al., 2010; Schmiedt et al., 1998). Thus, while hyperactive complement activation clearly promotes atherosclerosis, it is also evident that the presence of C3 is essential for limiting atherosclerosis.

In line with this, complement proteins involved in the initiation of the cascade has been reported to have atheroprotective effects. C1qa deficiency leads to larger aortic root lesion size and a significant increase in apoptotic cells in atherosclerosis-prone *Ldlr*$^{-/-}$ mice (Bhatia et al., 2007; Lewis et al., 2009), underlying the importance of C1q in mediating the removal of dying cells. Of note, uncontrolled activation of the classical pathway can also be pro-atherogenic in a C5-dependent manner and that is efficiently attenuated by the complex formation of C1q with ApoE (Yin et al., 2019). Physiologic lectin pathway activity is also beneficial in atherosclerosis, as selective MBL-A and MBL-C deficiency in macrophages results in increased lesion size in hypercholesterolemic mice (Matthijsen et al., 2009). Furthermore, although factor B deficiency on an *Apoe*$^{-/-}$ background was found to have no influence on lesion formation after regular chow feeding (Persson et al., 2004), *Fb*$^{-/-}$ *Ldlr*$^{-/-}$ mice develop exacerbated atherosclerosis compared to controls following high fat diet exposure as well as upon weekly administration of LPS, indicative of the protective effect of the initiation of the alternative pathway in atherosclerosis (Malik et al., 2010). Taken together, these findings suggest that complement has a central role in modulating plaque inflammation; however, only without translating into excessive C5a production and terminal pathway activation. This sheds a light on the importance of adequate complement regulators in fine-tuning the cascade activity.

1.3.3 Complement regulators in atherosclerosis

Even though efficient regulation of complement activation appears to be essential for preventing lesion formation and complement regulatory proteins are present in atherosclerotic lesions, our knowledge is very limited regarding the role of repressors in experimental atherosclerosis. Besides the previously discussed studies on C1q (Bhatia et al., 2007; Lewis et al., 2009), only the role of properdin has been assessed in atherosclerosis among fluid phase complement regulators. However, global properdin deficiency did not influence lesion formation in high fat diet-fed *Ldlr*$^{-/-}$ mice (Steiner et al., 2014). Among membrane-bound regulators, investigations on the effect of CD55 deficiency in atherosclerosis gave rather conflicting results. On an Ldlr deficient background, CD55 deficiency led to increased lesion formation and exaggerated deposition of terminal pathway

proteins (Leung et al., 2009), whereas *Cd55*$^{-/-}$*Apoe*$^{-/-}$ mice showed either similar or severely reduced lesion size compared to *Apoe*$^{-/-}$ controls in two independent studies (An et al., 2009; Lewis et al., 2011); although decreased cross sectional plaque area was associated with reduced serum triglyceride and cholesterol levels in *Cd55*$^{-/-}$*Apoe*$^{-/-}$ mice (Lewis et al., 2011). The function of the MAC inhibitory protein CD59 is more evident in atherosclerosis. CD59a or combined CD59a and CD59b deficiency aggravated atherosclerosis in five independent studies (An et al., 2009; Lewis et al., 2010; Liu et al., 2014; Wu et al., 2009; Yun et al., 2008). Moreover, selective overexpression of CD59 in the hematopoietic compartment as well as in endothelial cells reduced lesion size in *Apoe*$^{-/-}$ mice (Wu et al., 2009), again emphasizing the significance of local complement production.

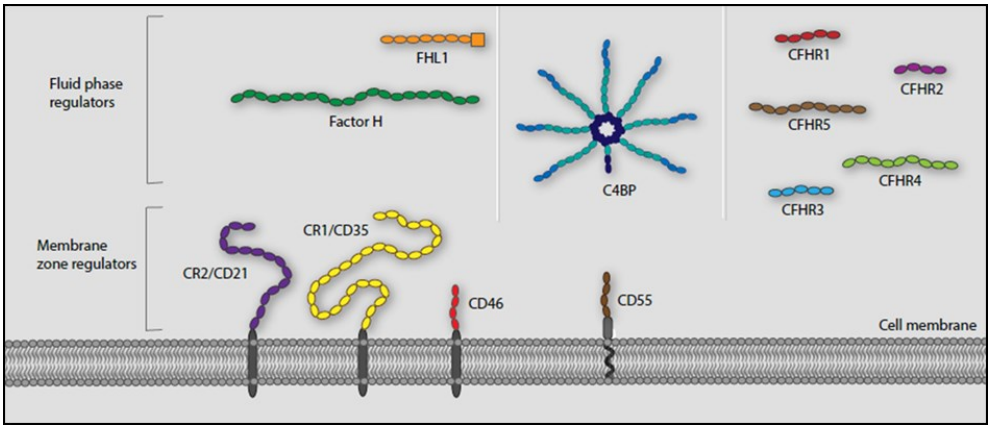

Figure 13 – Members of the regulators of complement activation (RCA) family – The RCA family is composed of both membrane zone regulators including CR1/CD35, CR2/CD21, CD46 and CD55 as well as fluid phase repressors, such as C4BP, CFH and its structurally related proteins, FHL-1 and CFH-related proteins 1-5 (CFHR1-5).

Surprisingly, besides the contradictory findings on CD55, the role of RCA family members (**Figure 13**) in atherosclerosis remains entirely unstudied. The RCA gene cluster is located on chromosome 1q32 in humans with a similar genetic location in mice. The individual genes of this cluster are thought to share a common ancestor from which they stem by gene duplication events (Rodriguez de Cordoba et al., 2004). These repressors are composed of 4 to 44 highly conserved structural units, so called short consensus repeats (SCR) or complement component proteins (CCP), with a length of approximately 60 amino acids linked with 3 to 8 amino acid spacers (Alexander and Quigg, 2007). They all exert natural affinity for C3b and/or C4b and are essential in distinguishing self from non-self thereby

preventing non-specific damage to the host. Therefore, they appear to have a crucial role in preventing advanced lesion formation.

The Binder laboratory has a profound interest in the role of RCA members in atherosclerosis and has intitated to investigate the effect of C4BP and CR2 (CD21) deficiency in lesion formation. While the thesis presented here will discuss the role of CFH in experimental atherosclerosis.

1.4 Complement factor H

Complement factor H (CFH) is the master regulator of the alternative pathway of complement activation. It inhibits the proteolytic cleavage of C3 by accelerating the decay of the C3 convertase C3bBb (Pickering and Cook, 2008). As one of the most abundant plasma proteins (100-500 µg/ml) expressed constitutively in the liver, CFH exerts its complement-regulatory function predominantly in the fluid phase (Ferreira et al., 2010). Extrahepatic production of CFH has been reported in various cell types including retinal pigment epithelial cells, endothelial cells, fibroblasts and podocytes (de Cordoba and de Jorge, 2008).

Indicative of its crucial role in controlling systemic complement activation, mice with global CFH deficiency exhibit secondary C3 deficiency as a result of continuous consumption of circulating C3 and develop spontaneous membranoproliferative glomerulonephritis (MPGN) with extensive complement and immune complex deposition on glomeruli by 8 months of age (Pickering et al., 2002). The pathologic effect is a direct consequence of alternative complement dysregulation, as additional deletion of factor B, which prevents C3 turnover, reverts the phenotype of CFH deficiency. In humans, impaired complement regulation due to reduced quantity or defective quality of CFH strongly predisposes to chronic diseases including MPGN, but also age-related macular degeneration (AMD), the number one cause of blindness among elderlies and atypical hemolytic uremic syndrome (aHUS), a rare, life-threatening progressive kidney disease (**Table 3;** (Noris and Remuzzi, 2008; Schmidt et al., 2008; Zipfel, 2001). Accordingly, renal diseases have been reported in 28 out of 33 individuals with severe CFH abnormalities (Pickering and Cook, 2008).

Disease	Pathology	Cause	Affected domain	Effect of CFHR1-CFHR3 deletion
Age-related macular degeneration (AMD)	Complement-containing drusen in the eye	Impaired binding to anionic molecules	SCR7, Y402H SNP	protective
Memranoproliferative glomerulonephritis type II (MPGN)	Complement-containing drusen in the glomeruli	Dysfunctional fluid phase regulation	Mainly SCR7, Y402H SNP	protective
Atypical hemolytic uremic syndrome (aHUS)	Renal endothelial injury and thrombosis	Impaired binding to anionic molecules	Mainly SCR19-20	Increased risk

Table 3 – Relevance of CFH in human diseases

CFH can also halt complement activation on cell surfaces by mediating co-factor activity for the inactivation of C3b into anti-inflammatory iC3b via factor I (Schmidt et al., 2008). Both the decay accelerating as well as the co-factor activity of CFH is mediated by the first 4 of its 20 short consensus repeat (SCR) domains. Other SCRs (including SCR 7, SCR 12-14 and SCR

19-20) contain heparin, glycosaminoglycan and sialic acid binding sites that promote the tethering of CFH on biological surfaces and simultaneously increase the affinity of CFH for surface-bound C3b (Jozsi et al., 2019). Therefore, C3b inactivation is highly dependent on the chemical composition of the surface (de Cordoba and de Jorge, 2008). Annexin A2, histones and DNA represent ligands for CFH on the surface of dying cells (Leffler et al., 2010). Furthermore, we have previously found that CFH can recognize the lipid peroxidation product malondialdehyde (MDA) and neutralize MDA-induced pro-inflammatory cytokine production by macrophages (Weismann et al., 2011). Moreover, CFH can exert its co-factor activity on MDA-decorated apoptotic cell surfaces, thereby facilitating local inactivation of complement (Weismann and Binder, 2012).

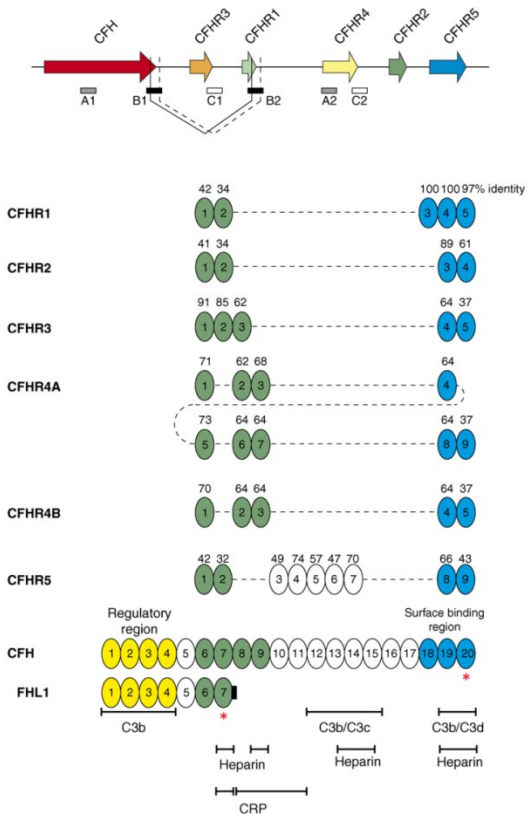

Figure 14 – The structure of CFH and its related proteins – Functional domains for decay accelerating and co-factor activity (*in yellow*) as well as for cell surface regulation (*in blue*) in CFH, FHL-1 and CFHRs are shown. Binding sites for anionic molecules and CRP are depicted in green. Red asterisks indicate MDA-binding sites. CFH is unique in the RCA family, as it solely contains SCRs aligned in tandem without intracytoplasmic regions or neighboring molecules arranged in multimers and uses its C-terminus for binding (*Alexander and Quigg, 2007*). *Adapted from (Jozsi and Zipfel, 2008).*

Importantly, six structurally related proteins with high similarity to CFH can be found in human plasma in much lower concentrations compared to CFH (**Figure 14**). Factor H-like protein 1 (FHL-1) is a product of alternative splicing, while CFH-related proteins 1-5 (CFHR1-5) originate from gene duplications (Jozsi and Zipfel, 2008). They can compete with CFH in complement regulation (FHL-1) or in cell surface attachment (CFHRs). Of note, FHL-1 is not present in mice and among CFHRs, only homologues for CFHR5 and CFHR3 can be detected in plasma, as well as in liver, heart and kidney samples. However, they derive from a separate gene, than CFH (Hellwage et al., 2006).

1.5 Aims of this thesis

Complement factor H (CFH) is the master regulator of alternative complement activation and has a crucial role in controlling systemic complement activation as well as in distinguishing self from non-self thereby protecting from complement-mediated host damage. The presence of CFH can be detected in human atherosclerotic lesions, where it is associated with proteoglycan-rich area and high C3d deposition. However, the mechanisms by which CFH can influence atherosclerotic lesion formation remain unknown. Thus, the main purpose of this thesis was to investigate the role of CFH in experimental atherosclerosis using CFH deficient mice. In particular, we aimed at:

1. Performing detailed immunological characterization of CFH deficient mice to assess the potential effect of CFH deficiency on the development and differentiation of immune cells in the steady-state
2. Identifying immune cells with the ability to produce CFH and investigating if and how hematopoietic CFH expression is regulated
3. Studying whether CFH can affect intracellular complement activation
4. Investigating whether CFH affects atherosclerosis-relevant macrophage functions in an autocrine or a systemic manner
5. Dissecting the role of hematopoietic CFH from liver-derived systemic effects

And most importantly,

6. Uncovering the effect of both global as well as hematopoietic CFH deficiency on experimental atherosclerosis

Results 2

2.1 Prologue

Even in an unchallenged setting, physiological complement activation has crucial functions in the silent removal of apoptotic cells and in fine-tuning adaptive immune responses, especially through modulating B cell differentiation and activation. Defective function of complement factor H (CFH) results in uncontrolled systemic complement activation, which is characterized by the continuous consumption of plasma C3. Consequently, mice deficient in CFH develop spontaneous membranoproliferative glomerulonephritis latest at the age of 8 months. However, it is not known whether the dysregulation of systemic complement activation associated with CFH deficiency affects the development and maturation of immune cells i.e. whether CFH deficient mice are immunocompromised per se.

In the article presented below, we performed immune-phenotyping of young, unchallenged littermate wildtype and CFH deficient mice that comprised the detailed characterization of the immune cell composition of major immune-relevant organs including the bone marrow, spleen, lymph node and peritoneum. We could demonstrate that due to its complement-regulatory effects, CFH has an important role in modulating splenic B cell differentiation and calibrating B cell responsiveness. By exerting these effects, CFH maintains the intact architecture of the spleen and restrains germinal center hyperactivity and autoantibody production. Thus, CFH prevents the development of B cell-dependent autoimmunity.

2.2 Manuscript #1

M.G. Kiss, M. Ozsvár-Kozma, F. Porsch, L. Göderle, N. Papac-Miličević, B. Bartolini-Gritti, D. Tsiantoulas, M.C. Pickering, C.J. Binder (2019) Complement factor H modulates splenic B cell development and limits autoantibody production. *Front Immunol* 10:1607. doi: 10.3389/fimmu.2019.01607.

Detailed author contribution: M. G. Kiss conceived the project, designed and performed experiments, analyzed and interpreted the data and wrote the manuscript; M.O.-K., F.P., L.G., N.P.-M., B.B.-G. performed experiments; D.T. critically revised and edited the manuscript; M.C.P. critically revised the manuscript and provided the *Cfh*$^{-/-}$ mice; C.J.B. conceived the project, designed experiments, interpreted the data and wrote the manuscript.

frontiers in Immunology

ORIGINAL RESEARCH
published: 11 July 2019
doi: 10.3389/fimmu.2019.01607

Complement Factor H Modulates Splenic B Cell Development and Limits Autoantibody Production

Máté G. Kiss[1,2], *Mária Ozsvár-Kozma*[1,2], *Florentina Porsch*[1,2], *Laura Göderle*[1,2], *Nikolina Papac-Miličević*[1,2], *Barbara Bartolini-Gritti*[1,2], *Dimitrios Tsiantoulas*[1,2], *Matthew C. Pickering*[3] *and Christoph J. Binder*[1,2]*

[1] Department for Laboratory Medicine, Medical University of Vienna, Vienna, Austria, [2] CeMM Research Center for Molecular Medicine of the Austrian Academy of Sciences, Vienna, Austria, [3] Centre for Inflammatory Disease, Imperial College, London, United Kingdom

Complement factor H (CFH) has a pivotal role in regulating alternative complement activation through its ability to inhibit the cleavage of the central complement component C3, which links innate and humoral immunity. However, insights into the role of CFH in B cell biology are limited. Here, we demonstrate that deficiency of CFH in mice leads to altered splenic B cell development characterized by the accumulation of marginal zone (MZ) B cells. Furthermore, B cells in *Cfh*$^{-/-}$ mice exhibit enhanced B cell receptor (BCR) signaling as evaluated by increased levels of phosphorylated Bruton's tyrosine kinase (pBTK) and phosphorylated spleen tyrosine kinase (pSYK). We show that enhanced BCR activation is associated with uncontrolled C3 consumption in the spleen and elevated complement receptor 2 (CR2, also known as CD21) levels on the surface of mature splenic B cells. Moreover, aged *Cfh*$^{-/-}$ mice developed splenomegaly with distorted spleen architecture and spontaneous B cell-dependent autoimmunity characterized by germinal center hyperactivity and a marked increase in anti-double stranded DNA (dsDNA) antibodies. Taken together, our data indicate that CFH, through its function as a complement repressor, acts as a negative regulator of BCR signaling and limits autoimmunity.

Keywords: complement factor H, complement, autoimmunity, B cell development, B cell receptor signaling

OPEN ACCESS

Edited by:
Harry W. Schroeder, University of Alabama at Birmingham, United States

Reviewed by:
Lee Ann Garrett-Sinha, University at Buffalo, United States
Masaki Hikida, Akita University, Japan

***Correspondence:**
Christoph J. Binder
christoph.binder@meduniwien.ac.at

Specialty section:
This article was submitted to B Cell Biology, a section of the journal Frontiers in Immunology

Received: *11 March 2019*
Accepted: *27 June 2019*
Published: *11 July 2019*

Citation:
Kiss MG, Ozsvár-Kozma M, Porsch F, Göderle L, Papac-Miličević N, Bartolini-Gritti B, Tsiantoulas D, Pickering MC and Binder CJ (2019) Complement Factor H Modulates Splenic B Cell Development and Limits Autoantibody Production. Front. Immunol. 10:1607. doi: 10.3389/fimmu.2019.01607

INTRODUCTION

The complement system is a multiprotein cascade of innate immunity that is specialized in facilitating the clearance of invading pathogens and unwanted host material (1, 2). Furthermore, it has been long appreciated that besides its role in inflammation, complement also participates in regulating adaptive immunity (3), especially through the modulation of B cell responses (4, 5).

Given the complexity of its catalytic nature, the complement cascade is tightly controlled by a wide range of repressors which serve as checkpoints in complement activation both on the cellular surface as well as in the fluid phase (6). Uncontrolled complement activation resulting from defective regulation leads to the accumulation of cellular waste which does not only promote proinflammatory and cytolytic effects inducing host tissue damage but also contributes to the rise of autoimmune conditions as it is seen upon either C1q (7), C4 (8, 9), or CR2/CD21 (10–12) deficiencies in mice as well as in humans (13). Although the role of the classical complement has

been well-studied in B cell biology, little is known about how regulators of the alternative pathway affect B cell-mediated immunity.

Complement factor H (CFH) is the master regulator of alternative complement activation. It accelerates the decay of the C3 convertase C3bBb thereby inhibiting the proteolytic cleavage of C3 (14). As one of the most abundant proteins in both human and rodent plasma (100–500 μg/ml), CFH exerts its complement-regulatory effects promptly in the fluid phase. Moreover, it regulates complement on cell surfaces by promoting Factor I-mediated inactivation of C3b into anti-inflammatory iC3b (15). Mice deficient in CFH with no detectable plasma CFH exhibit secondary C3 deficiency due to the constant consumption of circulating C3. Consequently, they develop spontaneous membranoproliferative glomerulonephritis (MPGN) with extensive complement and immune complex deposition on glomeruli (16). Accordingly, renal diseases have been reported in 28 out of 33 individuals with inherited complete deficiency of CFH (17). The pathologic effect has been shown to be dependent on the dysregulation of the alternative complement pathway as additional deletion of complement factor B (FB), which prevents C3 turnover, rescues the phenotype of CFH deficiency.

A recent study that aimed to investigate the contribution of humoral immunity to the development of glomerulopathy employed CFH deficiency as a model for MPGN and showed that $Cfh^{-/-}$ mice lacking B cells (backcrossed on the B cell-deficient μMT background) were protected from progressive glomerular disease (18). The authors proposed that antibodies with specificity to certain neo-epitopes exposed on damaged glomeruli exacerbate disease progression, in part by inducing local complement activation. However, it still remains unknown whether the protective effect of B cell deficiency in this model is indirectly linked to CFH deficiency or whether CFH has the capacity to attenuate autoimmunity by directly modulating B cell responsiveness.

Therefore, we characterized B cell immunity in $Cfh^{-/-}$ mice and found that in the absence of CFH, splenic B cells exhibit enhanced BCR signaling accompanied by abnormal B cell development. Loss of CFH leads to uncontrolled systemic complement activation which results in increased exposure to activated C3 fragments in the spleen associated with elevated surface levels of CD21 on mature B cells. Aged $Cfh^{-/-}$ mice spontaneously develop autoimmunity as judged by germinal center hyperactivity and robust titers of dsDNA-specific immunoglobulins. Our findings provide a novel role for CFH in directly calibrating B cell responsiveness and limiting autoimmunity.

MATERIALS AND METHODS

Mice

$Cfh^{-/-}$ mice on a C57BL/6 background were generated by Pickering et al. (16) and were bred in our in-house breeding facility. All experiments were performed with age- and sex-matched mice. Experiments were performed with mice between 9 and 11 weeks of age or 28 and 30 weeks of age, where stated. For the bone marrow transplantation study, 8 week-old C57BL/6 mice were lethally irradiated (2 × 6Gy) and were transplanted with 3 × 10^6 $Cfh^{+/+}$ or $Cfh^{-/-}$ bone marrow from 6 week-old donors. The recipient mice were sacrificed after 10 weeks of recovery period. Successful bone marrow reconstitution was verified by extracting and amplifying genomic DNA from the bone marrow of the recipient mice (**Supplementary Figure 9**). All experimental studies were approved by the Animal Ethics Committee of the Medical University of Vienna, Austria and were performed according to the guidelines for Good Scientific Practice of the Medical University of Vienna, Austria.

Primary Cell Isolation and Flow Cytometry

Spleens were mechanically dissociated through a 100 μm cell strainer (BD Biosciences) and red blood cells were lysed in red blood cell lysis buffer (Morphisto). Peripheral blood was collected via the vena cava and red blood cells were lysed in red blood cell lysis buffer. Bone marrow cell suspensions were isolated by flushing femurs and tibiae through a 26-gauge needle with 1% FCS in DPBS (Sigma) and red blood cells were lysed as stated above. Total viable cells were counted manually using a hemocytometer or by CASY cell counter & analyzer. For flow cytometric staining, 1 × 10^6 cells were added in a 96-well V-bottom plate (Thermo Scientific) and incubated with 2.5 μg/ml of a blocking anti-CD16/32 antibody (Clone 90, eBioscience) or anti-CD16/32 APC (Clone 90, eBioscience) diluted in DPBS (Sigma) supplemented with 1% FCS for 20 min at 4°C. After two washing steps, cells were stained with the following monoclonal antibodies: anti-CD45R (B220) PerCP-Cy5.5 (clone RA3-6B2, eBioscience), anti-CD43 PE (clone S7, BD Biosciences), anti-CD23 eFluor450 (clone B3B4, BD Biosciences), anti-CD21/35 BV605 (clone 7G6, BD Biosciences), anti-IgM APC (clone II/41, eBioscience) anti-IgD PE-Cy7 (clone 11-26C, eBioscience), anti-CD11b AlexaFluor700 (clone M1/70, eBioscience), anti-Ly6C BV605 (clone HK1.4, BioLegend), anti-.Ly6G PE (clone 1A8, BioLegend), anti-F4/80 PerCP-Cy5.5 (clone BM8, BioLegend), anti-CD11c APC-eFluor780 (clone N418, eBioscience), anti-CD19 APC (clone eBio1D3, eBioscience), anti-Igκ FITC (clone 197.1, BD Biosciences), biotinylated anti-Igλ. (clone RML-42, BioLegend), biotinylated anti-CD138 (clone 281-2, BioLegend), anti-GL7 eFluor450 (clone GL-7, eBioscience), biotinylated anti-CD21/35 (clone 7E9, BioLegend), anti-CD3e PE (clone 145-2C11, eBioscience), anti-CD4 FITC (clone GK1.5, eBioscience), anti-CD8a APC (clone 53-6.7; eBioscience), anti-CD185 (CXCR5) APC (clone SPRCL5, BD Biosciences), anti-CD279 (PD-1) (clone J43, eBioscience), mouse hematopoietic lineage antibody cocktail FITC (17A2, eBioscience), anti-CD117 (c-kit) APC-eFluor 780 (clone 2B8, eBioscience), anti-Sca1 (Ly6A/E) PE-Cy7 (clone D7, eBioscience), anti-CD34 eFluor450 (clone RAM34, eBioscience), anti-CD127 (IL7-R) PE (clone A7R34, eBioscience), anti-CD135 (Flt3) APC-eFluor 710 (clone A2F10, eBioscience), anti-C3b/iC3b,/C3c FITC (clone 3/26, Hycult), anti CD22 APC (clone OX-97, BioLegend), anti-Siglec G APC (clone SH2.1, eBioscience), anti MHCII AlexaFluor700 (clone M5/114.15.2, eBioscience), and streptavidin APC-eFluor 780 (eBioscience).

To determine the amount of intracellular Blimp-1, CD21 and of phosphorylated kinases pBtk and pSyk, cells were fixed and permeabilized with fixation and permeabilization solution (eBioscience) for 20 min at 4°C and then stained intracellularly in permeabilization buffer (eBioscience) with the following antibodies: anti-Blimp-1 Alexa Fluor 647 (clone 5E7; BD Biosciences), anti-CD21/35 PerCP-Cy5.5 (clone 7E9, BioLegend), pBTK/ITK (Y551/Y511) APC (clone M4G3LN; eBiosciences) and pSYK (Y348) APC (clone moch1ct, eBiosciences). Specificity of the intracellular staining was confirmed using Alexa Fluor 647-conjugated isotype controls (**Supplementary Figure 10**) including rat IgG2a kappa Alexa Fluor 647 (clone cBR2a, eBioscience), mouse IgG2b kappa Alexa Fluor 647 (clone MPC-11, BioLegend) and mouse IgG1 kappa Alexa Fluor 647 (clone P3.6.2.8.1, eBioscience). All stainings were carried out in DPBS (Sigma) supplemented with 1% FCS for 30 min at 4°C, followed by two washing steps. Finally, to identify dead cells staining with 7-AAD viability solution (eBiosciences) was performed. Data were acquired on a LSRII Fortessa (BD Biosciences, Billerica, MA, USA) and were analyzed using FlowJo software 10 (Tree Star, Ashland, OR, USA).

Antibody Measurements

Anti-dsDNA antibodies were measured as following: 96-well Nunc MaxiSorp plates (Thermo Scientific) were irradiated under UV light for 1 h and then coated with calf thymus DNA (5 μg/ml, Invitrogen) in DPBS. After overnight incubation at 4°C, plates were blocked in 1% BSA in DPBS and incubated in a wet chamber for 1 h at room temperature. Plasma samples were added at 1:80 (IgM) or 1:200 (IgG) dilutions and incubated for 2 h at 37°C. For detection, biotinylated rat anti-mouse IgM (1:2000, BD Pharmingen) or HRP-conjugated anti-mouse IgG (1:1000, GE Healthcare) was added and incubated for 1 h at 37°C. For anti-dsDNA IgM measurements, streptavidin-HRP (R&D Systems) was added in a 1:200 dilution for 30 min at 37°C. Samples were developed using TMB substrate solution according to the manufacturer's instructions. The reaction was stopped with 1M H_2SO_4 (Honeywell) and the absorbance was measured with a plate reader at 450 nm as the primary wavelength.

Total IgM, IgG1, IgG2b, IgG2c, IgG3, and IgA levels were measured by a chemiluminescence-based sandwich ELISA as described previously (19). IgE levels were determined using a mouse IgE-specific ELISA (BioLegend). MDA-LDL was prepared as described previously (19). Antigen-specific antibody titers were measured by chemiluminescent ELISA as previously described (20).

C3 Consumption Measurements

To measure extracellular concentrations of complement components, the spleens were mechanically dissociated through a 100 μm cell strainer (BD Biosciences) and spun down at 400 g for 5 min. The supernatant was collected and C3 and C3a levels were determined using a mouse C3 ELISA kit (Abcam) and a mouse C3a ELISA kit (MyBioSource) according to the manufacturers' instructions. As a measure of C3 consumption, C3a/C3 ratio was calculated based on total C3a concentrations divided by the total C3 levels of each individual sample. Total protein content of the samples was quantified using Pearce BCA Protein Assay Kit (Thermo Fisher Scientific).

Gene Expression Analysis

Total RNA was isolated from mouse spleen tissue using the RNeasy Mini Kit (PeqLab) and 500 ng of total RNA was reversely transcribed using the High Capacity cDNA Reverse Transcription kit (Applied Biosystems). Quantitative real-time PCR was performed using Kapa SYBR Fast Bio-Rad iCycler with ROX dye (Kapa Biosystems) in a CFX96 Real-time System (Bio-Rad Laboratories). All data were normalized to the housekeeping gene Cyclin B1 (CycB1). Values are expressed as the relative expression compared to the control group.

Primer Sequences

mm CycB1-forward: 5′-CAGCAAGTTCCATCGTGTCATCA-3′
mm CycB1-reverse: 5′-GGAAGCGCTCACCATAGATGCTC-3′
mm *C3*-forward: 5′-AGAAAGGGATCTGTGTGGCA-3′
mm *C3*-reverse: 5′- GAAGTAGCGATTCTTGGCGG-3′

For *Cd21* expression measurements, untouched B2 cells from $Cfh^{+/+}$ and $Cfh^{-/-}$ mice were purified with a B cell isolation kit (Miltenyi) and total RNA was isolated as stated above.

Primer Sequences

mm *Cd21*-forward: 5′-CCTCTAACTCATTGCCCCGA-3′
mm *Cd21*-reverse: 5′-AGGAAGCCTTGGTAGCAACT-3′

Tissue Preparation

Spleens and kidneys were fixed in 10% (v/v) normal buffered formalin, then dehydrated via a Tissue Processor (Leica, TP1020) and embedded in paraffin (Leica, EG1150H). Two micrometer sections were cut (Microm HM335E) and stained with a hematoxylin (Mayer's hematoxylin; Applichem, APC2-254766.1611) and eosin (Eosin Y solution; Sigma, HT110132-1L) stain. Kidneys were also stained with periodic acid (3%, Morphisto, 11839.00500) and Schiff's reagent (Carl Roth, X900.1). Images were taken with Axio Imager A1 from Zeiss.

Phosphorylated CD19 Staining

Spleen sections were stained for phosphorylated CD19 using an anti-CD19 (phospho Y531) antibody (1:200) by Abcam (ab203615) according to the manufacturers' instructions. Rabbit polyclonal IgG-ChIP Grade (ab27478) was used as isotype control. Biotinylated goat anti-rabbit IgG (H+L) by Vector (BA-1000) was used as a secondary antibody, followed by incubation with streptavidin-peroxidase polymer (Sigma-Aldrich, S2438) and detection with Liquid DAB Substrate (DAKO K3466). Hematoxylin (Mayer's hematoxylin; Applichem, APC2-254766.1611) was applied as counterstain. Images were taken with Axio Imager A1 from Zeiss.

Scoring of Spleen Architecture

Marginal zone morphology was evaluated as described by Birjandi et al. (21). Shortly, four well-separable white pulp areas were selected from each mouse and the architecture of the marginal zone (MZ) was scored based on two main parameters, the interface distortion and the percent of radius involvement per white pulp area on a scale ranging from 0 to 8 (0—most severe

distortions, 8—intact). Data shown are the average score of all white pulp areas per each mouse.

TUNEL Staining

Spleen sections were stained for TUNEL positivity using an *In Situ* Cell Death Detection Kit, TMR Red by Roche (12156792910) according to the manufacturers' instructions. At least three well-oriented white pulp areas were chosen from each mouse and the number of TUNEL$^+$ cells in the MZ area was determined. Data shown are the average score of all white pulp areas per each mouse. Images were taken with Axio Imager A1 from Zeiss.

Statistical Analysis

Statistical analyses were performed using Graph Pad Prism 7.03 for Windows (Graph Pad Software). Experimental groups were compared using two tailed Student's unpaired or paired *t*-test or Mann-Whitney U test as appropriate. Data are presented as mean ± SEM. A p-value of <0.05 was considered significant.

RESULTS

Complement Factor H Deficiency Results in Abnormal Splenic B2 Cell Development

Immunophenotypic characterization of *Cfh*$^{-/-}$ mice revealed that loss of complement factor H leads to markedly elevated counts of splenic CD21$^+$ CD23$^-$ and marginal zone (MZ) B cells (**Figures 1A,C**). We found no difference in the numbers of B-1 cells (**Figure 1B**), newly formed (NF) and transitional stage (T1) B2 cells (**Figure 1C**) between *Cfh*$^{+/+}$ and *Cfh*$^{-/-}$ mice. Moreover, CFH deficiency did not affect the numbers (**Supplementary Figure 1A**) or the kappa/lambda light chain ratio (**Supplementary Figure 1B**) of immature B cells in the bone marrow, suggesting that CFH impacts predominately the splenic B cell developmental process. Consistent with this, exclusion of transitional B220$^+$ CD93$^+$ B cells had no effect on the increased numbers of CD21$^+$ CD23$^-$ B cell found in CFH deficient animals (**Figure 1D**), which suggests an accumulation of mature B2 cells at this developmental stage in the spleen. Although the number of splenic FO/T2 B cells was unchanged in *Cfh*$^{-/-}$ mice (**Figure 1C**), they exhibited decreased surface expression of CD23 (**Figure 1E**). Similarly, reduced CD23 levels were found on circulating mature B cells in the blood as well as in the bone marrow (**Supplementary Figures 1D,F**, respectively), while the numbers were unaffected (**Supplementary Figures 1C,E**). Blimp1 has been shown to repress CD23 expression in FO B cells (22). In line with this, we detected increased Blimp-1 levels in CD21$^+$ CD23$^-$ B cells of Cfh$^{-/-}$ mice (**Figure 1F**). Together, these data indicate that CFH deficiency leads to an accumulation of mature splenic CD21$^+$CD23$^-$ B cells favoring MZ rather than follicular B cell commitment. Altered splenic B2 cell development in *Cfh*$^{-/-}$ mice had no major effect on total plasma immunoglobulin levels besides a reduction in IgG2c titers (**Supplementary Figure 2A**) which may be explained by an impaired antigen presentation capacity of splenic B cells due to decreased surface MHCII expression (**Supplementary Figure 2B**). We also found decreased IgM and IgG antibody levels against MDA-LDL in *Cfh*$^{-/-}$ mice (**Supplementary Figure 2C**), which can be indicative of increased consumption of MDA-specific immunoglobulins in the absence of the MDA-neutralizing function of CFH (23). In contrast, PC-BSA-specific antibody levels were not different (**Supplementary Figure 2D**).

Complement Factor H Deficiency Leads to Increased B Cell Receptor Signaling

The major driver of B2 cell differentiation toward MZ or FO cell fate is the strength of the BCR signaling (24, 25). B cell receptor (BCR) stimulation leads to the activation of downstream SRC family kinases, such as Bruton's tyrosine kinase (Btk) and spleen tyrosine kinase (Syk), which both have been reported to be crucial players in antigen-receptor signaling and B cell fate decision between MZ and FO B cells (26, 27). Therefore, to study the influence of CFH deficiency on BCR signaling, we chose to quantify phosphorylated Syk and Btk levels of splenic B cell subsets in *Cfh*$^{+/+}$ and *Cfh*$^{-/-}$ mice using a flow cytometry-based approach. First, we confirmed previous findings by our lab and others (24, 28, 29) that strong BCR signaling promotes MZ over FO B cell differentiation, as MZ B cells showed higher phosphorylated Btk levels compared to FO/T2 B cells of *Cfh*$^{+/+}$ mice (FO/T2 B cells, MFI $= 2206 \pm 113$; MZ B cells MFI $= 4783 \pm 310$, $p < 0.0001$). Moreover, we found that both MZ and FO/T2 B cells display elevated levels of phosphorylated Btk and Syk in *Cfh*$^{-/-}$ mice compared to control mice (**Figures 2A,B**), which could provide an explanation for the accumulation of MZ B cells as a result of CFH deficiency. Increased tyrosine kinase activation was also detected in CD21$^+$ CD23$^-$ B cells as well as in B-1 cells of *Cfh*$^{-/-}$ mice (**Figures 2A,B**). Importantly, NF and T1 cells, which require tonic BCR signaling for their survival, showed no difference in pSyk and pBtk levels between *Cfh*$^{+/+}$ and *Cfh*$^{-/-}$ mice (**Supplementary Figures 3A,B**). Taken together, mature splenic B cells exhibit heightened BCR signaling as a consequence of CFH deficiency which can contribute to the expansion of MZ B cells at the expense of appropriate FO B cell development.

Increased BCR Signaling Is Associated With Dysregulated Splenic Complement Activation Upon Complement Factor H Deficiency

BCR activation is tightly controlled by a variety of co-receptors, which can either inhibit or amplify BCR signaling strength. Therefore, we hypothesized that the effect of CFH deficiency on BCR signaling can be due to altered expression of inhibitory and stimulatory co-receptor signaling. There was no difference in surface levels of the main BCR repressors CD22 and Siglec G on B cells of *Cfh*$^{+/+}$ and *Cfh*$^{-/-}$ mice and similar data were obtained for the positive regulator CD19 (**Figure 3A**). However, we found significantly higher levels of the co-stimulatory molecule CD21 on the surface of total splenic B cells in *Cfh*$^{-/-}$ mice (**Figure 3A**), which was found on all mature splenic B cell subsets (**Figure 3B**). In line with this, mature B cells in the blood as well as in the bone marrow also displayed higher CD21 expression upon

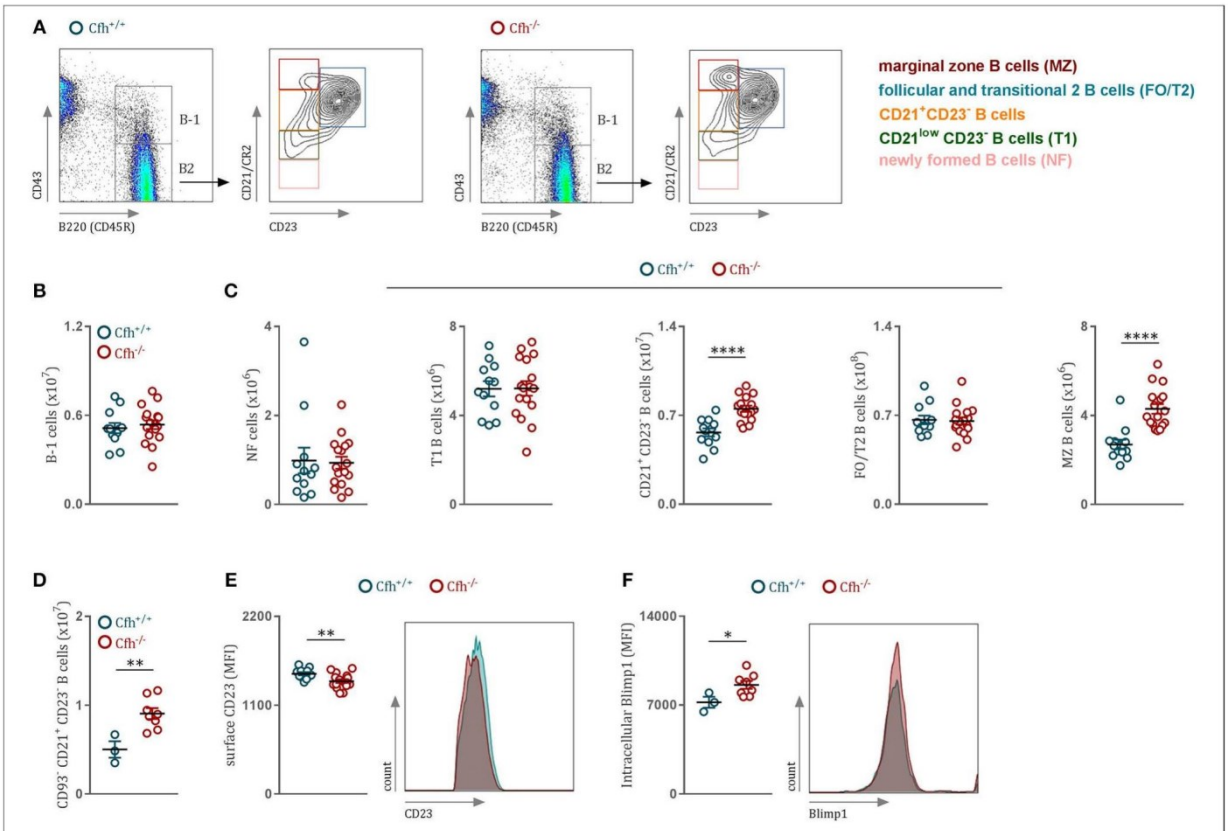

FIGURE 1 | CFH deficiency results in altered splenic B cell development. **(A)** Representative flow cytometry plots showing the gating strategy for B cells in both *Cfh*$^{+/+}$ and *Cfh*$^{-/-}$ mice. **(B)** Absolute numbers of splenic B220^{+}CD43^{+} B-1 cells and **(C)** splenic B2 cells in *Cfh*$^{+/+}$ (blue dots) and *Cfh*$^{-/-}$ (red dots) mice assessed by flow cytometry. **(D)** Absolute numbers of splenic B220^{+}CD43^{-}CD93^{-}CD21^{+}CD23^{-} B cells of *Cfh*$^{+/+}$ (blue dots) and *Cfh*$^{-/-}$ (red dots) mice analyzed by flow cytometry. **(E)** CD23 mean fluorescence intensity of FO/T2 B cells and **(F)** intracellular Blimp1 mean fluorescence intensity (MFI) of CD21^{+}CD23^{-} B cells of *Cfh*$^{+/+}$ (blue dots) and *Cfh*$^{-/-}$ (red dots) mice quantified by flow cytometry. Data shown are pooled from six independent experiments. All results show mean ± SEM, each symbol represents an individual mouse, $^{*}p < 0.05$, $^{**}p < 0.01$, $^{****}p < 0.0001$ (unpaired *t*-test).

CFH deficiency (**Supplementary Figures 4A,B**). The effect was not due to altered transcriptional regulation as *Cd21* mRNA expression was comparable in sorted splenic B cells from *Cfh*$^{+/+}$ and *Cfh*$^{-/-}$ mice (**Figure 3C**). In agreement with the latter, splenic B cell subsets of *Cfh*$^{-/-}$ mice showed no difference in intracellular CD21 levels (**Supplementary Figure 4C**). These findings suggest that increased BCR signaling upon loss of CFH can be in part mediated by enhanced surface CD21 signaling.

CD21 is a member of the B cell co-receptor complex and recognizes active cleavage products of complement component 3 (C3), such as iC3b and C3d (30). C3d acts as a molecular adjuvant in B cell response as interaction of antigen-coupled C3d with CD21 can substantially lower the threshold for BCR activation (31) in a CD19-dependent manner (32). Accordingly, we detected increased phosphorylated CD19 staining in spleen sections of *Cfh*$^{-/-}$ mice compared to littermate controls (**Figure 3D**). Heightened levels of surface CD21 on splenic B cells can be indicative of complement dysregulation in the spleen. In order to test this, we aimed to characterize local complement activation in the spleen of *Cfh*$^{+/+}$ and *Cfh*$^{-/-}$ mice. We found that spleen of CFH deficient mice contained less extracellular C3 compared to controls (**Figure 3E**). This was not due to reduced production of C3 by splenocytes (**Supplementary Figure 5**), but a result of enhanced C3 consumption as demonstrated by a higher C3a/C3 ratio in the spleen of CFH deficient mice (**Figure 3F**). Consistent with this, increased levels of activated C3b/iC3b/C3c fragments could be detected on the surface of splenocytes derived from *Cfh*$^{-/-}$ mice (**Figure 3G**). These data show that absence of CFH leads to uncontrolled complement activation in the spleen.

In order to further elucidate whether the influence of CFH on B cell activation is dependent on its systemic complement regulatory function and is not due to a B cell intrinsic effect, we performed a bone marrow transplantation study in which we transplanted lethally irradiated C57BL/6 mice with *Cfh*$^{+/+}$ or *Cfh*$^{-/-}$ bone marrow. Loss of hematopoietic CFH did not result

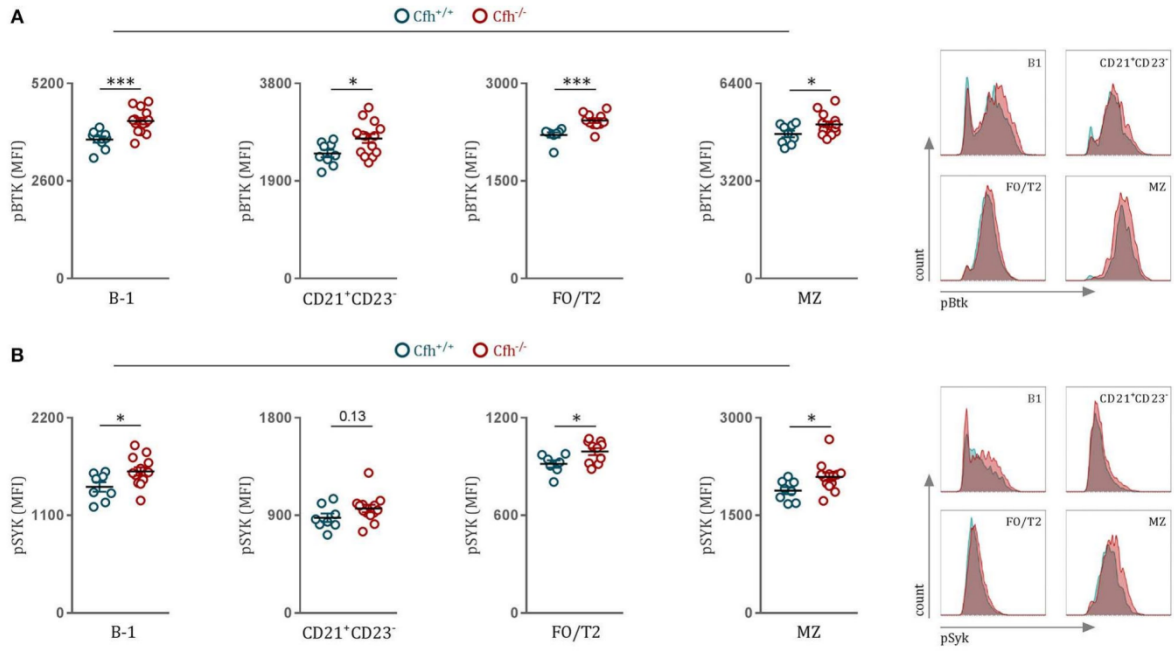

FIGURE 2 | CFH deficiency leads to heightened B cell receptor signaling *in vivo*. **(A,B)** Dot plots and representative flow cytometry plots show the MFI for **(A)** pBTK and **(B)** pSYK levels of B-1, CD21^{+}CD23^{-}, FO/T2, and MZ B cells (as defined in **Figure 1A**) of *Cfh*$^{+/+}$ (blue dots) and *Cfh*$^{-/-}$ (red dots) mice. Data shown are pooled from four independent experiments. All results show mean ± SEM, each symbol represents an individual mouse, $^{*}p < 0.05$, $^{***}p < 0.001$ (unpaired *t*-test).

in systemic complement activation as indicated by comparable plasma C3 and C3a levels (**Supplementary Figures 6A,B**). Moreover, hematopoietic CFH deficiency did not lead to an expansion of MZ B cells (**Supplementary Figure 6C**) and had no effect on surface CD21/CR2 levels of mature B cells (**Supplementary Figure 6D**). Consistent with this, intracellular levels of phosphorylated Btk and Syk were unchanged between the two groups (**Supplementary Figures 6E,F**). These data provide strong evidence, that CFH modulates splenic B cell activation and maturation through its systemic complement regulatory activity.

Complement Factor H Deficient Mice Develop Germinal Center Hyperactivity With Robust Autoantibody Titers

Growing evidence suggests that even modest discrepancies in BCR signaling can promote autoreactivity in the naïve B cell repertoire and predispose to autoimmunity (33). As we found that CFH deficiency results in enhanced B cell activation, we hypothesized that *Cfh*$^{-/-}$ mice develop spontaneous B cell-dependent autoimmune phenotype over time. Indeed, 8 month-old *Cfh*$^{-/-}$ mice presented with splenomegaly (**Figure 4A**) associated with an increase in dying splenocytes (**Figure 4B**) compared to age-matched controls. Moreover, CFH deficiency caused severe morphological disruption of the splenic architecture. While spleens of aged *Cfh*$^{+/+}$ mice showed a well-organized white pulp with easily separable marginal zone and lymphoid follicle area, the MZ area of *Cfh*$^{-/-}$ mice were diffuse, poorly discernable, displayed a high degree of distortion (**Figure 4C**) and contained increased numbers of TUNEL^{+} cells (**Figure 4D**). The accumulation of dying cells in *Cfh*$^{-/-}$ mice was accompanied by increased splenic inflammatory cell counts including neutrophils, Ly6C^{high} monocytes, Ly6C^{low} monocytes and subsets of macrophages and dendritic cells (**Supplementary Figure 7A**). This was a consequence of excessive extramedullary hematopoiesis in the spleen (**Supplementary Figure 7B**) which also led to elevated numbers of inflammatory cells in the periphery (**Supplementary Figure 7C**).

Importantly, splenic B cells of *Cfh*$^{-/-}$ mice displayed a decreased kappa to lambda chain ratio (**Figure 4E** and **Supplementary Figure 8**), suggesting an altered BCR repertoire. Because mature—but not immature—bone marrow B cells of *Cfh*$^{-/-}$ mice showed the same alterations in kappa to lambda ratio as splenic B cells (**Figure 4F**), we again concluded that the effect is not due to altered BCR editing in the bone marrow, but specific to splenic maturation. The persistence of autoantigens derived from apoptotic material combined with dysregulated BCR signaling can promote germinal center hyperactivity (34). Moreover, autoreactive B cells have the ability to coordinate the expansion of cognate follicular helper T cells to further orchestrate spontaneous germinal center formation. Consistent

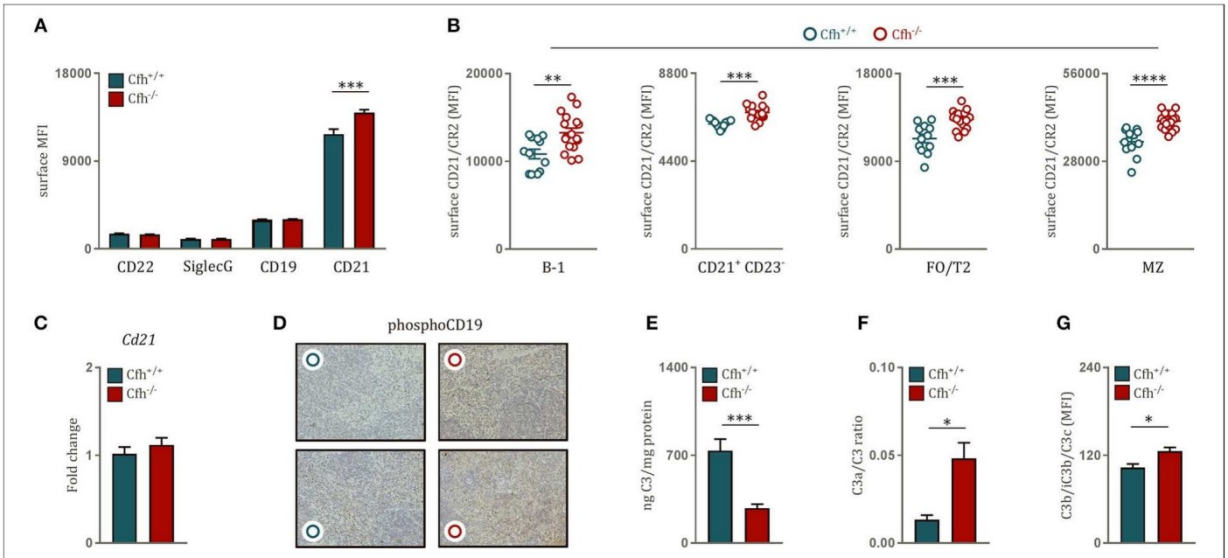

FIGURE 3 | Increased B cell receptor signaling is associated with uncontrolled splenic complement activation upon CFH deficiency. **(A)** Bar graphs showing the MFI of CD22, SiglecG, CD19 and CD21 levels on the surface of B220$^+$ B cells of *Cfh*$^{+/+}$ (blue bar) and *Cfh*$^{-/-}$ (red bar) mice measured by flow cytometry. **(B)** Dot plots demonstrating the MFI of surface CD21 levels on B-1, CD21$^+$CD23$^-$, FO/T2, and MZ B cells (as defined in **Figure 1A**) of *Cfh*$^{+/+}$ (blue dots) and *Cfh*$^{-/-}$ (red dots) mice analyzed by flow cytometry. **(C)** Relative gene expression of *Cd21* normalized to *CycB1* expression in sorted splenic B2 cells of *Cfh*$^{+/+}$ (blue bar) and *Cfh*$^{-/-}$ (red bar) mice assessed by quantitative PCR. **(D)** Representative images show phosphorylated (Y531) CD19 staining of splenic sections from *Cfh*$^{+/+}$ (blue dots) and *Cfh*$^{-/-}$ (red dots) mice. **(E)** Bar graphs showing total splenic C3 levels of *Cfh*$^{+/+}$ (blue) and *Cfh*$^{-/-}$ (red) mice measured by quantitative C3 ELISA in spleen homogenates. **(F)** C3a/C3 ratio, a measure of complement activation determined by total splenic C3a and C3 levels by quantitative ELISAs. **(G)** Deposition of C3 cleavage products (C3b/iC3b/C3c) on the surface of splenocytes of *Cfh*$^{+/+}$ (blue bar) and *Cfh*$^{-/-}$(red bar) mice analyzed by flow cytometry, shown as MFI. Data shown are pooled from four independent experiments. All results show mean ± SEM, each symbol represents an individual mouse, $^*p < 0.05$, $^{**}p < 0.01$, $^{***}p < 0.001$, $^{****}p < 0.0001$ (unpaired *t*-test).

with this, *Cfh*$^{-/-}$ mice had elevated numbers of germinal center B cells (**Figure 4G**) as well as follicular helper T cells (**Figure 4H**) compared to controls. Furthermore, we found increased numbers of plasma cells and plasmablasts both in the spleen (**Figure 4I**) as well as in the lymph nodes (**Figure 4J**) of *Cfh*$^{-/-}$ mice, indicative of heightened germinal center activity. In order to test whether the generated plasma cells are autoreactive, we measured anti-dsDNA IgG titers in the plasma of *Cfh*$^{+/+}$ and *Cfh*$^{-/-}$ mice. CFH deficiency resulted in markedly increased levels of dsDNA-specific autoantibodies (**Figures 4K,L**).

Notably, even in 10 week-old *Cfh*$^{-/-}$ mice increased anti-dsDNA IgG antibodies could be detected (**Supplementary Figure 7G**) while extramedullary hematopoiesis (**Supplementary Figure 7E**) as well as splenic and peripheral inflammatory cell counts were unaffected (**Supplementary Figures 7D,F**) and no overt signs of glomerulonephritis were observed (**Supplementary Figure 7H**). Thus, CFH deficiency promotes B cell autoimmunity and this precedes chronic inflammation and the development of glomerulonephritis in *Cfh*$^{-/-}$ mice.

DISCUSSION

CFH deficiency causes uncontrolled complement activation characterized by the continuous cleavage of newly generated C3. Active C3 fragments are crucial mediators of adaptive immune responses. However, whether CFH directly impacts B cells and humoral immunity remains unknown. Here, we demonstrate that CFH deficiency results in heightened BCR signaling which affects splenic B cell development and leads to B cell-dependent autoimmunity with increased levels of dsDNA autoantibodies.

Genetic variants in CFH and CFH-related proteins (CFHRs) have been associated with systemic lupus erythematosus (SLE) development (35). Furthermore, patients with circulating IgG autoantibodies against CFH, which have been shown to inactivate the repressor function of CFH, have increased serum anti-nuclear antibody (ANA) titers (36) and anti-CFH autoantibodies are found in patients positive for lupus anticoagulants (37). Additionally, experimental evidence showed that *Cfh*$^{-/-}$ mice backcrossed on the lupus-prone MRL-lpr background develop accelerated lupus nephritis (LN) which could recapitulate many symptoms of human LN including marked albuminuria and azotemia and resulted in increased mortality at 14 weeks of age (38). However, the exact mechanism behind the development of nephropathies upon CFH deficiency has not yet been addressed. Recently, evidence for a B cell-mediated pathological effect of CFH deficiency came from a study, in which *Cfh*$^{-/-}$ mice were crossed with mice lacking functional B cells (18). While aged *Cfh*$^{-/-}$ mice developed spontaneous renal disease with omnipresent deposition of complement components on the glomeruli, CFH deficient mice lacking B cells were protected

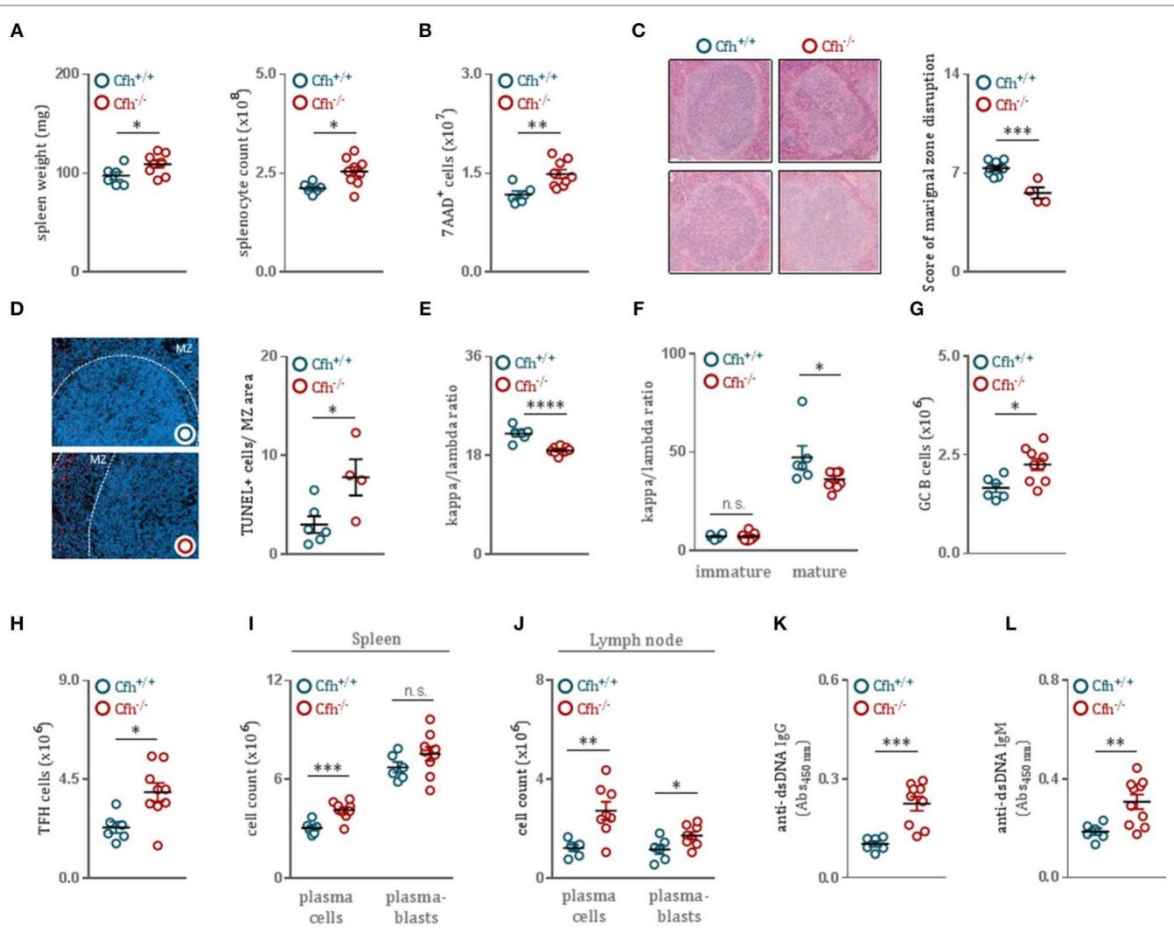

FIGURE 4 | CFH deficient mice develop germinal center hyperactivity with robust autoantibody titers. **(A)** Spleen weight and absolute splenocyte count of 8 month-old $Cfh^{+/+}$ (blue dots) and $Cfh^{-/-}$ (red dots) mice. **(B)** Total numbers of $7AAD^{+}$ dying splenocytes of $Cfh^{+/+}$ (blue dots) and $Cfh^{-/-}$ (red dots) mice, measured by flow cytometry. **(C)** Representative images demonstrating the white pulp architecture of 8 month-old $Cfh^{+/+}$ and $Cfh^{-/-}$ mice. Dot plots show the score of marginal zone disruption in the spleens of $Cfh^{+/+}$ (blue dots) and $Cfh^{-/-}$ (red dots) mice. **(D)** Representative images showing TUNEL staining of spleen sections from 8 month-old $Cfh^{+/+}$ and $Cfh^{-/-}$ mice. Dot plots indicate the average numbers of $TUNEL^{+}$ cells in the marginal zone area in the spleens of $Cfh^{+/+}$ (blue dots) and $Cfh^{-/-}$ (red dots) mice. Dot plots represent the kappa/lambda light chain ratio of **(E)** $IgD^{+}CD19^{+}CD43^{-}$ mature splenic B cells as well as **(F)** $B220^{hi}CD23^{+}CD43^{-}$ mature and $B220^{lo}CD23^{-}CD43^{-}$ immature splenic B cells of $Cfh^{+/+}$ (blue dots) and $Cfh^{-/-}$ (red dots) mice assessed by flow cytometry. Absolute numbers of (G) $GL\text{-}7^{+}B220^{+}$ germinal center B cells and **(H)** $CD3^{+}CD4^{+}CXCR5^{+}PD\text{-}1^{+}$ follicular helper T cells in the spleen of $Cfh^{+/+}$ (blue dots) and $Cfh^{-/-}$ (red dots) mice quantified by flow cytometry. **(I,J)** Quantification of $CD138^{+}B220^{-}$ plasma cells and $CD138^{+}B220^{+}$ plasmablasts in the spleen as well as in the lymph node of $Cfh^{+/+}$ (blue dots) and $Cfh^{-/-}$ (red dots) mice by flow cytometry. **(K)** IgG and **(L)** IgM titers specific for double stranded-DNA in the plasma of aged $Cfh^{+/+}$ (blue dots) and $Cfh^{-/-}$ (red dots) mice determined by ELISA. All results show mean ± SEM, each symbol represents an individual mouse, $^{*}p < 0.05$, $^{**}p < 0.01$, $^{***}p < 0.001$, $^{****}p < 0.0001$ (unpaired *t*-test).

from renal damage. In accordance with this, our data provide a direct link between CFH and B-cell dependent autoimmunity, as we found that CFH controls splenic C3 cleavage and modulates BCR signaling, thus contributing to physiological B cell development.

The strength of BCR signaling is the major determinant of the developmental fate of mature splenic B cells toward MZ or FO B cell maturation (25). Initially, BCR signaling strength was thought to be directly associated with FO B cell differentiation (39, 40). We and others have provided direct evidence that strong BCR signaling favors MZ B cell over FO cell development (24, 28, 29). Mice deficient in secreted IgM displayed increased MZ B cell and decreased FO B cell numbers and low-dose treatment of $sIgM^{-/-}$ mice with the Btk inhibitor Ibrutinib promoted differentiation of FO B cells while restricting MZ B cell formation. This is in accordance with our current report that enhanced BCR signaling in CFH deficient mice leads to the doubling of the MZ B cell pool, although other potential mechanisms independent of BCR signaling may also contribute to increased MZ B cell numbers. It is important to note that similar to mice with CFH

deficiency, $sIgM^{-/-}$ mice also develop high autoantibody titers and autoimmunity (41). The protective effect of secreted IgM is attributed to its ability to dampen self-antigen-induced BCR signaling (24). Sources of such self-antigens include cell debris, dying cells and microvesicles (42, 43). Similarly, CFH is able to bind immunogenic ligands such as MDA (23), DNA, histones and annexin-II (44) on the surface of apoptotic and necrotic cells and mediate their anti-inflammatory disposal. The importance of cell surface recognition by CFH is well-illustrated in a study showing that mice with a mutant CFH that lack its surface recognition domains (including an MDA-binding site) develop spontaneous kidney disease (45). While in this study we did not investigate whether CFH could neutralize MDA-induced stimulatory effects on B cell activation, we found that CFH deficient mice show decreased plasma levels of antibodies specific to MDA epitopes, likely due to increased consumption of MDA-reactive antibodies. Therefore, it is plausible that CFH might control B cell activation in part by sequestering self-antigens.

B cell activation is tightly modulated by accessory transmembrane molecules in the close proximity of the BCR (46). CD21 is part of the stimulatory BCR co-receptor complex and its differential expression defines the developmental stage of splenic B cells. It has been suggested that complement factor H-related protein 3 (CFHR3) binds C3d and can abrogate its interaction with CD21 thereby preventing the interaction of the BCR with the co-receptor complex on human B cells (47). Here, we identify CFH as a crucial modulator of surface CD21 expression on mature B cells in mice. While CD21 levels and the BCR signaling strength were comparable in immature B cells of $Cfh^{+/+}$ and $Cfh^{-/-}$ mice, we detected increased CD21 expression on the surface of mature B cells in the absence of CFH concurrent with heightened BCR signaling. CD21 binds active C3 cleavage products and we show that uncontrolled systemic C3 activation as a consequence of CFH deficiency also results in increased C3 activation in the spleen. Therefore, we propose that increased exposure to C3d-coated antigens initiates an amplification loop in B cell activation, which leads to increased CD21 surface levels further enhancing BCR signaling.

Inadequate BCR signaling can culminate in the escape and activation of autoreactive B cells by facilitating the formation of autoimmune germinal centers in lymphoid follicles (33, 48). Accordingly, autoantibody-secreting B cells derived from patients with SLE often display somatic hypermutation (49). Consistent with this, we found that CFH deficiency results in germinal center hyperactivity, elevated numbers of germinal center B cells and follicular helper T cells and an altered BCR repertoire. High levels of pathogenic autoantibodies secreted by autoreactive plasma cells are a hallmark of autoimmunity. Here we demonstrate that $Cfh^{-/-}$ mice have increased titers of anti-dsDNA immunoglobulins and develop systemic autoimmunity over time. In our hands, the presence of autoantibodies preceded the progression of glomerulonephritis as we could detect anti-dsDNA IgGs upon CFH deficiency as early as at 10 weeks of age while no apparent renal pathology could be seen between $Cfh^{+/+}$ and $Cfh^{-/-}$ mice at this age. The occurrence of autoantibodies was concurrent with heightened BCR signaling in $Cfh^{-/-}$ mice, thereby implicating the loss of B cell tolerance in the development of autoantibodies upon CFH deficiency. This is supported by studies showing that transgenic mice overexpressing Btk have increased circulating ANAs (50, 51) and develop a lupus-like disease. Therefore, it is tempting to speculate that treatment of $Cfh^{-/-}$ mice with Ibrutinib would reverse the adverse effects of CFH deficiency on germinal center hyperactivity and autoantibody production (52, 53).

In conclusion, we found that upon aging, $Cfh^{-/-}$ mice develop high titers of anti-dsDNA IgG antibodies and suffer from autoimmunity joint with chronic inflammation as a consequence of excessive hematopoiesis in the spleen. In the absence of CFH, uncontrolled complement activation results in heightened BCR signaling, altered splenic B cell development and germinal center hyperactivity leading to the expansion of autoreactive plasma cells. Our findings identify a previously undefined role for CFH in protecting from autoimmunity and chronic inflammation.

DATA AVAILABILITY

This manuscript contains previously unpublished data. The name of the repository and accession number are not available.

ETHICS STATEMENT

This study was carried out in accordance with the recommendations of the guidelines of Good Scientific Practice of the Medical University of Vienna (Austria). The protocol was approved by the Animal Ethics Committee of the Medical University of Vienna (Austria) 66.009/0132-WF/V/3b/2015.

AUTHOR CONTRIBUTIONS

MK conceived the project, designed and performed experiments, analyzed and interpreted the data, and wrote the manuscript. MO-K, FP, LG, NP-M, and BB-G performed experiments. DT critically revised and edited the manuscript. MP critically revised the manuscript and provided the $Cfh^{-/-}$ mice. CB conceived the project, designed experiments, interpreted the data, and wrote the manuscript.

FUNDING

This work was supported by fellowships of the doctoral program Cell Communication in Health and Disease (CCHD; to MK and FP) and by SFB Lipotox F30, both funded by the Austrian Science Fund.

ACKNOWLEDGMENTS

We are particularly thankful to Dr. Dávid Medgyesi for providing protocols and for helpful discussions, to Anastasiya Hladik for providing protocols and reagents and to Astrid Fabry for excellent technical support.

SUPPLEMENTARY MATERIAL

The Supplementary Material for this article can be found online at: https://www.frontiersin.org/articles/10.3389/fimmu.2019.01607/full#supplementary-material

Supplementary Figure 1 | CFH deficiency limits CD23 expression of circulating and bone marrow B cells without affecting their numbers. **(A)** Representative flow cytometry plots showing the gating strategy for B cells and dot plots demonstrating immature bone marrow B cell numbers in $Cfh^{+/+}$ (blue dots) and $Cfh^{-/-}$ (red dots) mice quantified by flow cytometry. **(B)** Bar graphs representing the kappa/lambda light chain ratio of immature B cells in the bone marrow of $Cfh^{+/+}$ (blue bar) and $Cfh^{-/-}$ (red bar) mice analyzed by flow cytometry. **(C)** Absolute numbers of mature bone marrow B cells and **(D)** their CD23 expression in $Cfh^{+/+}$ (blue dots) and $Cfh^{-/-}$ (red dots) mice measured by flow cytometry. **(E)** Representative flow cytometry plots showing the gating strategy for circulating $CD23^+$ B cells and dot plots indicating the count and **(F)** CD23 expression of $CD23^+$ B cells in $Cfh^{+/+}$ (blue dots) and $Cfh^{-/-}$ (red dots) mice quantified by flow cytometry. Data shown are pooled from two independent experiments. All results show mean ± SEM, each symbol represents an individual mouse, $*p < 0.05$, $**p < 0.01$ (unpaired *t*-test).

Supplementary Figure 2 | Immunoglobulin levels in $Cfh^{+/+}$ and $Cfh^{-/-}$ mice. **(A)** Quantification of total IgM, IgG1, IgG2b, IgG2c, IgG3, IgA, and IgE levels in the plasma of $Cfh^{+/+}$ (blue dots) and $Cfh^{-/-}$ (red dots) mice measured by quantitative ELISAs. **(B)** Dot plots demonstrate the MFI of surface MHCII levels on FO/T2 and MZ B cells (as defined in **Figure 1A**) of $Cfh^{+/+}$ (blue dots) and $Cfh^{-/-}$ (red dots) mice analyzed by flow cytometry. **(C)** MDA-LDL specific antibody levels (IgM, IgG1, IgG2b, IgG2c, and IgG3) and **(D)** PC-BSA specific antibody levels (IgM and IgG) in the plasma of $Cfh^{+/+}$ (blue dots) and $Cfh^{-/-}$ (red dots) mice determined by ELISA, shown as relative light unit (RLU)/100 ms. All results show mean ± SEM, each symbol represents an individual mouse, $*p < 0.05$, $**p < 0.01$ (unpaired *t*-test).

Supplementary Figure 3 | CFH deficiency does not influence BCR signaling of newly formed (NF) and T1 B cells in the spleen. **(A)** Dot plots show the mean fluorescence intensity (MFI) for **(A)** pBTK and **(B)** pSYK levels of NF and T1 B cells (as defined in **Figure 1A**) in $Cfh^{+/+}$ (blue dots) and $Cfh^{-/-}$ (red dots) mice. Data shown are pooled from four independent experiments. All results show mean ± SEM (unpaired *t*-test), each symbol represents an individual mouse.

Supplementary Figure 4 | Blood and bone marrow B cells display increased CD21 expression upon loss of CFH. **(A)** CD21 mean fluorescence intensity (MFI) of circulating $CD23^+$ B cells (as defined in **Supplementary Figure 1E**) and **(B)** mature bone marrow B cells (as defined in **Supplementary Figure 1A**) in $Cfh^{+/+}$ (blue dots) and $Cfh^{-/-}$ (red dots) mice analyzed by flow cytometry. **(C)** Intracellular CD21 levels (MFI) of B-1, $CD21^+CD23^-$, FO/T2 and MZ B cells (as defined in **Figure 1A**) of $Cfh^{+/+}$ (blue dots) and $Cfh^{-/-}$ (red dots) mice quantified by flow cytometry. Data shown are representative of three independent experiments. All results show mean ± SEM, $*p < 0.05$, $**p < 0.01$ (unpaired *t*-test), each symbol represents an individual mouse.

Supplementary Figure 5 | CFH does not alter splenic C3 production. Relative gene expression of *C3* normalized to *CycB1* expression in the spleen of $Cfh^{+/+}$ (blue bar) and $Cfh^{-/-}$ (red bar) mice assessed by quantitative PCR. Data shown are pooled from four independent experiments.

Supplementary Figure 6 | Hematopoietic deletion of CFH does not affect systemic complement activation, B cell signaling and maturation. **(A,B)** Dot plots showing total plasma **(A)** C3 and **(B)** C3a levels of C57BL/6 mice receiving $Cfh^{+/+}$ (blue) or $Cfh^{-/-}$ (red) bone marrow measured by quantitative ELISAs. **(C)** Absolute numbers of MZ B cells of C57BL/6 mice receiving $Cfh^{+/+}$ (blue) or $Cfh^{-/-}$ (red) bone marrow assessed by flow cytometry. **(D)** Dot plots demonstrating the MFI of surface CD21 levels on B-1, $CD21^+CD23^-$, FO/T2 and MZ B cells (as defined in **Figure 1A**) of C57BL/6 mice receiving $Cfh^{+/+}$ (blue) or $Cfh^{-/-}$ (red) bone marrow analyzed by flow cytometry. **(E,F)** Dot plots showing the MFI for **(E)** pBTK and **(F)** pSYK levels of B-1, $CD21^+CD23^-$, FO/T2, and MZ B cells (as defined in **Figure 1A**) of C57BL/6 mice transplanted with $Cfh^{+/+}$ (blue) or $Cfh^{-/-}$ (red) bone marrow measured by flow cytometry.

Supplementary Figure 7 | Autoantibody production precedes chronic inflammation and renal pathology in CFH deficient mice. **(A,D)** Absolute numbers of $CD11b^+Ly6C^+Ly6G^+$ neutrophils, $CD11b^+Ly6C^{hi}Ly6G^-$ monocytes, $CD11b^+Ly6C^{lo}Ly6G^-$ monocytes, $CD11b^-F4/80^+$ macrophages, $CD11b^+F4/80^+$ macrophages, $CD11b^-CD11c^+$ dendritic cells, and $CD11b^+CD11c^+$ dendritic cells in the spleen of **(A)** 8 month-old and **(D)** 10 week-old $Cfh^{+/+}$ (blue dots) and $Cfh^{-/-}$ (red dots) mice quantified by flow cytometry. **(B,E)** Absolute numbers of $Lin^-c\text{-}kit^+Sca\text{-}1^+$ LSKs and $Lin^-c\text{-}kit^+Sca\text{-}1^-CD34^+CD16/32^{hi}$ granulocyte-macrophage progenitors (GMP) in the spleen of **(B)** 8 month-old and **(E)** 10 week-old $Cfh^{+/+}$ (blue dots) and $Cfh^{-/-}$ (red dots) mice by flow cytometry. **(C,F)** Absolute numbers of $CD11b^+Ly6C^+Ly6G^+$ neutrophils, $CD11b^+Ly6C^{hi}Ly6G^-$ monocytes and $CD11b^+Ly6C^{lo}Ly6G^-$ monocytes in the peripheral blood of **(C)** 8 month-old and **(F)** 10 week-old $Cfh^{+/+}$ (blue dots) and $Cfh^{-/-}$ (red dots) mice analyzed by flow cytometry. **(G)** IgG titers specific for double stranded-DNA in the plasma of 10 week-old $Cfh^{+/+}$ (blue dots) and $Cfh^{-/-}$ (red dots) mice determined by ELISA. Data shown are pooled from four independent experiments. **(H)** Hematoxylin-eosin and Periodic acid-Schiff staining of kidney sections of 10 week-old $Cfh^{+/+}$ (blue dots) and $Cfh^{-/-}$ (red dots) mice, images are representative of 5 mice per group. All results show mean ± SEM, each symbol represents an individual mouse, $*p < 0.05$, $**p < 0.01$ (unpaired *t*-test).

Supplementary Figure 8 | CFH deficiency leads to decreased kappa to lambda chain ratio of both FO/T2 B cells and MZ B cells. Dot plots represent the kappa/lambda light chain ratio of FO/T2 and MZ B cells (as defined in **Figure 1A**) of $Cfh^{+/+}$ (blue dots) and $Cfh^{-/-}$ (red dots) mice assessed by flow cytometry. Results show mean ± SEM, each symbol represents an individual mouse, $*p < 0.05$ (unpaired *t*-test).

Supplementary Figure 9 | Successful bone marrow reconstitution. At time of sacrifice bone marrow cells were collected from recipient mice reconstituted with $Cfh^{+/+}$ and $Cfh^{-/-}$ donor cells and genomic DNA was extracted and amplified for the *Cfh* gene. Tail DNA from $Cfh^{+/+}$, $Cfh^{+/-}$ and $Cfh^{-/-}$ mice were used as positive and negative controls.

Supplementary Figure 10 | Isotype control staining of intracellular Blimp1, pBTK, and pSYK levels. Histograms show Blimp1 and isotype rat IgG2a kappa staining of $B220^+$ B cells as well as pBTK and isotype mouse IgG2b kappa and pSYK and isotype mouse IgG1 kappa staining of $B220^+CD43^-CD21^{hi}CD23^-$ marginal zone B cells of $Cfh^{+/+}$ (blue histograms) and $Cfh^{-/-}$ (red histograms) mice assessed by flow cytometry.

REFERENCES

1. Walport MJ. Complement. First of two parts. *N Engl J Med*. (2001) 344:1058–66. doi: 10.1056/NEJM200104053441406
2. Walport MJ. Complement. Second of two parts. *N Engl J Med*. (2001) 344:1140–4. doi: 10.1056/NEJM200104123441506
3. Carroll MC. The complement system in regulation of adaptive immunity. *Nat Immunol*. (2004) 5:981–6. doi: 10.1038/ni1113
4. Carroll MC. The complement system in B cell regulation. *Mol Immunol*. (2004) 41:141–6. doi: 10.1016/S0161-5890(04)00079-3
5. Carroll MC, Isenman DE. Regulation of humoral immunity by complement. *Immunity*. (2012) 37:199–207. doi: 10.1016/j.immuni.2012.08.002
6. Zipfel PF, Skerka C. Complement regulators and inhibitory proteins. *Nat Rev Immunol*. (2009) 9:729–40. doi: 10.1038/nri2620
7. Botto M, Dell'Agnola C, Bygrave AE, Thompson EM, Cook HT, Petry F, et al. Homozygous C1q deficiency causes glomerulonephritis associated with multiple apoptotic bodies. *Nat Genet*. (1998) 19:56–9. doi: 10.1038/ng0598-56
8. Paul E, Pozdnyakova OO, Mitchell E, Carroll MC. Anti-DNA autoreactivity in C4-deficient mice. *Eur J Immunol*. (2002) 32:2672–9. doi: 10.1002/1521-4141(200209)32:9<2672::AID-IMMU2672>3.0.CO;2-X

9. Chen Z, Koralov SB, Kelsoe G. Complement C4 inhibits systemic autoimmunity through a mechanism independent of complement receptors CR1 and CR2. *J Exp Med*. (2000) 192:1339–52. doi: 10.1084/jem.192.9.1339
10. Prodeus AP, Goerg S, Shen LM, Pozdnyakova OO, Chu L, Alicot EM, et al. A critical role for complement in maintenance of self-tolerance. *Immunity*. (1998) 9:721–31. doi: 10.1016/S1074-7613(00)80669-X
11. Wu X, Jiang N, Deppong C, Singh J, Dolecki G, Mao D, et al. A role for the Cr2 gene in modifying autoantibody production in systemic lupus erythematosus. *J Immunol*. (2002) 169:1587–92. doi: 10.4049/jimmunol.169.3.1587
12. Boackle SA, Holers VM, Chen X, Szakonyi G, Karp DR, Wakeland EK, et al. Cr2, a candidate gene in the murine Sle1c lupus susceptibility locus, encodes a dysfunctional protein. *Immunity*. (2001) 15:775–85. doi: 10.1016/S1074-7613(01)00228-X
13. Walport MJ. Complement and systemic lupus erythematosus. *Arthritis Res*. (2002) 4:S279–93. doi: 10.1186/ar586
14. Zipfel PF. Complement factor H: physiology and pathophysiology. *Semin Thromb Hemost*. (2001) 27:191–9. doi: 10.1055/s-2001-15248
15. Ferreira VP, Pangburn MK, Cortés C. Complement control protein factor H: the good, the bad, and the inadequate. *Mol Immunol*. (2010) 47:2187–97. doi: 10.1016/j.molimm.2010.05.007
16. Pickering MC, Cook HT, Warren J, Bygrave AE, Moss J, Walport MJ, et al. Uncontrolled C3 activation causes membranoproliferative glomerulonephritis in mice deficient in complement factor H. *Nat Genet*. (2002) 31:424–8. doi: 10.1038/ng912
17. Pickering MC, Cook HT. Translational mini-review series on complement factor H: renal diseases associated with complement factor H: novel insights from humans and animals. *Clin Exp Immunol*. (2008) 151:210–30. doi: 10.1111/j.1365-2249.2007.03574.x
18. Panzer SE, Laskowski J, Renner B, Kulik L, Ljubanovic D, Huber KM, et al. IgM exacerbates glomerular disease progression in complement-induced glomerulopathy. *Kidney Int*. (2015) 88:528–37. doi: 10.1038/ki.2015.120
19. Chou MY, Fogelstrand L, Hartvigsen K, Hansen LF, Woelkers D, Shaw PX, et al. Oxidation-specific epitopes are dominant targets of innate natural antibodies in mice and humans. *J Clin Invest*. (2009) 119:1335–49. doi: 10.1172/JCI36800
20. Binder CJ, Hörkkö S, Dewan A, Chang MK, Kieu EP, Goodyear CS, et al. Pneumococcal vaccination decreases atherosclerotic lesion formation: molecular mimicry between Streptococcus pneumoniae and oxidized LDL. *Nat Med*. (2003) 9:736–43. doi: 10.1038/nm876
21. Birjandi SZ, Ippolito JA, Ramadorai AK, Witte PL. Alterations in marginal zone macrophages and marginal zone B cells in old mice. *J Immunol*. (2011) 186:3441–51. doi: 10.4049/jimmunol.1001271
22. Hug E, Hobeika E, Reth M, Jumaa H. Inducible expression of hyperactive Syk in B cells activates Blimp-1-dependent terminal differentiation. *Oncogene*. (2014) 33:3730–41. doi: 10.1038/onc.2013.326
23. Weismann D, Hartvigsen K, Lauer N, Bennett KL, Scholl HP, Charbel Issa P, et al. Complement factor H binds malondialdehyde epitopes and protects from oxidative stress. *Nature*. (2011) 478:76–81. doi: 10.1038/nature10449
24. Tsiantoulas D, Kiss M, Bartolini-Gritti B, Bergthaler A, Mallat Z, Jumaa H, et al. Secreted IgM deficiency leads to increased BCR signaling that results in abnormal splenic B cell development. *Sci Rep*. (2017) 7:3540. doi: 10.1038/s41598-017-03688-8
25. Pillai S, Cariappa A. The follicular versus marginal zone B lymphocyte cell fate decision. *Nat Rev Immunol*. (2009) 9:767–77. doi: 10.1038/nri2656
26. Cariappa A, Tang M, Parng C, Nebelitskiy E, Carroll M, Georgopoulos K, et al. The follicular versus marginal zone B lymphocyte cell fate decision is regulated by Aiolos, Btk, and CD21. *Immunity*. (2001) 14:603–15. doi: 10.1016/S1074-7613(01)00135-2
27. Cornall RJ, Cheng AM, Pawson T, Goodnow CC. Role of Syk in B-cell development and antigen-receptor signaling. *Proc Natl Acad Sci USA*. (2000) 97:1713–8. doi: 10.1073/pnas.97.4.1713
28. Wen L, Brill-Dashoff J, Shinton SA, Asano M, Hardy RR, Hayakawa K. Evidence of marginal-zone B cell-positive selection in spleen. *Immunity*. (2005) 23:297–308. doi: 10.1016/j.immuni.2005.08.007
29. Geier CB, Sauerwein KMT, Leiss-Piller A, Zmek I, Fischer MB, Eibl,. M. M, et al. Hypomorphic mutations in the BCR signalosome lead to selective immunoglobulin M deficiency and impaired B-cell homeostasis. *Front Immunol*. (2018) 9:2984. doi: 10.3389/fimmu.2018.02984
30. Roozendaal R, Carroll MC. Complement receptors CD21 and CD35 in humoral immunity. *Immunol Rev*. (2007) 219:157–66. doi: 10.1111/j.1600-065X.2007.00556.x
31. Dempsey PW, Allison MED, Akkaraju S, Goodnow CC, Fearon DT. C3d of complement as a molecular adjuvant: bridging innate and acquired immunity. *Science*. (1996) 271:348–50. doi: 10.1126/science.271.5247.348
32. Barrington RA, Schneider TJ, Pitcher LA, Mempel TR, Ma M, Barteneva NS, et al. Uncoupling CD21 and CD19 of the B-cell coreceptor. *Proc Natl Acad Sci USA*. (2009) 106:14490–5. doi: 10.1073/pnas.0903477106
33. Rawlings DJ, Metzler G, Wray-Dutra M, Jackson SW. Altered B cell signalling in autoimmunity. *Nat Rev Immunol*. (2017) 17:421–36. doi: 10.1038/nri.2017.24
34. Dörner T, Giesecke C, Lipsky PE. Mechanisms of B cell autoimmunity in SLE. *Arthritis Res Ther*. (2011) 13:243. doi: 10.1186/ar3433
35. Zhao J, Wu H, Khosravi M, Cui H, Qian X, Kelly JA. Association of genetic variants in complement factor H and factor H-related genes with systemic lupus erythematosus susceptibility. *PLoS Genet*. 7:e1002079. doi: 10.1371/journal.pgen.1002079
36. Dragon-Durey MA, Loirat C, Cloarec S, Macher MA, Blouin J, Nivet H, et al. Anti-factor H autoantibodies associated with atypical hemolytic uremic syndrome. *J Am Soc Nephrol*. (2005) 16:555–63. doi: 10.1681/ASN.2004050380
37. Foltyn Zadura A, Memon AA, Stojanovich L, Perricone C, Conti F, Valesini G, et al. Factor H autoantibodies in patients with antiphospholipid syndrome and thrombosis. *J Rheumatol*. (2015) 42:1786–93. doi: 10.3899/jrheum.150185
38. Bao L, Haas M, Quigg RJ. Complement factor H deficiency accelerates development of lupus nephritis. *J Am Soc Nephrol*. (2011) 22:285–95. doi: 10.1681/ASN.2010060647
39. Loder F, Mutschler B, Ray RJ, Paige CJ, Sideras P, Torres R, et al. B cell development in the spleen takes place in discrete steps and is determined by the quality of B cell receptor-derived signals. *J Exp Med*. (1999) 190:75–89. doi: 10.1084/jem.190.1.75
40. Wen R, Chen Y, Xue L, Schuman J, Yang S, Morris SW, et al. Phospholipase Cgamma2 provides survival signals via Bcl2 and A1 in different subpopulations of B cells. *J Biol Chem*. (2003) 278:43654–62. doi: 10.1074/jbc.M307318200
41. Boes M, Schmidt T, Linkemann K, Beaudette BC, Marshak-Rothstein A, Chen J. Accelerated development of IgG autoantibodies and autoimmune disease in the absence of secreted IgM. *Proc Natl Acad Sci USA*. (2000) 97:1184–9. doi: 10.1073/pnas.97.3.1184
42. Ehrenstein MR, Notley CA. The importance of natural IgM: scavenger, protector and regulator. *Nat Rev Immunol*. (2010) 10:778–86. doi: 10.1038/nri2849
43. Tsiantoulas D, Perkmann T, Afonyuskhin T, Mangold A, Prohaska TA, Papac-Milicevic N, et al. Circulating microparticles carry oxidation-specific epitopes and are recognized by natural IgM antibodies. *J Lipid Res*. (2015) 56:440–8. doi: 10.1194/jlr.P054569
44. Leffler J, Herbert AP, Norström E, Schmidt CQ, Barlow PN, Blom AM, et al. Annexin-II, DNA, and histones serve as factor H ligands on the surface of apoptotic cells. *J Biol Chem*. (2010) 285:3766–76. doi: 10.1074/jbc.M109.045427
45. Pickering MC, de Jorge EG, Martinez-Barricarte R, Recalde S, Garcia-Layana A, Rose KL, et al. Spontaneous hemolytic uremic syndrome triggered by complement factor H lacking surface recognition domains. *J Exp Med*. (2007) 204:1249–56. doi: 10.1084/jem.20070301
46. O'Rourke L, Tooze R, Fearon DT. Co-receptors of B lymphocytes. *Curr Opin Immunol*. (1997) 9:324–9. doi: 10.1016/S0952-7915(97)80077-5
47. Buhlmann D, Eberhardt HU, Medyukhina A, Prodinger WM, Figge MT, Zipfel PF, et al. FHR3 Blocks C3d-mediated coactivation of human B cells. *J Immunol*. (2016) 197:620–9. doi: 10.4049/jimmunol.1600053

48. Grammer AC, Lipsky PE. B cell abnormalities in systemic lupus erythematosus. *Arthritis Res Ther*. (2003) 5:S22–7. doi: 10.1186/ar1009
49. Wellmann U, Letz M, Herrmann M, Angermüller S, Kalden JR, Winkler TH. The evolution of human anti-double-stranded DNA autoantibodies. *Proc Natl Acad Sci USA*. (2005) 102:9258–63. doi: 10.1073/pnas.0500132102
50. Kil LP, de Bruijn MJ, van Nimwegen M, Corneth OB, van Hamburg JP, Dingjan GM, et al. Btk levels set the threshold for B-cell activation and negative selection of autoreactive B cells in mice. *Blood*. (2012) 119:3744–56. doi: 10.1182/blood-2011-12-397919
51. Satterthwaite AB. Bruton's tyrosine kinase, a component of B cell signaling pathways, has multiple roles in the pathogenesis of lupus. *Front Immunol*. (2018) 8:1986. doi: 10.3389/fimmu.2017.01986
52. Hutcheson J, Vanarsa K, Bashmakov A, Grewal S, Sajitharan D, Chang BY, et al. Modulating proximal cell signaling by targeting Btk ameliorates humoral autoimmunity and end-organ disease in murine lupus. *Arthritis Res Ther*. (2012) 14:R243. doi: 10.1186/ar4086
53. Mina-Osorio P, LaStant J, Keirstead N, Whittard T, Ayala J, Stefanova S, et al. Suppression of glomerulonephritis in lupus-prone NZB × NZW mice by RN486, a selective inhibitor of Bruton's tyrosine kinase. *Arthritis Rheum*. (2013) 65:2380–91. doi: 10.1002/art.38047

Conflict of Interest Statement: The authors declare that the research was conducted in the absence of any commercial or financial relationships that could be construed as a potential conflict of interest.

Supplementary information

Supplementary Figure 1

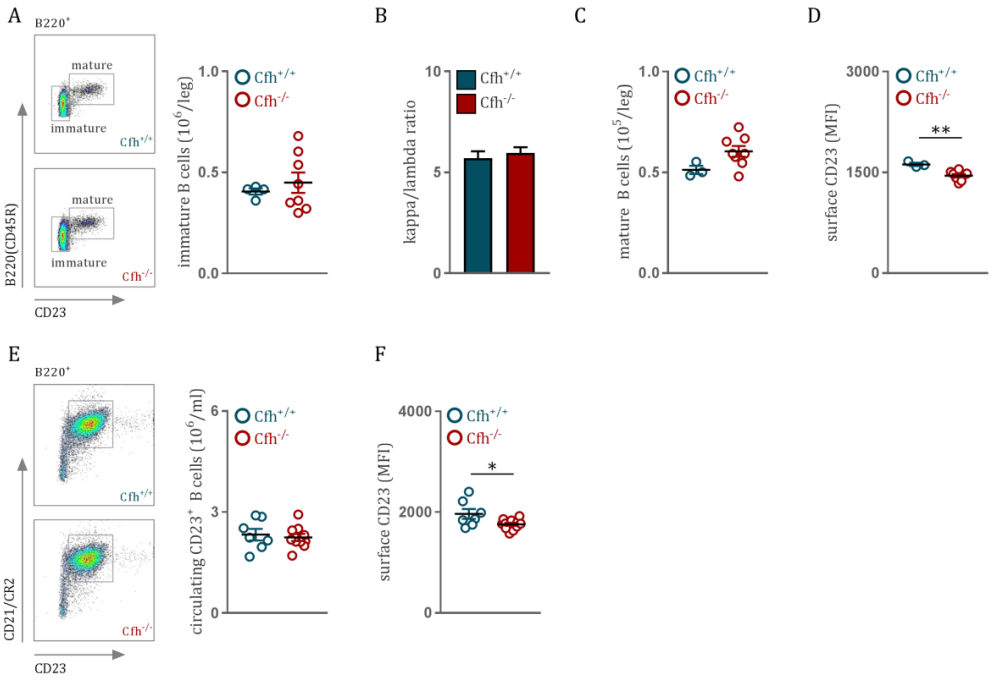

Supplementary Figure 2

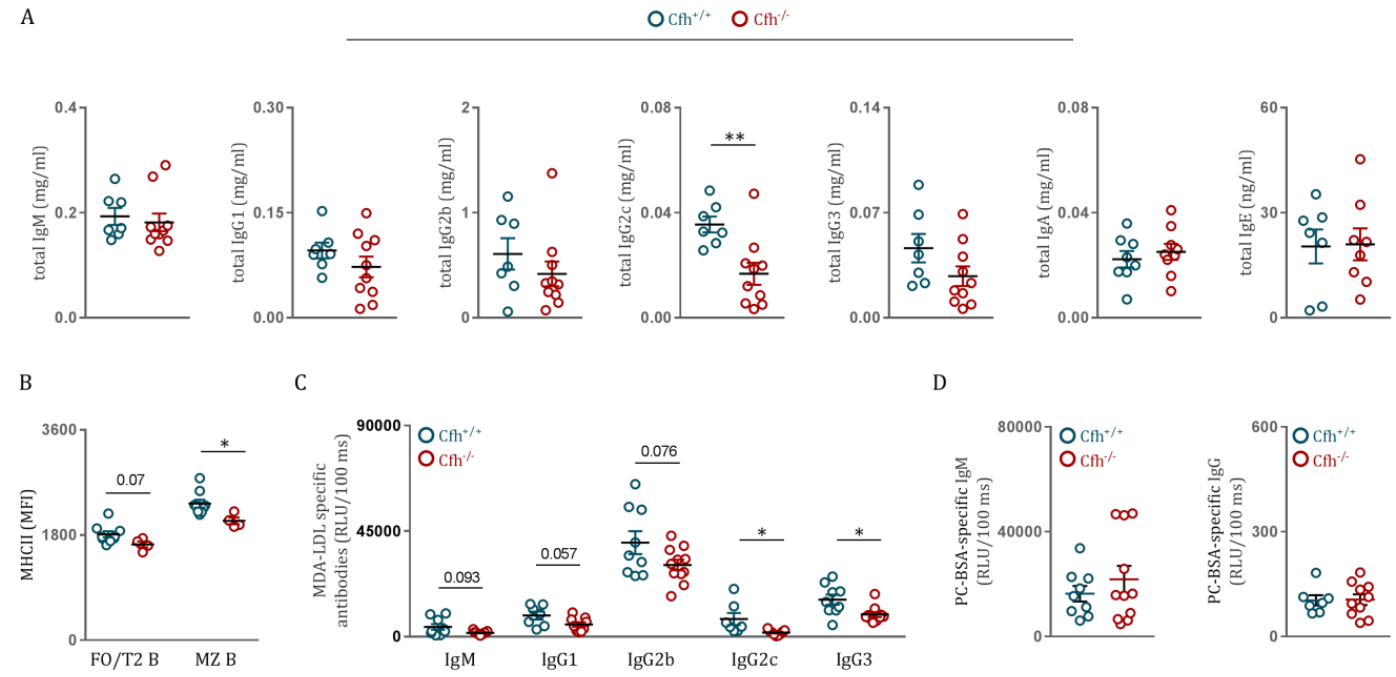

Supplementary Figure 3

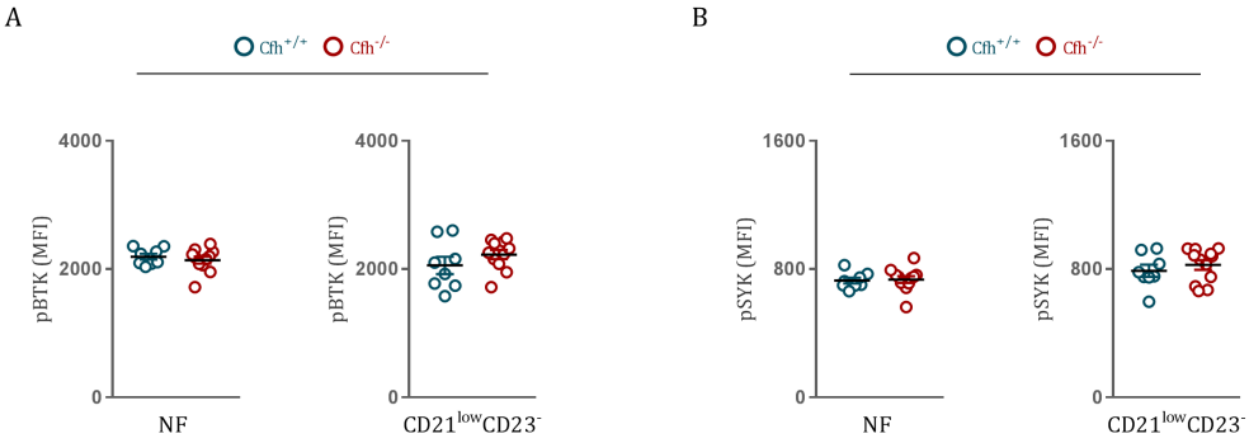

Supplementary Figure 4

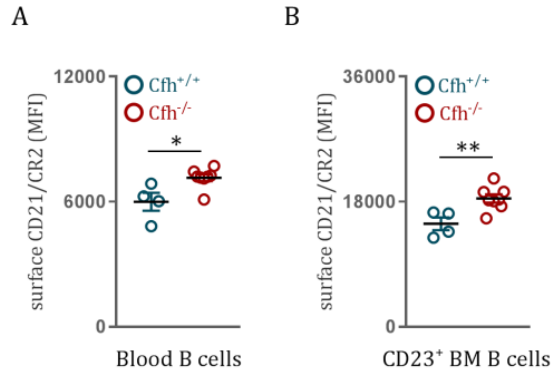

Supplementary Figure 5

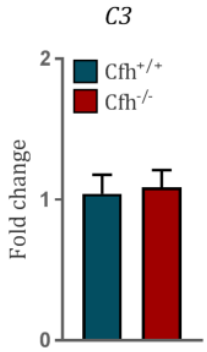

Supplementary Figure 6

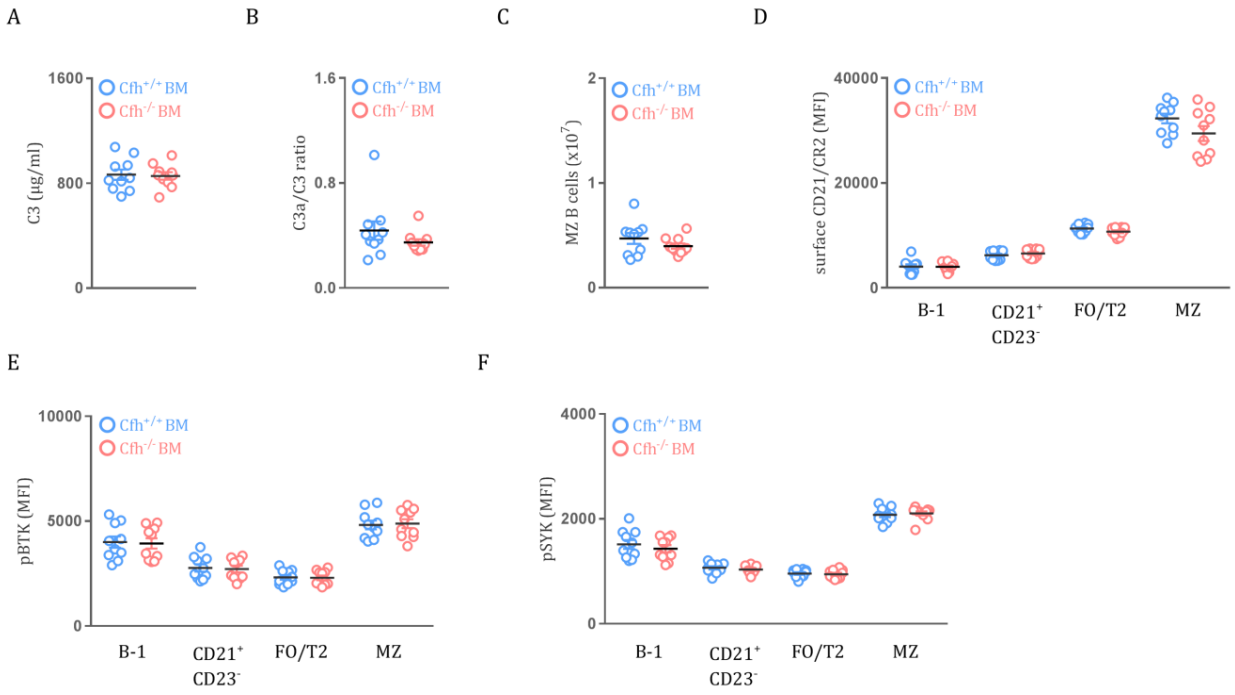

Supplementary Figure 7

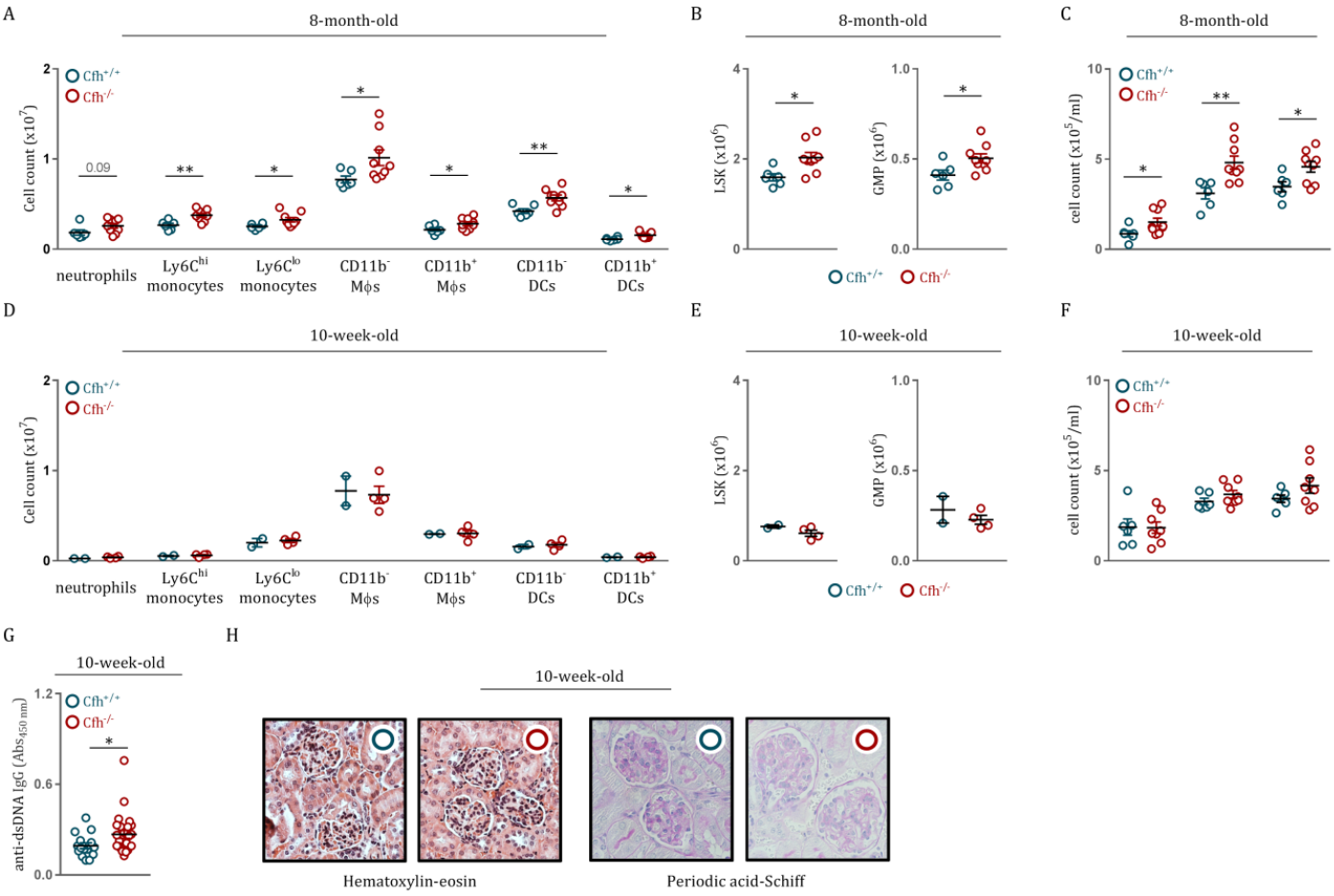

Supplementary Figure 8

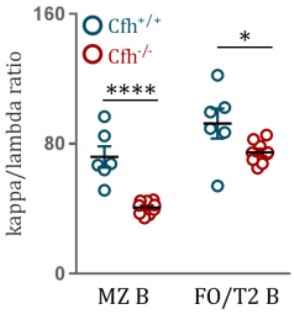

Supplementary Figure 9

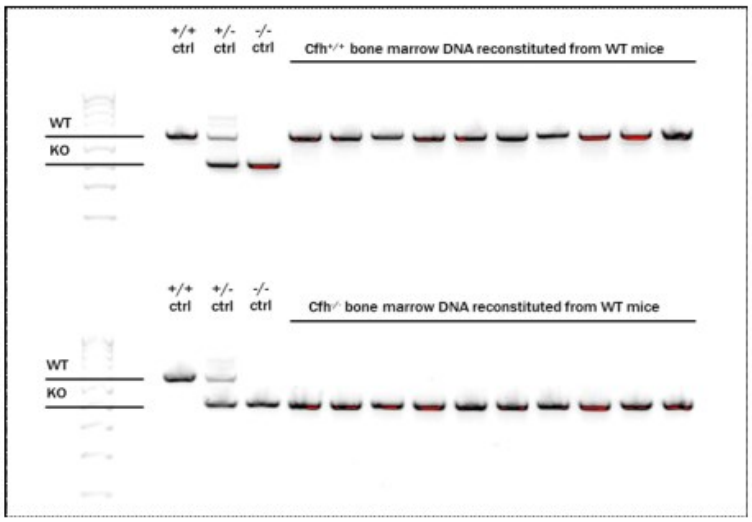

2.3 Interlude

Liver-derived, serum-circulating complement has been long known to have a pivotal role in the clearance of invading pathogens and modified host cells. Therefore, complement is a potent effector of humoral immunity. However, key complement proteins representing mainly the alternative pathway appeared evolutionarily in the *Porifera* class of sponges that have no circulatory system or organs. The discovery of intracellular complement activation strongly supports that complement had operated originally as an intracellular sentinel system in single cell organisms and became secreted eventually during evolution. In line with this, intracellular complement activation is now appreciated to control basic cellular processes, such as cell survival and autophagy. However, if and how intracellular complement activation is regulated remains elusive.

In the following manuscript, we investigated the expression pattern of canonical complement regulators in a wide array of splenic immune cells and identified a unique expression pattern for complement factor H (CFH) that is restricted to monocytes, in particular, inflammatory monocytes. We documented that the expression of CFH is under inflammatory regulation and is upregulated upon hypercholesterolemia. Unexpectedly, we found that selective CFH deficiency in the hematopoietic compartment protects from atherosclerosis by promoting lesional efferocytosis. This effect is dependent on the role of CFH in regulating intracellular C3 levels in inflammatory macrophages. Finally, we could demonstrate the dominant effect of hematopoietic CFH over systemic, liver-derived CFH in atherosclerotic lesion formation.

2.4 Manuscript #2

M.G. Kiss, N. Papac-Miličević, D. Tsiantoulas, T. Hendrikx, F. Porsch, M.-S. Narzt, L. Göderle, M. Ozsvár-Kozma, A. Hladik, T. Penz, N. Fortelny, M. Schuster, C. Bock, S. Knapp, F. Gruber, M.C. Pickering, F.K. Swirski, C. Kemper, C.J. Binder. Enhanced cell autonomous complement activation limits atherosclerosis by promoting macrophage efferocytosis. *To be submitted.*

Detailed author contribution: M. G. Kiss conceived the project, designed and performed experiments, analyzed and interpreted the data and wrote the manuscript; N.P.-M., D.T., T.H., F.P., L.G., M.-S. N., M.O.-K. and A.H. performed experiments; T. W.-P., N.F. and M.S. conducted and analyzed 10X genomics and RNA sequencing experiments. C.B., S.K., F.G. critically revised the manuscript; M.C.P. critically revised the manuscript and provided the *Cfh*$^{-/-}$ mice; F.K.S., C.K. critically revised and edited the manuscript; C.J.B. conceived the project, designed experiments, interpreted the data and wrote the manuscript.

TITLE: Enhanced cell autonomous complement activation limits atherosclerosis by promoting macrophage efferocytosis

One sentence summary: Local complement factor H production restrains efficient efferocytosis by controlling on-demand C3 activation in monocyte-derived macrophages during inflammation

Authors:

Máté G. Kiss[1,2], Nikolina Papac-Miličević[1,2], Dimitrios Tsiantoulas[1,2], Tim Hendrikx[1,2], Florentina Porsch[1,2], Marie-Sophie Narzt[3], Laura Göderle[1,2] Mária Ozsvár-Kozma[1,2], Anastasiya Hladik[2,4], Thomas Winkler-Penz[2], Nikolaus Fortelny[2], Michael Schuster[2], Christoph Bock[2], Sylvia Knapp[2,4], Florian Gruber[3], Matthew C. Pickering[5], Filip K. Swirski[6], Claudia Kemper[7,8,9], Christoph J. Binder[1,2]

Affiliations:

[1] Department of Laboratory Medicine, Medical University of Vienna, Austria

[2] CeMM Research Center for Molecular Medicine of the Austrian Academy of Sciences, Vienna, Austria

[3] Department of Dermatology, Medical University of Vienna, Vienna, Austria; Christian Doppler Laboratory for Biotechnology of Skin Aging, Austria

[4] Department of Medicine I, Laboratory of Infection Biology, Medical University of Vienna, Vienna, Austria

[5] Centre for Inflammatory Disease, Imperial College, London, United Kingdom

[6] Center for Systems Biology, Massachusetts General Hospital and Harvard Medical School, Boston, Massachusetts, United States

[7] Laboratory of Molecular Immunology and Immunology Center, National Heart, Lung and Blood Institute, Bethesda, MD 20892, USA

[8] Faculty of Life Sciences and Medicine, King's College London, London SE1 9RT, United Kingdom

[9] Institute for Systemic Inflammation Research, University of Lübeck, Lübeck 23562, Germany

Correspondence: Prof. Christoph J. Binder, Department for Laboratory Medicine, Medical University of Vienna, Vienna, Austria and CeMM Research Center for Molecular Medicine of the Austrian Academy of Sciences, Lazarettgasse 14, AKH BT 25.2, A-1090, Vienna, Austria, christoph.binder@meduniwien.ac.at

ABSTRACT

Complement is a crucial effector system of innate immunity and is critical for the clearance of invading pathogens and cellular debris. While it has been widely recognized as a serum-effective cascade, it is now evident that complement activation also occurs within cells and can mediate basic cellular processes. However, if and how intracellular complement activation is regulated has been elusive. Here, we investigated the potential role of canonical complement repressors in controlling autonomous complement activation in immune cells. We found that only the expression of complement factor H (CFH), the major regulator of alternative complement, is restricted to monocytes, upregulated during inflammation and coincides with the accumulation of intracellular C3. In monocyte-derived inflammatory macrophages, the absence of CFH leads to uncontrolled intracellular C3 cleavage without increased downstream C5 activation and a heightened efferocytotic capacity promoting the resolution of inflammation. Moreover, hematopoietic deletion of CFH in atherosclerosis-prone, low-density lipoprotein receptor-deficient mice resulted in enhanced lesional efferocytosis and reduced plaque formation. These data demonstrate the capacity of a canonical complement repressor to control intracellular C3 consumption in macrophages in a cell autonomous manner, supporting a concept of on-demand complement regulation during inflammation.

MAIN TEXT

Complement represents the serum-effective protease cascade of innate immunity with a critical role in detecting and clearing invading microorganisms and dying cells[1,2]. The proteolytic cleavage of the central complement component C3 is the convergence point in the activation of three separate complement activation pathways[3], among which the alternative complement cascade is continuously triggered by a tick-over mechanism acting as its own catalyst[4].

While most of the complement components are primarily produced in the liver, extrahepatic sources of C3 have been reported[5]. Although systemic and local complement activities were considered to be confined to the extracellular space, recent work in human T cells demonstrated that tonic generation of bioactive C3 cleavage products by cell-specific proteases occurs also intracellularly[6]. Importantly, intracellular stores of C3 are not exclusive to T cells[6], but are also present in other cell types suggesting that complement may have additional physiological functions[7]. Indeed, intracellular complement activation has been shown to control T cell homeostasis[6], nutrient influx, metabolic reprogramming[8] as well as pancreatic beta cell survival[9].

In addition, intracellular C3 stores can also serve as a cytosolic surveillance system against self and non-self danger signals[10]. For example, intracellular C3 drives autophagy-mediated growth restriction of cyto-invasive bacteria[11] and proteasome-mediated degradation of viruses[12]. Furthermore, intracellular C5a (a downstream complement cleavage product) has been shown to regulate inflammasome activation following the accumulation of reactive oxygen species (ROS)[13]. Thus, intracellular complement has a fundamental role in orchestrating cellular immunity and homeostasis[14]. However, as most cellular processes, also intracellular C3 activation must require active regulation and it is not known if and how this regulation takes place. Therefore, we investigated whether cell autonomous complement activation is controlled on a cellular level, whether it is mediated by canonical complement repressors, and how this affects inflammatory responses.

Atherosclerosis is a lipid-driven chronic inflammatory disease of the arterial wall and the underlying cause of myocardial infarction and stroke, the leading causes of death worldwide[15]. Monocyte-derived macrophages represent central cells in the maladaptive, non-resolving inflammatory response within atherosclerotic lesions that has been shown to result from inadequate cyto-protective functions due to excessive lipid accumulation[16]. Complement proteins are present in human atherosclerotic plaques[17], and the effects of certain complement components have been investigated in experimental atherosclerosis[18,19].

However, the role and regulation of intracellular complement activation in atherosclerotic lesion formation has been unexplored.

To identify key factors in cell autonomous complement regulation, we first investigated the expression profile of canonical complement repressors among various immune cell subsets of murine splenocytes by single cell RNA sequencing. We focused on regulators that are known to modulate systemic C3 activation and/or the effector functions of bioactive C3 cleavage products[20]. These include the most common fluid phase mediators such as C4b binding protein (C4BP), complement factor H (CFH), complement factor I (CFI), complement factor D (CFD) and factor H-related protein B (FHR-B) as well as membrane-bound receptors such as complement receptor 1-related protein Y (Crry/Cr1l), CD55 (also known as decay accelerating factor; DAF) and its isoform CD55b. Based on the expression levels of the most variable genes, we could successfully classify and annotate all major splenic immune cell subsets and found a unique expression pattern for the primary alternative complement regulator *Cfh* with a restriction to monocytes, while the rest of the regulators was either undetectable (*C4bp, Cfi, Cfd, Fhr-b, Cd55b*) or ubiquitously expressed (*Cr1l*, *Cd55*) **(Fig 1A)**. We confirmed our finding by qRT-PCR analysis of sorted splenic leukocyte subsets, which further revealed that inflammatory Ly6C^{hi} monocytes account predominantly for *Cfh* expression **(Fig 1B).** This suggested an inflammatory regulation of CFH production by monocytes. Indeed, expression of *Cfh* was further induced in circulating Ly6C^{hi} monocytes of mice challenged with the sterile inflammatory trigger thioglycollate, while other complement regulators were unaffected **(Fig 1C)**. Furthermore, we could show that IFNγ treatment leads to an upregulation of *Cfh* in both BMDMs **(Fig 1D)** as well as increased intracellular CFH levels in THP-1 monocyte-derived macrophages **(Fig 1E)**, which were also capable of secreting CFH (**Fig 1F**).

Given the unexpected observation that CFH is the sole complement regulator with a compartmentalized expression pattern, we sought to investigate the significance of monocyte-derived CFH during inflammation. Ly6C^{hi} monocytes are hallmark cells of atherosclerosis being induced by hypercholesterolemia and preferentially accumulating in atherosclerotic lesions where they differentiate to inflammatory macrophages[21]. Importantly, we could demonstrate an increased *Cfh* expression in both blood as well as splenic Ly6C^{hi} monocytes of *Ldlr*$^{-/-}$ mice fed an atherogenic diet (AD) compared to standard diet-fed (SD) mice **(Fig 2A)**. Of note, hepatic *Cfh* expression was not significantly induced by AD **(Fig 2B)** suggesting that hypercholesterolemia triggers *Cfh* expression primarily in monocytes. Therefore, we tested whether monocyte-derived CFH affects lesion formation. We generated *Ldlr*$^{-/-}$ mice reconstituted with bone marrow of *Cfh*$^{+/+}$ or *Cfh*$^{-/-}$ mice and fed them an atherogenic diet for 12 weeks **(Fig 2C)**. While global loss of CFH in mice results in

uncontrolled systemic complement activation due to the continuous consumption of circulating C3[22,23], we found that hematopoietic CFH deficiency did not influence total CFH levels **(Fig 2D)** or systemic complement activation **(Fig 2E & 2F)**. Moreover, there was no effect on body weights, plasma cholesterol and triglyceride levels **(Fig S1A-C)**. Nevertheless, *Cfh*$^{-/-}$ bone marrow chimeric mice developed less atherosclerosis in the entire aorta **(Fig S2A)** as well as in cross sections of the aortic root **(Fig 2H & I)**. Furthermore, hematopoietic CFH deficiency also resulted in a more than 80% reduction of the necrotic core area **(Fig 2J)**. *Cfh*$^{-/-}$ bone marrow chimeric *Ldlr*$^{-/-}$ mice were also protected from hepatic inflammation as demonstrated by decreased macrophage content **(Fig S2B)** as well as reduced *Cxcl1, Cxcl2* and *Tnfa* expression in the liver **(Fig S2C)**. Thus, CFH deficiency in monocytes protects from atherosclerosis despite the abundant presence of liver-derived CFH in plasma.

Although the atheroprotective effect of hematopoietic CFH deficiency is clearly independent of systemic C3 activation, we wondered whether monocyte-derived CFH modulates inflammation by mediating C3 consumption on a cellular level. In order to test this, we first investigated if inflammation promotes monocyte-specific C3 expression. We confirmed that – similarly to *Cfh* – *C3* is primarily expressed in monocytes among immune cells (**Fig S3A**), and upregulated in blood and splenic Ly6C^{hi} monocytes, but not in the liver of *Ldlr*$^{-/-}$ mice upon hypercholesterolemia (**Fig 3A & 3B**). Consistent with the upregulation of C3 during inflammation, we also found increased C3 expression in circulating Ly6C^{hi} monocytes of thioglycollate-injected mice (**Fig S3B**). Notably, properdin (Cfp), the upstream activator of the alternative complement pathway was also upregulated in this setting, which suggests an on-demand production of alternative complement components by Ly6C^{hi} monocytes upon an inflammatory challenge (**Fig S3C**). Circulating Ly6C^{hi} monocytes rapidly differentiate into inflammatory macrophages after being recruited to the peritoneum[24]. Intracellular flow cytometry staining revealed that >80% of infiltrating peritoneal Ly6C^{hi} monocytes contained intracellular C3 while patrolling Ly6C^{lo} monocytes had minimal C3 content (**Fig S4A & 3C**). Moreover, peritoneal C3^{+} Ly6C^{hi} monocytes also displayed elevated surface levels of the macrophage markers F4/80 and C5aR1, indicating that C3 accumulation is associated with macrophage differentiation **(Fig S4B)**. Indeed, inflammatory monocyte-derived macrophages (Mo-Macs) isolated from the peritoneum of thioglycollate-injected mice displayed significantly higher intracellular C3 levels compared to resident macrophages (Res-Macs) from control mice, as determined by intracellular flow cytometry **(Fig 3D)** as well as ELISA **(Fig 3E)**. Notably, surface-bound levels of C3 were minute **(Fig S5A)** and comparable between Mo-Macs and Res-Macs **(Fig S5B)**. Active cleavage of C3 was demonstrated by the parallel intracellular accumulation of the C3 cleavage product C3a in Mo-Macs **(Fig 3F)**. Thus, inflammatory stimuli trigger the intracellular accumulation and activation of C3 in Mo-Macs.

To determine whether the loss of CFH affects intracellular C3 activation in inflammatory monocytes and macrophages, we first sorted Ly6C^{hi} monocytes from the peritoneum of thioglycollate-injected *Cfh*$^{+/+}$ and *Cfh*$^{-/-}$ mice and measured intracellular C3 levels. Intriguingly, monocytes from *Cfh*$^{-/-}$ mice contained less intact C3 compared to wildtype controls **(Fig 3G and 3H)**. This effect was also observed in sorted circulating Ly6C^{hi} monocytes from unchallenged *Cfh*$^{+/+}$ and *Cfh*$^{-/-}$ mice, albeit to a minor extent due to lower intracellular C3 levels **(Fig S6)**. Consistent with this, CFH deficient Mo-Macs had dramatically reduced intracellular C3 levels compared to wildtype controls **(Fig 3I & 3J, Fig S7**), which was due to enhanced C3 cleavage as judged by increased intracellular C3a levels **(Fig 3K)** and a higher C3a/C3 ratio **(Fig 3L)**.

Intracellular complement activation has been shown to drive C5aR1-dependent NLRP3 inflammasome activity in human T cells[13]. Surprisingly, intracellular C5a levels were not elevated, but significantly decreased in *Cfh*$^{-/-}$ Mo-Macs **(Fig 3M)**, indicating that uncontrolled C3 activation as a result of CFH deficiency does not translate to increased C5 activation. Furthermore, we found no difference in spontaneous interleukin 1-beta (IL-1β) secretion between *Cfh*$^{+/+}$ and *Cfh*$^{-/-}$ Mo-Macs **(Fig S8)**. On the contrary, *Cfh*$^{-/-}$ mice displayed accelerated resolution of sterile peritonitis as indicated by decreased numbers of peritoneal Mo-Macs both 3 days (as previously reported[25]) and 7 days after thioglycollate injection **(Fig 3N)**. Next, we investigated the contribution of monocyte-derived CFH to intracellular C3 consumption in the context of inflammation. Therefore, we transplanted *Cfh*$^{-/-}$ mice with *Cfh*$^{-/-}$ or *Cfh*$^{+/+}$ bone marrow and subjected them to sterile peritonitis **(Fig 3O)**. Reconstitution of CFH production in the hematopoietic compartment of CFH deficient mice normalized intracellular C3 levels in Mo-Macs **(Fig 3P)** and was sufficient to delay the resolution of sterile peritonitis as judged by increased Mo-Macs in the peritoneal lavage fluid (**Fig 3Q**). Thus, our data clearly demonstrate the significance of cell autonomous CFH production in regulating C3 cleavage within macrophages and supports a functional role for cellular complement regulation during inflammation.

To assess the effects of enhanced intracellular C3 activation on the function of inflammatory macrophages we performed RNA sequencing of Mo-Macs from *Cfh*$^{+/+}$ and *Cfh*$^{-/-}$ mice. Expression of over 4,000 genes was significantly altered in CFH-deficient Mo-Macs compared to wildtype controls **(**$q < 0.1$; **Fig 4A)**. Importantly, genes associated with the complement cascade, the clearance of apoptotic cells i.e. efferocytosis and the resolution of inflammation were primarily upregulated in CFH deficient Mo-Macs **(Fig 4B & 4C; FigS9)**. Moreover, we found a robust increase in the expression of receptors triggering an autophagy-related process involved in efficient efferocytosis, called LC3-associated phagocytosis (LAP)[26] **(Fig 4D**). LAP promotes rapid phagolysosomal fusion and the

hydrolytic degradation of apoptotic material by conjugating lipids to LC3-bound phagosomal membranes[27]. Therefore, we evaluated the conversion of cellular LC3-I to the lipid-associated LC3-II form in Mo-Macs by Western blotting. Lysates of *Cfh*$^{-/-}$ Mo-Macs displayed an elevated LC3-II/LC3-I ratio compared to wildtype controls **(Fig 4E)**. This is also consistent with the previously described ATG16L1-dependent role of intracellular C3 in autophagy[9,11]. To perform functional validation, we carried out *ex vivo* efferocytosis assays, in which equivalent numbers of isolated Mo-Macs from the peritoneal cavities of *Cfh*$^{+/+}$ and *Cfh*$^{-/-}$ mice were incubated with CMFDA-labelled apoptotic RAW macrophages for 1.5 hours. As expected, quantification of CMFDA^{+} Mo-Macs by flow cytometry revealed that CFH deficient macrophages indeed display heightened efferocytotic capacity compared to wildtype macrophages **(Fig 4F)**. Accordingly, we found decreased frequencies of late apoptotic (AnnV^{+} 7-AAD^{+}) and necrotic (AnnV^{-} 7-AAD^{+}) macrophages in the peritoneum of thioglycollate-injected *Cfh*$^{-/-}$ mice compared to wildtype controls as assessed by Annexin V (AnnV) and 7-aminoactinomycin D (7-AAD) staining **(Fig S10)**. The frequencies of AnnV^{+} 7-AAD^{-} Mo-Macs were not different between *Cfh*$^{+/+}$ mice and *Cfh*$^{-/-}$ mice, suggesting that the rate of apoptosis was not affected **(Fig S10)**.

Next, we tested whether the enhanced efferocytotic capacity of inflammatory macrophages is responsible for the atheroprotective role of hematopoietic CFH deficiency. Importantly, we could confirm that the reduction in necrotic core formation – that is typically a consequence of defective efferocytosis[27] - was associated with a significant decrease in lesional TUNEL^{+} macrophages **(Fig 4G)**. Indeed, a striking reduction in the ratio of 'free' to 'macrophage-associated' apoptotic cells indicated enhanced lesional efferocytosis **(Fig 4H)**. Furthermore, lesions of recipients of *Cfh*$^{-/-}$ bone marrow displayed higher ATG5 expression in macrophage-rich regions **(Fig 4I)**, in line with the previously described role of this key autophagy protein in autophagosome formation[28] and macrophage efferocytosis and in the protection from necrotic core formation[29]. Therefore, CFH deficiency in monocytes protects from atherosclerosis by promoting lesional efferocytosis and resolution of inflammation.

Last, we evaluated whether the protective effect on lesion composition associated with the absence of monocyte-derived CFH is also present in mice with global CFH deficiency. Therefore, we bred littermates of *Cfh*$^{+/+}$*Ldlr*$^{-/-}$ and *Cfh*$^{-/-}$*Ldlr*$^{-/-}$ mice and fed them an atherogenic diet for 10 weeks. Body weights, plasma cholesterol and triglyceride levels **(Fig S11A-C)** were not different between the two groups. Consistent with previous data by us[30] and others[23], *Cfh*$^{-/-}$*Ldlr*$^{-/-}$ mice had severely reduced plasma C3 levels **(Fig S11F)** and increased circulating anti-dsDNA autoantibodies **(Fig S11G)** compared to *Cfh*$^{+/+}$*Ldlr*$^{-/-}$ controls. Nevertheless, global loss of CFH still resulted in a marked decrease in necrotic core

formation (**Fig 4E**) in lesions of similar size **(Fig 4D),** which suggests a dominant effect of monocyte-derived CFH in atherosclerosis.

Our findings describe a novel immune-regulatory mechanism by which cell autonomous complement activation controls crucial cyto-protective functions in monocyte-derived macrophages during inflammation. This is in line with the notion that early C3 activation evolved to be a part of an intracellular sensor system that armors individual cells against cellular stress and injury[7,31]. C3 activation within macrophages in the context of inflammation may involve a C3-cleaving enzyme, e.g. an intracellular C3 convertase or other cell-specific proteases, such as cathepsin L[6]; however, it also requires active regulation. Here, we identify that complement factor H (CFH), the canonical repressor of alternative complement activation in serum, is highly upregulated in inflammatory macrophages where it suppresses C3 cleavage. Although we do not know the exact mechanism of action, CFH might accelerate the decay of an intracellular C3 convertase or inhibits a cell-specific protease with C3-cleaving ability[32].

We show that loss of CFH results in uncontrolled intracellular C3 consumption without activating the proinflammatory C5a-inflammasome axis. Consistent with the previously reported function of C3 in promoting autophagy[9,11], we found that C3 overactivation as a result of CFH deficiency enhances macrophage autophagy and consequently efferocytosis in models of both acute and chronic inflammation. Importantly, we provide evidence for the non-redundant role of macrophage-derived CFH in this context. Therefore, our data clearly demonstrate the impact of regulating cell autonomous complement activation during inflammatory processes.

We also found that the levels of properdin, the upstream alternative complement activator are also under inflammatory regulation. Thus, Ly6C^{hi} monocytes appear to carry their own set of alternative complement proteins to the site of inflammation, where they differentiate into effector phagocytes. This likely allows them to actively fine tune both local as well as cell autonomous complement activation and thereby modulate host-protective cellular functions, supporting a concept of local ‘on-demand’ complement activation during inflammation. Macrophage-derived CFH appears to have a crucial role in modulating ‘on-demand’ complement. The local availability of macrophage-derived CFH may be dependent on the extent of accumulating apoptotic cells, which have been shown to be bound by CFH. In turn, this may limit the amount of free CFH for (re-)uptake by macrophages and thereby indirectly modulate intracellular complement activity[33]. Thus, our data suggest a model in which the interaction of CFH with apoptotic cells regulates the resolution of inflammation.

The accumulation of apoptotic macrophages is one of the major characteristics of advanced atherosclerotic lesions[16]. Therefore, complement has been widely studied in experimental atherosclerosis[19], due to its critical homeostatic role in clearing dying cells. While the protective effect of the classical complement pathway via C1q has been well described[34-36], the effect of alternative complement activation on lesion formation is less clear. Global C3 deficiency has been found to accelerate atherosclerosis and to result in greater lesional macrophage content[18,37]. This is in line with our current findings that uncontrolled C3 activation associated with CFH deficiency promotes lesional efferocytosis and protects from atherosclerosis. However, studies on the role of CFB and CFP in lesion formation gave conflicting results and the identification of potential cell autonomous effects is largely complicated by the strong influence of both CFB and CFP deficiency on systemic C3 activation[37-39]. Thus, in light of our findings, the re-evaluation of studies discussing the effect of systemic complement on atherosclerosis may be warranted with respect to complement activation in macrophages and future investigations should aim to dissect the cell autonomous effects of complement components.

In summary, we here identify a novel mechanism by which uncontrolled cell autonomous C3 activation resulting from CFH deficiency induces cyto-protective autophagy in macrophages, promotes lesional efferocytosis and mitigates atherosclerosis development. The need for alternative strategies in treating atherosclerotic vascular diseases – such as inducing resolution - is apparent, as anti-inflammatory drug therapies can potentially suppress host defense and lead to fatal infections[40]. Our findings indicate that targeting intracellular complement regulation may provide novel opportunities in next generation therapeutics against chronic inflammatory diseases without dampening host defense mechanisms.

METHODS

Methods and any associated references are available in the online version of the paper.

FIGURE LEGENDS

Figure 1. Complement factor H is exclusively expressed by monocytes among immune cells and is upregulated during inflammation (A) t-SNE representation of aligned gene expression data in single cells extracted from the spleen of a C57BL/6 mouse. Gene expression profiles of complement genes (*Cfh, C4bp, Fhr-b, Cfi, Cfd, Cd55, Cd55b, Cr1l*) are shown. **(B)** Relative gene expression of *Cfh* in FACS-sorted splenic immune cell subsets of unchallenged C57BL6/J mice measured by qRT-PCR. Data are shown relative to *Cfh* expression in Ly6C^{hi} monocytes. Bars represent the mean±SEM of three mice. **(C)** qRT-PCR analysis of transcript levels of complement regulatory proteins (*C4bp, Cr1l, Cd55b, Cd55, Cfi, Cfd, Fhr-b* and *Cfh*) in circulating Ly6C^{hi} monocytes sorted from the blood of thioglycollate-injected (24 hours) vs control C57BL6/J mice. **(D)** qRT-PCR analysis of *Cfh* transcript levels in untreated vs 100 ng/ml IFNγ-stimulated bone marrow-derived macrophages. Data are expressed relative to *Cfh* expression in untreated BMDMs. **(E)** Representative flow cytometry histograms show intracellular CFH levels of untreated vs 100 ng/ml IFNγ-stimulated THP-1 macrophages evaluated by flow cytometry. **(F)** Total secreted CFH levels in the supernatant of THP-1 monocyte-derived macrophages treated with 100 ng/ml IFNγ. Each symbol represents individual mice. Data are representative of two or more independent experiments. Statistical significance was evaluated by two-tailed Student's *t* tests (*P < 0.05, ***P < 0.001, ****P < 0.0001). Error bars indicate SEM.

Figure 2. Hematopoietic deletion of complement factor H attenuates atherosclerosis independent of systemic complement activation (A-B) *Ldlr*$^{-/-}$ mice were fed a standard (SD) or atherogenic diet (AD) for 12 weeks (n=8 vs n=10). qRT-PCR analysis of *Cfh* transcript levels in **(A)** circulating and splenic Ly6C^{hi} monocytes as well as in **(B)** total liver samples. Data are expressed relative to gene expression in standard diet-fed mice. **(C)** Schematic representation of chimeric models of hematopoietic CFH deficiency. **(D-J)** Lethally irradiated *Ldlr*$^{-/-}$ mice were reconstituted with bone marrow from *Cfh*$^{+/+}$ vs *Cfh*$^{-/-}$ mice and were fed an atherogenic diet for 12 weeks, starting 5 weeks after transplantation (n=14 vs n=12). **(D-F)** Total plasma **(D)** CFH, **(E)** C3 as well as **(F)** C3a and C5a levels quantified by ELISA. **(G)** Quantification of aortic root plaque size. Representative images of Masson's trichrome-stained sections are shown. Original magnification, 50X; scale bars, 200 μm. **(H)** Measurement of lesion volume. The dot plots represent the average μm^2 of nine sections throughout the entire aortic origin (400 μm), bar graphs show total lesion volume (mm^3). **(I)** Assessment of necrotic core formation in cross sections at the aortic origin. Percentages of

necrotic area (of sections at 150 µm depth) of total lesion area are shown. Representative images are shown, where necrotic area is delineated by red lines. Each symbol represents individual mice. Statistical significance was evaluated by two-tailed Student's *t* tests (**P* < 0.05, ***P* < 0.01, ****P* < 0.001, *****P* < 0.0001). Error bars indicate SEM.

Figure 3. Complement factor H controls cell autonomous C3 activation in monocyte-derived macrophages and delays the resolution of inflammation (A-B) *Ldlr*$^{-/-}$ mice were fed a standard (SD) or atherogenic diet (AD) for 12 weeks (n=8 vs n=10). qRT-PCR analysis of *C3* transcript levels in **(A)** circulating and splenic Ly6C^{hi} monocytes as well as in **(B)** total liver samples. Data are expressed relative to gene expression in standard diet-fed mice. **(C)** C3 levels of peritoneal Ly6C^{hi} and Ly6c^{lo} monocytes of thioglycollate-injected mice determined by intracellular flow cytometry. (**D-F)** Characterization of resident macrophages (Res-Macs) vs monocyte-derived macrophages (Mo-Macs) in the peritoneal lavage fluid of control vs thioglycollate-injected (24 hours) C57BL/6J mice. **(D&E)** Intracellular C3 levels quantified by **(D)** flow cytometry and **(E)** in the lysates of adherent macrophages by ELISA. Representative histograms for **(D)** are shown. **(F)** Intracellular C3a levels relative to total protein content measured in lysates of adherent macrophages by ELISA. **(G)** Intracellular C3 levels normalized to cellular protein content in lysates of peritoneal Ly6C^{hi} monocytes of thioglycollate-injected (24 hours) *Cfh*$^{+/+}$ and *Cfh*$^{-/-}$ mice quantified by ELISA. **(H)** Representative histograms show C3 levels within peritoneal Ly6C^{hi} monocytes of thioglycollate-injected *Cfh*$^{+/+}$ and *Cfh*$^{-/-}$ mice assessed by intracellular flow cytometry. **(I-M)** Characterization of monocyte-derived macrophages (Mo-Macs) in the peritoneal lavage fluid of thioglycollate-injected (72 hours) *Cfh*$^{+/+}$ vs *Cfh*$^{-/-}$ mice. **(I)** Intracellular C3 levels normalized to cellular protein content measured in lysates of adherent Mo-MACS by ELISA. **(J)** Representative histograms show C3 levels measured by intracellular flow cytometry. **(K)** C3a mean fluorescence intensity (MFI) measured by intracellular flow cytometry. **(L)** C3a/C3 ratio, a measure of complement activation, as judged by total intracellular C3a and C3 levels in lysates of adherent Mo-MACS quantified by ELISA. **(M)** C5a levels normalized to cellular protein content in lysates of adherent Mo-MACS measured by ELISA. **(N)** Absolute numbers of Mo-Macs (Cd11b^{int}F4/80^{int}Ly6C^{lo}) in the peritoneal lavage fluid of *Cfh*$^{+/+}$ vs *Cfh*$^{-/-}$ mice 24, 72 and 168 hours after thioglycollate injection, quantified by flow cytometry. **(O)** Schematic representation of chimeric models of CFH deficiency. **(P)** Intracellular C3 levels normalized to cellular protein content in lysates of adherent Mo-Macs of bone marrow chimeric mice (see Figure 2N) measured by ELISA. **(Q)** Absolute numbers of numbers of Mo-Macs (Cd11b^{int}F4/80^{int}Ly6C^{lo}) in the peritoneal lavage fluid of bone marrow chimeric mice (see Figure 2N) 72 hours after thioglycollate injection, quantified by flow cytometry. Each symbol represents individual mice. Data are representative of at least three independent

experiments. Statistical significance was evaluated by two-tailed Student's *t* tests (**P* < 0.05, ***P* < 0.01, ****P* < 0.001, *****P* < 0.0001). Error bars indicate SEM.

Figure 4. Complement factor H-deficient macrophages display heightened efferocytotic capacity (A-F) Characterization of monocyte-derived macrophages (Mo-Macs) in the peritoneal lavage fluid of thioglycollate-injected (72 hours) *Cfh*$^{+/+}$ vs *Cfh*$^{-/-}$ mice. **(A)** Volcano plot of genes with expression change exceeding a factor of 1.5 (q < 0.05) from a genome-wide transcriptome profiling by RNA sequencing. **(B-C)** *Enrichr* analysis of genome-wide transcriptome profiling by RNA sequencing. The eight most overrepresented **(B)** biological pathways as well as **(C)** biological processes are shown in CFH deficient Mo-Macs compared with all *Mus musculus* genes. **(D)** Heat map of LAP-associated genes highly upregulated in CFH-deficient macrophages from a genome-wide transcriptome profiling by RNA sequencing. **(E)** Western blot analysis of intracellular LC3-I and LC3-II levels in lysates of adherent Mo-Macs isolated from the peritoneal cavity of thioglycollate-injected *Cfh*$^{+/+}$ vs *Cfh*$^{-/-}$ mice. A representative blot is shown. **(F)** *Ex vivo* efferocytosis assay using adherent Mo-Macs isolated from the peritoneal cavity of thioglycollate-injected *Cfh*$^{+/+}$ vs *Cfh*$^{-/-}$ mice. Mo-Macs were cultured in the presence of 1% of respective sera and were subsequently incubated with CMFDA-labelled apoptotic RAW macrophages for 1.5 hours. Percentages of CMFDA^{+} efferocytotic Mo-Macs were quantified by flow cytometry. Representative histograms are shown. Bars represent the mean±SEM of three technical replicates. **(G-I)** Lethally irradiated *Ldlr*$^{-/-}$ mice were reconstituted with bone marrow from *Cfh*$^{+/+}$ vs *Cfh*$^{-/-}$ mice and were fed an atherogenic diet for 12 weeks, starting 5 weeks after transplantation (n=14 vs n=12). **(G)** Quantification of dying F4/80^{+} macrophages per cellular area (mm^2) by TUNEL staining using fluorescence microscopy. **(H)** Evaluation of lesional efferocytosis. Efferocytotic capacity was determined as the ratio of free apoptotic cells vs macrophage-associated apoptotic cells using fluorescence microscopy. Representative images of sections stained with DAPI, TUNEL and F4/80 are shown. DAPI, 4',6-diamidino-2-phenylindole. Yellow hashtags (#) show free apoptotic cells and pink asterisks (*) indicate macrophage-associated apoptotic cells. Scale bars 100 µm. **(I)** Quantification of ATG5^{+} lesional area per total cellular area by immunohistochemistry. Each symbol represents individual mice. Representative images are shown. Statistical significance was evaluated by two-tailed Student's *t* tests (**P* < 0.05, ***P* < 0.01, ****P* < 0.001, *****P* < 0.0001). Error bars indicate SEM.

AUTHOR CONTRIBUTIONS

M.G.K. conceived the project, designed and performed experiments, analyzed and interpreted the data and wrote the manuscript; N.P.-M., D.T., T.H., F.P., L.G., M.-S. N., M.O.-K. and A.H. performed experiments; T. W.-P., N.F. and M.S. conducted and analyzed 10X genomics and RNA sequencing experiments. C.B., S.K., F.G. critically revised the manuscript; M.C.P. critically revised the manuscript and provided the *Cfh*$^{-/-}$ mice; F.K.S., C.K. critically revised and edited the manuscript; C.J.B. conceived the project, designed experiments, interpreted the data and wrote the manuscript.

COMPETING FINANCIAL INTERESTS

The authors declare no competing financial interests. Correspondence and requests for materials should be addressed to christoph.binder@meduniwien.ac.at.

REFERENCES AND NOTES:

1. M.J. Walport, *N Eng J Med*. 344(14):1058-66 (2001)
2. M.J. Walport, *N Eng J Med*. 344(15):1140-4 (2001)
3. V.M. Holers, *Annu Rev Immunol.* 32:433-59 (2014)
4. M. Elvington, M.K. Liszewski, P. Bertram, H.S. Kulkarni, J.P. Atkinson, *J Clin Inv.* 127(3):970-981 (2017)
5. G. Arbore, C. Kemper, M. Kolev, *Mol Immunol.* 89:2-9 (2017)
6. M.K. Liszewski, M. Kolev, G. Le Friec, M. Leung, P.G. Bertram, A.F. Fara, M. Subias, M.C. Pickering, C. Drouet, S. Meri, T.P. Arstila, P.T. Pekkarinen, M. Ma, A. Cope, T. Reinheckel, S. Rodriguez de Cordoba, B. Afzali, J.P. Atkinson, C. Kemper, *Immunity.* 39(6):1143-57 (2013)
7. M. Kolev, C. Kemper, *Front Immunol.* 8:1 (2017)
8. M. Kolev, S. Dimeloe, G. Le Friec, A. Navarini, G. Arbore, G.A. Povoleri, M. Fischer, R. Belle, J. Loeliger, L. Develioglu, G.R. Bantug, J. Watson, L. Couzi, B. Afzali, P. Lavender, C. Hess, C. Kemper. *Immunity*. 42(6):1033-47 (2015).
9. B.C. King, K. Kulak, U. Krus, R. Rosberg, E. Golec, K. Wozniak, M.F. Gomez, E. Zhang, D.J. O'Connell, E. Renström, A.M. Blom, *Cell Metab.* 29(1):202-210.e6 (2019)
10. M. Elvington, M.K. Liszewski, J.P. Atkinson, *Immunol Rev.* 274(1):9-15 (2016)
11. M.T. Sorbara, E.G. Foerster, J. Tsalikis, M. Abdel-Nour, J. Mangiapane, I. Sirluck-Schroeder, I. Tattoli, R. van Dalen, D.E. Isenman, J.R. Rohde, S.E. Girardin, D.J. Philpott, *Cell Host Microbe*. May 9;23(5):644-652.e5 (2018)
12. J.C. Tam, S.R. Bidgood, W.A. McEwan, L.C. James, *Science*. 5;345(6201):1256070 (2014)
13. G. Arbore, E.E. West, R. Spolski, A.A.B. Robertson, A. Klos, C. Rheinheimer, P. Dutow, T.M. Woodruff, Z.X. Yu, L.A. O'Neill, R.C. Coll, A. Sher, W.J. Leonard, J. Köhl, P. Monk, M.A. Cooper, M. Arno, B. Afzali, H.J. Lachmann, A.P. Cope, K.D. Mayer-Barber, C. Kemper, *Science.* 352(6292):aad1210 (2016)
14. C. Hess, C. Kemper, *Immunity*. 16;45(2):240-54 (2016)
15. C. Weber, H. Noels, *Nat Med.* 17(11):1410-22 (2011)
16. K.J. Moore, I. Tabas, *Cell*. 145(3):341-55. doi: 10.1016/j.cell.2011.04.005 (2011)
17. R. Oksjoki, P.T. Kovanen, M.O. Pentikäinen, *Curr Opin Lipidol.* 14(5):477-82 (2003)
18. C. Buono, C.E. Come, J.L. Witztum, G.F. Maguire, P.W. Connelly, M. Carroll, A.H. Lichtman, *Circulation*. 105(25):3025-31 (2002)
19. W.S. Speidl, S.P. Kastl, K. Huber, J. Wojta*, J Thromb Haemost*. 9(3):428-40 (2011)
20. P.F. Zipfel, C. Skerka, *Nat Rev Immunol*. 9(10):729-40 (2009)
21. F.K. Swirski, M. Nahrendorf, *Science*. 339(6116):161-6 (2013)

22. P.F. Zipfel, *Semin Thromb Hemost*. 27(3):191-9 (2001)
23. M.C. Pickering, H.T. Cook, J. Warren, A.E. Bygrave, J. Moss, M.J. Walport, M. Botto, *Nat Genet*. 31(4):424-8 (2002)
24. E.E. Ghosn, A.A. Cassado, G.R. Govoni, T. Fukuhara, Y. Yang, D.M. Monack, K.R. Bortoluci, S.R. Almeida, L.A. Herzenberg, L.A. Herzenberg, *Proc Natl Acad Sci USA.* 107(6):2568-73 (2010)
25. B. Calippe, S. Augustin, F. Beguier, H. Charles-Messance, L. Poupel, J.B. Conart, S.J. Hu, S. Lavalette, A. Fauvet, J. Rayes, O. Levy, W. Raoul, C. Fitting, T. Denèfle, M.C. Pickering, C. Harris, S. Jorieux, P.M. Sullivan, J.A. Sahel, P. Karoyan, P. Sapieha, X. Guillonneau, E.L. Gautier, F. Sennlaub, *Immunity*. 46(2):261-272 (2017)
26. J. Martinez, J. Almendinger, A. Oberst, R. Ness, C.P. Dillon, P. Fitzgerald, M.O. Hengartner, D.R. Green, *Proc Natl Acad Sci U.S.A.* 108(42):17396-401 (2011)
27. A. Yurdagul Jr, A.C. Doran, B. Cai, G. Fredman, I.A. Tabas, *Front Cardiovasc Med*. 4:86 (2018)
28. I. Đikić, Z. Elazar, *Nat Rev Mol Cell Biol*. 19(6):349-364 (2018)
29. X. Liao, J.C. Sluimer, Y. Wang, M. Subramanian, K. Brown, J.S. Pattison, J. Robbins, J. Martinez, I. Tabas, *Cell Metabol* 15(4):545-53 (2012)
30. M.G. Kiss, M. Ozsvár-Kozma, F. Porsch, L. Göderle, N. Papac-Miličević, B. Bartolini-Gritti, D. Tsiantoulas, M.C. Pickering, C.J. Binder, *Front Immunol*. 10:1607 (2019)
31. E.E. West, C. Kemper, *Immunometabolism*. 1:e190006.
32. M. Kolev, G. Le Friec, C. Kemper, *Nat Rev Immunol*. 14(12):811-20 (2014)
33. M. Martin, J. Leffler, K.I. Smoląg, J. Mytych, A. Björk, L.D. Chaves, J.J. Alexander, R.J. Quigg, A.M. Blom, *Cell Death Differ*. 23(5):903-11 (2016)
34. V.K. Bhatia, S. Yun, V. Leung, D.C. Grimsditch, G.M. Benson, M.B. Botto, J.J. Boyle, D.O. Haskard, *Am J Pathol*. 170(1):416-26 (2007)
35. M.J. Lewis, T.H. Malik, M.R. Ehrenstein, J.J. Boyle, M. Botto, D.O. Haskard, *Circulation*. 120(5):417-26 (2009)
36. C. Yin, S. Ackermann, Z. Ma, S.K. Mohanta, C. Zhang, Y. Li, S. Nietzsche, M. Westermann, L. Peng, D. Hu, S.V. Bontha, P. Srikakulapu, M. Beer, R.T.A. Megens, S. Steffens, M. Hildner, L.D. Halder, H.H. Eckstein, J. Pelisek, J. Herms, S. Roeber, T. Arzberger, A. Borodovsky, L. Habenicht, C.J. Binder, C. Weber, P.F. Zipfel, C. Skerka, A.J.R. Habenicht, *Nat Med*. 25(3):496-506 (2019)
37. L. Persson, J. Borén, A.K. Robertson, V. Wallenius, G.K. Hansson, M. Pekna, *Arterioscler Thromb Vasc Biol*. 24(6):1062-7 (2004)
38. T.H. Malik, A. Cortini, D. Carassiti, J.J. Boyle, D.O. Haskard, M. Botto, *Circulation*.122(19):1948-56 (2010)

39. T. Steiner, L. Francescut, S. Byrne, T. Hughes, A. Jayanthi, I. Guschina, J. Harwood, K. Cianflone, C. Stover, S. Francis, PLoS One. 9(3):e92404 (2014)
40. P.M. Ridker, B.M. Everett, T. Thuren, J.G. MacFadyen, W.H. Chang, C. Ballantyne, F. Fonseca, J, Nicolau, W. Koenig, S.D. Anker, J.J.P. Kastelein, J.H. Cornel, P. Pais, D. Pella, J. Genest, R. Cifkova, A. Lorenzatti, T. Forster, Z. Kobalava, L. Vida-Simiti, M. Flather, H. Shimokawa, H. Ogawa, M. Dellborg, P.R.F. Rossi, R.P.T. Troquay, P. Libby, R.J. Glynn; CANTOS Trial Group, *N Engl J Med*. 21;377(12):1119-1131 (2017)

ACKNOWLEDGEMENTS

This work was supported by fellowships of the doctoral program Cell Communication in Health and Disease (CCHD; to M.G.K. and F.P.) and by SFB Lipotox F30, both funded by the Austrian Science Fund.

SUPPLEMENTARY INFORMATION

Fig S1. Hematopoietic deletion of complement factor H does not affect weight gain or lipid metabolism (A-C) Lethally irradiated *Ldlr*$^{-/-}$ mice were reconstituted with bone marrow from *Cfh*$^{+/+}$ vs *Cfh*$^{-/-}$ mice and were fed an atherogenic diet for 12 weeks, starting 5 weeks after transplantation (n=14 vs n=12). **(A)** Final body weight. **(B-C)** Plasma **(B)** cholesterol and **(C)** triglyceride levels measured by an enzymatic automated method. Each symbol represents individual mice. Statistical significance was evaluated by two-tailed Student's *t* tests.

Fig S2. Hematopoietic complement factor H deficiency mitigates hepatic inflammation (A-C) Lethally irradiated *Ldlr*$^{-/-}$ mice were reconstituted with bone marrow from *Cfh*$^{+/+}$ vs *Cfh*$^{-/-}$ mice and were fed an atherogenic diet for 12 weeks, starting 5 weeks after transplantation (n=14 vs n=12). **(A)** Quantitative analysis of atherosclerosis in the aorta. Data are expressed as percentage of Sudan IV stained area of the entire aorta. Representative images are shown. **(B)** Quantification of infiltrating macrophages in liver sections. Data are expressed as number of positive cells per mm^2. Representative images of Mac-1-stained liver sections are shown. Original magnification, 200X; scale bars, 100 µm. **(C)** qRT-PCR analyses of transcript levels of inflammatory genes (*Cxcl1, Cxcl2* and *TNFα*) in total liver samples. Data are expressed relative to the expression of individual genes in control *Cfh*$^{+/+}$ bone marrow chimeric mice. Bars represent the mean±SEM of 14 vs 12 mice. Statistical significance was evaluated by two-tailed Student's *t* tests (**P* < 0.05, ***P* < 0.01). Error bars indicate SEM.

Fig S3. Ly6C^{hi} monocytes upregulate alternative complement genes during acute inflammation (A) t-SNE representation of aligned gene expression data in single cells extracted from the spleen of a C57BL/6 mouse. Gene expression profiles of complement genes (*C3*) are shown. **(B-C)** qRT-PCR analysis of transcript levels of **(B)** *C3* and **(C)** *Cfp* in circulating Ly6C^{hi} monocytes sorted from the blood of thioglycollate-injected (24 hours) vs control C57BL6/J mice. Statistical significance was evaluated by two-tailed Student's *t* tests (**P* < 0.05, ****P* < 0.001). Error bars indicate SEM.

Fig S4. Accumulation of intracellular C3 in Ly6C^{hi} monocytes is in association with the expression of macrophage markers (A) Representative flow cytometry plot shows the percentage of intracellular C3$^+$ Ly6C^{hi} monocytes in the peritoneal lavage fluid of

thioglycollate-injected mice (24 hours) assessed by flow cytometry. **(B)** Mean fluorescence intensity (MFI) of macrophage markers (F4/80, C5aR1) on the surface of $C3^-$ and $C3^+$ $Ly6C^{hi}$ monocytes in the peritoneal lavage fluid of thioglycollate-injected mice quantified by flow cytometry. Bars represent the mean±SEM of 4 mice. Statistical significance was evaluated by two-tailed Student's *t* tests (****P* < 0.001, *****P* < 0.0001). Error bars indicate SEM.

Fig S5. Intracellular but not extracellular C3 levels are increased in monocyte-derived macrophages during inflammation (A) Extracellular and intracellular C3 mean fluorescence intensity (MFI) of monocyte-derived macrophages from the peritoneal cavity of thioglycollate-injected mice (24 hours) measured by flow cytometry. Representative flow cytometry histograms are shown. Bars represent the mean±SEM of 4 mice. **(B)** Surface levels of C3 on monocyte-derived macrophages vs resident macrophages in the peritoneal lavage fluid of thioglycollate-injected vs control C57BL/6J mice assessed by flow cytometry. Bars represent the mean±SEM of 4 vs 4 mice. Statistical significance was evaluated by two-tailed Student's *t* tests (*****P* < 0.0001). Error bars indicate SEM.

Fig S6. Complement factor H deficiency results in reduced intracellular C3 levels in circulating $Ly6C^{hi}$ monocytes Intracellular C3 levels normalized to cellular protein content in lysates of circulating $Ly6C^{hi}$ monocytes sorted from the blood of $Cfh^{+/+}$ vs $Cfh^{-/-}$ mice. Statistical significance was evaluated by two-tailed Student's *t* tests (*****P* < 0.0001). Error bars indicate SEM.

Fig S7. Purity of adherent monocyte-derived macrophages isolated from the peritoneal cavity of $Cfh^{+/+}$ and $Cfh^{-/-}$ mice Representative flow cytometry plots show the percentage of $CD11b^+F4/80^+$ cells among adherent cells after plating total peritoneal cells isolated from $Cfh^{+/+}$ and $Cfh^{-/-}$ mice measured by flow cytometry.

Fig S8. Uncontrolled complement activation associated with complement factor H deficiency does not lead to increased IL-1β secretion IL-1β levels in the supernatant of monocyte-derived macrophages isolated from peritoneal cavity of thioglycollate-injected $Cfh^{+/+}$ vs $Cfh^{-/-}$ mice measured by ELISA. Each symbol represents individual mice. Statistical significance was evaluated by two-tailed Student's *t* tests. Error bars indicate SEM.

Fig S9. **CFH deficiency leads to a pro-efferocytotic gene expression signature in monocyte-derived macrophages** Heat map of selected genes highly upregulated in CFH deficient Mo-Macs from a genome-wide transcriptome profiling by RNA sequencing.

Fig S10. Complement factor H deficiency enhances the clearance of dying macrophages during sterile peritonitis (A) Enumeration of dying Mo-Macs in the peritoneal lavage fluid of thioglycollate-injected $Cfh^{+/+}$ vs $Cfh^{-/-}$ mice using Annexin V (AnnV)

and 7-aminoactinomycin D (7-AAD) double staining. Representative flow cytometry plots and bar graphs show the frequency of viable ($AnnV^-7\text{-}AAD^-$), apoptotic ($AnnV^+7\text{-}AAD^-$), late apoptotic ($AnnV^+$ $7\text{-}AAD^+$) and necrotic ($AnnV^-$ $7\text{-}AAD^+$) macrophages. The frequencies of necrotic ($AnnV^-$ $7\text{-}AAD^+$), late apoptotic ($AnnV^+$ $7\text{-}AAD^+$) and apoptotic ($AnnV^+7\text{-}AAD^-$) monocyte-derived macrophages (Mo-Macs) in the peritoneal lavage fluid of thioglycollate-injected (72 hours) $Cfh^{+/+}$ vs $Cfh^{-/-}$ mice quantified by flow cytometry. Statistical significance was evaluated by two-tailed Student's *t* tests (**P* < 0.05, ***P* < 0.001). Error bars indicate SEM.

Fig S11. Global complement factor H deficiency does not affect weight gain or lipid levels, but protects from necrotic core formation despite plasma C3 exhaustion and autoantibody production (A-G) $Cfh^{+/+}$ $Ldlr^{-/-}$ vs $Cfh^{-/-}$ $Ldlr^{-/-}$ mice were fed an atherogenic diet for 10 weeks (n=12 vs n=14). **(A)** Final body weight. **(B-C)** Plasma **(B)** cholesterol and **(C)** triglyceride levels measured by an enzymatic automated method. **(D)** Quantification of aortic root plaque size. Values represent the average μm^2 of nine sections throughout the entire aortic origin (400 µm). Representative images of Masson's trichrome-stained sections are shown. Original magnification, 50X; scale bars, 200 µm. **(E)** Assessment of necrotic core formation in cross sections at the aortic origin. Values indicate the percentage of necrotic area per total lesional area throughout the entire aortic origin (400 µm). Representative images of Masson's trichrome-stained sections are shown. Original magnification, 50X; scale bars, 200 µm. Bar graphs show total percentage of necrotic core formation per total lesional area. Each symbol represents individual mice. Representative images are shown. Scale bar, 200 µm. **(F)** Total plasma C3 levels quantified by ELISA. **(G)** Plasma IgG titers specific for double stranded-DNA measured by ELISA. Each symbol represents individual mice. Statistical significance was evaluated by two-tailed Student's *t* tests (**P* < 0.05, ***P* < 0.01, *****P* < 0.0001). Error bars indicate SEM.

MATERIAL AND METHODS

Mice

All experimental studies were approved by the Animal Ethics Committee of the Medical University of Vienna, Austria and were performed according to the guidelines for Good Scientific Practice of the Medical University of Vienna, Austria. All mice were on a C57BL/6 background. *Cfh*$^{-/-}$ mice were generated by Matthew C. Pickering (Pickering et al. 2012). *C3*$^{-/-}$ and *Ldlr*$^{-/-}$ mice were purchased originally from The Jackson Laboratories (Bar Harbor, ME, USA). *Cfh*$^{-/-}$, *C3*$^{-/-}$ and *Ldlr*$^{-/-}$ mice were further crossed to generate *Cfh*$^{-/-}$ *C3*$^{-/-}$, *Cfh*$^{-/-}$ *Ldlr*$^{-/-}$, *C3*$^{-/-}$ *Ldlr*$^{-/-}$ and *Cfh*$^{-/-}$ *C3*$^{-/-}$ *Ldlr*$^{-/-}$ mice.

Bone marrow transplantation studies were performed as previously described (Binder et al. 2004). In short, 8-week-old *Ldlr*$^{-/-}$ mice or 10-week-old *Cfh*$^{-/-}$ mice were lethally irradiated (2x 6Gy) and were subsequently injected intravenously via the retro-orbital plexus with $3x10^6$ *Cfh*$^{+/+}$ or *Cfh*$^{-/-}$ bone marrow from 6-week-old donors. The recipient mice were given a 5-week recovery period before intervention studies. Successful bone marrow reconstitution was verified by extracting and amplyfing genomic DNA from the bone marrow of the recipient mice.

For inducing sterile peritonitis, mice were intraperitoneally injected with a single dose of 50µl/g/body weight sterile thioglycollate (Thermo Fisher Scientific, Difco Laboratories, Waltham, MA, USA) and were sacrificed 24 hours, 72 hours or 168 hours post injection.

All mice were bred in our in-house breeding facility. All experiments were performed with age- and sex-matched adult littermates (i.e. 8 weeks of age or older).

Diets

If not indicated otherwise, all mice received non-atherogenic rodent chow. For dietary intervention studies, experimental mice were fed a Western type diet containing 21% milk fat and 0.2% cholesterol (E15721-347, Ssniff Spezialdiäten GmbH, Soest, Germany) for 10-12 weeks.

Evaluation of atherosclerosis

The extent of atherosclerosis was assessed as previously described (Binder et al. 2003). Shortly, lesion formation in the entire aorta was evaluated in *en face* preparations by staining the luminal surface with Sudan IV (Sigma Aldrich, St. Louis, MO, USA). Atherosclerosis in

the aortic origin was quantified in modified elastin-trichrome stained, 5 µm-thick serial sections through a 400 µm segment of the aortic root starting upon the appearance of all 3 valve leaflets. For each mouse, 9 sections separated by 50 µm were examined and total lesion volume was determined. Necrotic core formation was quantified as the percent of acellular area compared to total lesional area. Each section was photographed using the AxioVison software (Carl Zeiss AG, Jena, Germany) and lesion size was assessed in a blinded fashion by computer-assisted image analysis using Adobe Photoshop CS5 (Adobe Inc., San Jose, CA, USA) and ImageJ software,

Immunohistochemistry in aortic root lesions

For the quantification of lesional macrophage content or ATG5 expression, sections of aortic root lesions were stained with an anti–mouse MAC-3 antibody (clone M3/84, BD Pharmingen, San Diego, CA, USA) or with a polyclonal anti-mouse ATG5 antibody (Novus Biologicals, Centennial, CO, USA), respectively. Sections were then stained with a biotinylated goat anti-rat IgG (VectorLabs, Burlingame, CA, USA) and were developed with streptavidin-peroxidase polymer (Sigma Aldrich). Quantification was performed with computer-assisted image analysis using Adobe Photoshop CS5 (Adobe Inc.) and ImageJ software.

Quantification of lesional apoptosis and *in situ* efferocytosis assay

Sections of aortic root lesions were de-paraffinized with xylene (Carl Roth, Karlsruhe, Germany) and were rehydrated in decreasing concentrations of ethanol (Carl Roth). The specimens were then boiled in 1x citrate buffer (Sigma Aldrich; pH 6.0) for antigen retrieval. After cooling, the sections were incubated with TUNEL using the In Situ Cell Death Detection Kit TMR-Red (Roche Diagnostics, Rotkreuz, Switzerland) according to the manufacturer's instructions at 37°C for 60 min in a dark, humidified atmosphere and then washed 3 times with 1X DPBS (Sigma Aldrich). Sections were then blocked with 10% donkey serum (Sigma Aldrich) in 1X DPBS supplemented with 1% bovine serum albumin (BSA; PAN-Biotech GmbH, Aldenbach, Germany) for 60 min and were incubated overnight at 4°C with a rabbit anti-mouse F4/80 antibody (clone: D2S9R, Cell Signaling Technology, Cambridge, UK; 1:200). Following 3 washing steps with 1X DPBS, sections were incubated with a polyclonal donkey anti-rabbit IgG (H+L) antibody conjugated to Alexa Fluor 647 (Jackson ImmunoResearch, West Grove, PA, USA; 1:500) for 2 hours and after intensive washing with 1X DPBS, were counterstained with 4',6-diamidino-2-phenylindole (DAPI, Sigma Aldrich; 1:2000) for 5 min. Slides were mounted in Fluoromount (Thermo Fisher Scientific). Representative fields (six to eight fields of each valve leaflet in a 200 µm depth) were

photographed with Axio Imager A1 (Carl Zeiss AG). For the quantification of apoptotic macrophages, only TUNEL$^+$F4/80$^+$ cells that co-localized with DAPI-stained nuclei were counted as being positive. *In situ* efferocytosis was quantified as described by Wang et al. 2017. Shortly, the ratio of TUNEL$^+$ nuclei that were associated with F4/80$^+$ macrophages ('macrophage-associated' apoptotic cells), indicative of efferocytosis, or not associated with F4/80$^+$ macrophages ('free' apoptotic cells) was determined.

Liver Histology

The left lobe of each liver was isolated and four equal pieces were snap frozen in liquid nitrogen for further analyses. To assess the level of macrophage infiltration, 7 µm-thick frozen liver sections were stained with an anti-Mac1 antibody (clone M1/70; R&D Systems, Minneapolis, MN, USA; 1:500) as described previously (Busch & Hendrikx et al. 2017). Cell nuclei were counterstained with hematoxylin (VWR, Klinipath, Radnor, PA, USA). Pictures were taken with a Nikon digital camera DMX1200 (Nikon, Tokyo, Japan) and ACT-1 v2.63 software. To determine the extent of liver inflammation, the number of Mac1$^+$ cells was counted in a blinded fashion using six images (200X) per each liver.

Primary cell isolation, flourescence-activated cell sorting and flow cytometry

Spleens were mechanically dissociated through a 100 µm cell strainer (BD Biosciences, Franklin Lakes, NJ, USA) and red blood cells were lysed in red blood cell lysis buffer (Morphisto, Frankfurt am Main, Germany). Peripheral blood was collected via the vena cava (in a MiniCollect EDTA blood collection TUBE; Greiner Bio-One, Kremsmünster, Austria) and red blood cells were lysed in red blood cell lysis buffer. Peritoneal exudate cells were harvested by peritoneal lavage using ice-cold HBSS (Thermo Fisher Scientific) supplemented with 2% fetal calf serum (FCS; Thermo Fisher Scientific, Gibco). Total viable cells were counted manually using a hemocytometer or by CASY cell counter & analyzer (OLS-OMNI Life Science GmbH, Bremen, Germany). For flourescence-activated cell sorting, the whole cell suspension was incubated with 2.5 µg/ml of a blocking anti-CD16/32 antibody (Clone 90, Thermo Fisher Scientific, eBioscience) diluted in 1X DPBS (Sigma Aldrich) supplemented with 1% FCS for 20 min at 4°C. After two washing steps, cells were stained with the following monoclonal antibodies: anti-CD11b APC (clone M1/70, Thermo Fisher Scientific, eBioscience), anti-Ly6C FITC (clone HK1.4, BioLegend, San Diego, CA, USA), anti-Ly6G PE (clone 1A8, BioLegend), anti-F4/80 PerCP-Cy5.5 (clone BM8, BioLegend), anti-CD45R (B220) PerCP-Cy5.5 (clone RA3-6B2, Thermo Fisher Scientific, eBioscience), anti-CD43 PE (clone S7, BD Biosciences), anti-CD23 FITC (clone B3B4, BD Biosciences), biotinylated anti-CD21/35 (clone 7E9, BioLegend), anti-CD3e PE (clone 145-2C11, Thermo

Fisher Scientific, eBioscience), anti-CD4 FITC (clone GK1.5, Thermo Fisher Scientific, eBioscience), anti-CD8a APC (clone 53-6.7; Thermo Fisher Scientific, eBioscience) and streptavidin APC (Thermo Fisher Scientific, eBioscience). Data were acquired on a SH800S Cell Sorter (Sony Biotechnology, San Jose, CA, USA) and were analyzed using FlowJo software 10 (Tree Star, Ashland, OR, USA).

For flow cytometry, $1x10^6$ cells were added in a 96-well V-bottom plate (Thermo Fisher Scientific) and incubated with 2.5 µg/ml of a blocking anti-CD16/32 antibody (Clone 90, Thermo Fisher Scientific, eBioscience) diluted in 1X DPBS supplemented with 1% FCS for 20 min at 4°C. After two washing steps, cells were stained with the following monoclonal antibodies: anti-CD11b APC (clone M1/70, Thermo Fisher Scientific, eBioscience), anti-Ly6C FITC (clone HK1.4, BioLegend), anti-Ly6G PE (clone 1A8, BioLegend), anti-F4/80 PerCP-Cy5.5 (clone BM8, BioLegend), anti-C5aR1 (CD88) PE-Cy7 (clone 20/70, BioLegend), anti-C5aR2 (C5L2) Alexa Fluor 700 (clone 468705, R&D Systems, Minneapolis, MN, USA), anti-C3aR Alexa Fluor 488 (14D4, Hycult Biotech, Wayne, PA, USA), anti-C3/C3b/iC3b,/C3c Alexa Fluor 488 (clone 3/26, Hycult) and anti-C3a Alexa Fluor 488 (clone mAb 3/11, Hycult). All unconjugated antibodies were labelled using the Alexa Fluor 488 Antibody Labeling Kit (Thermo Fisher Scientific, Invitrogen).

To determine the amount of intracellular C3, C3a, C3aR, C5aR1 and C5aR2, cells were first incubated with the unconjugated form of the respective antibody and were fixed and permeabilized with Fixation and Permeabilization Solution (Thermo Fisher Scientific, eBioscience) for 20 minutes at 4 °C and then stained intracellularly in permeabilization buffer (Thermo Fisher Scientific, eBioscience) with the respective conjugated antibodies stated above. For intracellular human CFH staining, THP-1 macrophages were fixed and permeabilized as stated above and then stained intracellularly in permeabilization buffer (Thermo Fisher Scientific, eBioscience) with anti-CFH (clone OX-24, Cedarlane Laboratories, Burlington, ON, Canada) followed by a secondary antibody staining using anti-IgG1 kappa APC (clone P3.6.2.8.1, Thermo Fisher Scientific, eBioscience). All stainings were carried out in 1X DPBS supplemented with 1% FCS for 30 min at 4°C, followed by two washing steps. Finally, to identify early and late dead cells staining with Annexin V and 7-AAD viability solution was performed according to the manufacturer's protocol (Thermo Fisher Scientific, eBioscience). Data were acquired on a BD FACSCalibur (BD Biosciences) or BD LSRII Fortessa (BD Biosciences) and were analyzed using FlowJo software 10 (Tree Star).

Plasma cholesterol and triglyceride quantification

Blood was collected from the vena cava (in a MiniCollect EDTA blood collection TUBE; Greiner Bio-One) at the time of sacrifice. Blood was centrifuged at 1000g for 30 minutes at room temperature. Plasma total cholesterol and triglyceride were measured in an ISO 15189 accredited medical laboratory under standardized conditions on Beckman Coulter AU5400 (Beckman Coulter, Brea, CA, USA) instruments, using the Beckman Coulter OSR6516 reagent.

Quantification of complement component levels

To measure plasma concentrations of complement components, peripheral blood was collected from the vena cava (in a MiniCollect EDTA blood collection TUBE; Greiner Bio-One) at the time of sacrifice. Blood was centrifuged at 1000g for 30 minutes at room temperature and plasma samples were snap frozen in liquid nitrogen for further use. To determine the intracellular levels of complement components in monocyte-derived macrophages (Mo-Macs), peritoneal exudate cells were harvested from thioglycollate-injected wildtype and *Cfh*$^{-/-}$ mice by peritoneal lavage using ice-cold HBSS (Thermo Fisher Scientific, Gibco) supplemented with 2% fetal calf serum (FCS; Thermo Fisher Scientific, Gibco). Total viable cells were counted by CASY cell counter & analyzer (OLS-OMNI Life Science GmbH) and cells were plated in equivalent numbers in RPMI-1640 medium (Thermo Fisher Scientific, Invitrogen) containing 10% FCS at 37°C for 60 minutes. Non-adherent cells were removed by washing three times with ice-cold 1X DPBS (Sigma Aldrich). The purity of adherent Mo-Macs was confirmed by flow cytometry as above. Adherent Mo-Macs were lysed in an IP protein lysis buffer containing 50 mM Tris (Sigma Aldrich, pH 7.5), 150 mM NaCl (Carl Roth), 5 mM EDTA (Sigma Aldrich), 5 mM EGTA (Sigma Aldrich) and 1% NP-40 (Merck, Calbiochem, Darmstadt, Germany). Lysates of adherent Mo-Macs were kept at -20°C or used immediately. The concentration of complement components was determined by specific ELISA kits including the Mouse C3 ELISA kit (Abcam, Cambridge, UK), the Mouse C3a ELISA Kit (MyBioSource, San Diego, CA, USA) and the Mouse Complement Component C5a DuoSet ELISA (R&D Systems), according to the manufacturer's recommendations. To quantify plasma CFH levels, a self-established sandwich ELISA was set up using a monoclonal and a polyclonal anti-mouse CFH antibody (both R&D systems). As a measure of C3 consumption, C3a/C3 ratio was calculated based on total C3a concentrations divided by the total C3 levels of each individual sample. For intracellular measurements, total protein content of the lysates was quantified using Pearce BCA Protein Assay Kit (Thermo Fisher Scientific) and was used to normalize complement component levels.

Quantification of secreted interleukin-1 beta

Mo-Macs were isolated and plates as stated above. Adherent Mo-Macs were cultured in RPMI-1640 medium (Thermo Fisher Scientific, Invitrogen) containing 10% fetal calf serum (FCS; Thermo Fisher Scientific, Gibco) at 37°C for 24 hours and the supernatant were collected and spun down at 400g for 5 minutes. The concentrations of interleukin-1 beta in cell supernatants were quantified by the IL-1 beta Mouse Uncoated ELISA Kit (Thermo Fisher Scientific, Life Technologies) according to the manufacturer's instructions. Samples were developed using TMB substrate solution (BD Biosciences) and the reaction was terminated with 1M H_2SO_4 (Honeywell, Morristown, NJ, USA). The absorbance was measured with a Synergy 2 plate reader (BioTek Instruments, Winooski, VT, USA) at 450 nm as the primary wavelength.

Antibody measurements

Anti-dsDNA IgG antibodies were quantified as previously described (Kiss et al. 2019). In short, 96-well Nunc MaxiSorp plates (Thermo Fisher Scientific) were irradiated with UV light and coated with calf thymus DNA (Thermo Fisher Scientific, Invitrogen; 5 µg/ml) in 1X DPBS (Sigma Aldrich). After overnight incubation at 4°C, plates were blocked in 1% bovine serum albumin (BSA; PAN-Biotech GmbH) in 1X DPBS. Plasma samples were added in 1:200 dilutions and the signal was detected with HRP-conjugated anti-mouse IgG (1:1000, GE Healthcare, Chicago, IL, USA). The absorbance was measured with a Synergy 2 plate reader (BioTek Instruments) at 450 nm as the primary wavelength.

Cell lines

Human THP-1 monocytic cells and murine RAW 264.7 macrophages were purchased from ATCC (Manassas, VA, USA) and were maintained in presence of RPMI-1640 (Thermo Fisher Scientific, Invitrogen) supplemented with 10% heat-inactivated fetal calf serum (FCS; Thermo Fisher Scientific, Gibco). All cells were incubated in a humidity-controlled environment at 37°C, 5% CO_2 (Thermo Scientific Heraeus Cytoperm 2).

Generation and stimulation of THP-1-derived macrophages

To obtain THP-1-derived macrophages, cells were stimulated for 24 hours with 100 nM phorbol-12-myristate-13-acetate (PMA; Sigma Aldrich). After 1-2 days, THP-1 macrophages were stimulated in culture medium containing 100 ng/ml recombinant human interferon-gamma (BioLegend).

Generation of CMFDA-labeled apoptotic RAW 264.7 macrophages

RAW 264.7 macrophages were plated on a cell culture dish (100x20 mm, CELLSTAR, Greiner Bio-One) and were incubated in RPMI-1640 medium (Thermo Fisher Scientific, Invitrogen) containing 5 µM CellTracker Green chloromethylfluorescein diacetate (CMFDA; Thermo Fisher Scientific, Invitrogen) in the absence of serum for 30 min at 37°C. After replacing the medium with 1X DPBS (Sigma Aldrich), apoptosis of RAW 264.7 macrophages was induced by UVC irradiation (100mJ/cm^2) using a UVP CX-2000 UV Crosslinker (Analytik Jena, Jena, Germany). Following the irradiation, cells were maintained in RPMI-1640 medium containing sterile bovine serum albumin (BSA; PAN-Biotech GmbH; 50µg/ml) in a humidity-controlled environment at 37°C, 5% CO2 for 16 hours.

***Ex vivo* efferocytosis assay**

Peritoneal exudate cells were harvested as stated above. Non-adherent cells were removed by two times washing with fresh medium. Adherent monocyte-derived macrophages (Mo-Macs) were cultured in RPMI-1640 medium (Thermo Fisher Scientific, Invitrogen) in the presence of 1% of respective sera at 37°C overnight and were subsequently incubated with CMFDA-labeled apoptotic RAW macrophages in a 1:3 ratio for 1.5 hours. After discarding the supernatant, cells were washed three times in ice-cold 1x DPBS (Sigma Aldrich) and were detached using a cell scraper (Sigma Aldrich). Mo-Macs were then taken in collection tubes and the percentages of CMFDA$^+$ efferocytotic cells were quantified on a BD FACSCalibur (BD Biosciences) and were analyzed using FlowJo software 10 (Tree Star).

LC3 conversion assay

Protein loading was normalized in each lysate of adherent monocyte-derived macrophages using a Pearce BCA Protein Assay Kit (Thermo Fisher Scientific, Gibco). After resuspending the lysates in 1x Laemmli buffer (Bio-Rad Laboratories, Hercules, CA, USA) and heating the samples up to 96°C, proteins were separated on a polyacrylamide gel (Bio-Rad Laboratories), transferred to polyvinylidenfluorid (PVDF) membranes (Bio-Rad Laboratories), blocked with 5% non-fat dry milk (Bio-Rad Laboratories) in 1x TBS (Sigma Aldrich, St. Louis, MO, USA) containing 1% bovine serum albumin (BSA; PAN-Biotech GmbH, Aldenbach, Germany) and incubated with a goat anti-mouse LC3 antibody (GeneTex, Irvine, CA, USA; 1:1000). As secondary antibody, goat anti-rabbit IgG-HRP (Bio-Rad Laboratories) was used and the subsequent chemiluminescent quantification was performed on ChemiDoc imager (Bio-Rad Laboratories). The signal was measured with Image Lab 4.1 analysis software (Bio-Rad Laboratories).

Generation and stimulation of bone-marrow-derived macrophages

To obtain bone-marrow derived macrophages (BMDM), bone marrow cell suspensions were isolated by flushing femurs and tibiae of C57BL/6J mice through a 26-gauge needle (BD Biosciences) with 1% fetal calf serum (FCS; Thermo Fisher Scientific, Gibco) in 1x DPBS (Sigma Aldrich) and red blood cells were lysed as stated above. BMDMs were then cultured in the presence of RPMI-1640 (Thermo Fisher Scientific, Invitrogen), 10% heat-inactivated FCS, penicillin (100 U/ml), streptomycin (100 µg/ml) and antimycotics (all Sigma Aldrich), supplemented with 10% L929-conditioned medium. After 7-8 days, BMDMs were stimulated in culture medium containing 100 ng/ml recombinant mouse interferon-gamma (R&D Systems).

Gene expression analyses

Total RNA was isolated from tissue, cell culture or sorted cell subsets using the RNeasy Mini Kit (VWR, PeqLab) and total RNA was reversely transcribed using the High Capacity cDNA Reverse Transcription kit (Thermo Fisher Scientific, Applied Biosystems). Quantitative real-time PCR was performed using Kapa SYBR Fast Bio-Rad iCycler with ROX dye (Roche Diagnostics, Kapa Biosystems) in a CFX96 Real-time System (Bio-Rad Laboratories). All data were normalized to the housekeeping gene Cyclin B1 (CycB1) and/or 36B4. Values are expressed as the relative expression compared to untreated samples or the control group/cell type.

Primer sequences

mm CycB1-forward: 5'-CAGCAAGTTCCATCGTGTCATCA-3'

mm CycB1-reverse: 5'-GGAAGCGCTCACCATAGATGCTC-3'

mm 36B4-forward: 5'-AGGGCGACCTGGAAGTCC-3'

mm 36B4-reverse: 5'-CCCACAATGAAGCATTTTGGA-3'

mm Cfh-forward: 5'-ACCACATGTGCCAAATGCTA-3'

mm Cfh-reverse: 5'-TGTTGAGTCTCGGCACTTTG-3'

mm C4bp-forward: 5'-CCTGGCTATGGTAGGGGAAT-3'

mm C4bp-reverse: 5'-CCTCGGACCTCACAAGAACT-3'

mm Cr1l-forward: 5’-ACTCAACCTGGACGAGTGCT-3’

mm Cr1l-reverse: 5’-CTGGGGGTATCTCACAAGGA-3’

mm Cd55b-forward: 5’-TCAACATACCAACCGGCATA-3’

mm Cd55b-reverse: 5’-TTGGTGGGTCTGGACAAAAT-3’

mm Cd55-forward: 5’-TAATGCGAGGGGAAAGTGAC-3’

mm Cd55-reverse: 5’-TGAGGGGGTTCCTGTACTTG-3’

mm Cfi-forward: 5’-TGTGTGAATGGGAAGCACAT-3’

mm Cfi-reverse: 5’-CACAACGGCTCTCATCTTCA-3’

mm Cfd-forward: 5’-TGCACAGCTCCGTGTACTTC-3’

mm Cfd-reverse: 5’-CACCTGCACAGAGTCGTCAT-3’

mm Fhr-b-forward: 5’-GTACAGAGAATGGCTGGTC-3’

mm Fhr-b-reverse: 5’-AGTGATCCTCTTGCTTTCTG-3’

mm Cxcl1-forward: 5’-TGCACCCAAACCGAAGTCAT-3’

mm Cxcl1-reverse: 5’-TTGTCAGAAGCCAGCGTTCAC-3’

mm Cxcl2-forward: 5’-AGTGAACTGCGCTGTCAATGC-3’

mm Cxcl2-reverse: 5’-AGGCAAACTTTTTGACCGCC-3’

mm Tnfa-forward: 5’-CATCTTCTCAAAATTCGAGTGACAA-3’

mm Tnfa-reverse: 5’-TGGGAGTAGACAAGGTACAACCC-3’

mm C3-forward: 5’-AGAAAGGGATCTGTGTGGCA-3’

mm C3-reverse: 5’- GAAGTAGCGATTCTTGGCGG-3’

10X Genomics

10x Genomics Single Cell Gene Expression workflow was performed with the Chromium Single Cell 3' v3 Chemistry according to manufacturer's recommendations. Raw reads were demultiplexed using cellranger (version 2.1.0) mkfastq. Demultiplexed reads were aligned to the mouse genome provided by 10x genomics (mm10 genome version 1.2.0) using cellranger count. Data were analyzed and visualized using Loupe Cell Browser 3.1.1.

RNA-sequencing

NGS Library Preparation

Total RNA concentration was quantified by using the Qubit 2.0 Fluorometric Quantitation System (Life Technologies, Carlsbad, CA, USA). The RNA integrity number (RIN) was determined by applying the Experion Automated Electrophoresis System (Bio-Rad, Hercules, CA, USA). RNA-seq libraries were prepared by using the TruSeq Stranded mRNA LT sample preparation kit (Illumina, San Diego, CA, USA) and the Sciclone and Zephyr liquid handling workstations (PerkinElmer, Waltham, MA, USA) for pre- as well as post-PCR procedures, respectively. Library concentrations were measured with the Qubit 2.0 Fluorometric Quantitation System (Life Technologies, Carlsbad, CA, USA) and the size distribution was evaluated by using the Experion Automated Electrophoresis System (Bio-Rad, Hercules, CA, USA). For the sequencing step, samples were diluted and pooled into Next-Generation Sequencing (NGS) libraries in equimolar amounts.

Sequencing and Raw Data Processing

Expression profiling libraries were sequenced by HiSeq 3000/4000 instruments (Illumina, San Diego, CA, USA) in 50-base-pair, single-end conditions. The base calls were provided by the real-time analysis (RTA) software (Illumina, San Diego, CA, USA) and were subsequently converted into multiplexed, unaligned BAM format followed by demultiplexing into sample-specific, unaligned BAM files. For the raw data processing of the instruments, Picard-tool based custom programs were used.

Transcriptome Analysis

[Tuxedo Suite]

Transcriptome analysis was carried out with the Tuxedo suite. For each individual sample, NGS reads tested by vendor quality filtering were aligned to the UCSC Genome Browser

[mm10] flavor of the Genome Reference Consortium [GRCm38] assembly with TopHat2 (v2.1.1), a splice junction mapper using the Bowtie2 (v2.2.9) short read aligner. Therefore, "basic" Ensembl transcript annotation (version e87; December 2016) served as reference transcriptome. Based on spliced read alignments and the reference transcriptome joint with raw transcript quantification, Cufflinks (v2.2.1) allowed for transcriptome assembly. Ahead of differential expression calling with Cuffdiff (included in Cufflinks v2.2.1), transcriptome sets of each individual sample of each group was combined via the Cuffmerge algorithm. Lastly, the cummeRbund and biomaRt Bioconductor packages were used in custom R scripts for performing quality assessment and further refinement of the results from the analysis.

[STAR Aligner and DESeq2]

NGS reads were mapped onto the Genome Reference Consortium [GRCm38] assembly together with the “Spliced Transcripts Alignment to a Reference” (STAR) aligner using the “basic” Ensembl transcript annotation (version e87; December 2016) serving as the reference transcriptome. As the [mm10] assembly flavor of the UCSC Genome Browser was favored for alignment as well as for downstream data processing with Bioconductor packages, Ensembl transcript annotation needed to be adjusted to UCSC Genome Browser sequence region names ahead of the alignment. Reads overlapping transcript features were determined by using the summarizeOverlaps() function of the Bioconductor GenomicAlignments package also taking into consideration that the Illumina TruSeq stranded mRNA protocol results in sequencing of the second strand, therefore all reads required inverting before counting. The Bioconductor DESeq2 package was then applied to model the data set and identify differentially expressed genes.

Statistical analysis

Statistical analyses were performed using Graph Pad Prism 8 for Windows (Graph Pad Software, La Jolia, CA, USA). Normal distribution of data was assessed and experimental groups were compared using two tailed Student’s unpaired or paired t test or Mann-Whitney U test, as appropriate. Data points, which were more than 2X SD of the mean, were excluded as statistical outliers. Data are presented as mean ± SEM and considered significant at $p \leq 0.05$ (*$p \leq 0.05$, **$p \leq 0.01$, ***$p \leq 0.001$ and ****$p \leq 0.0001$, respectively).

Figure 1

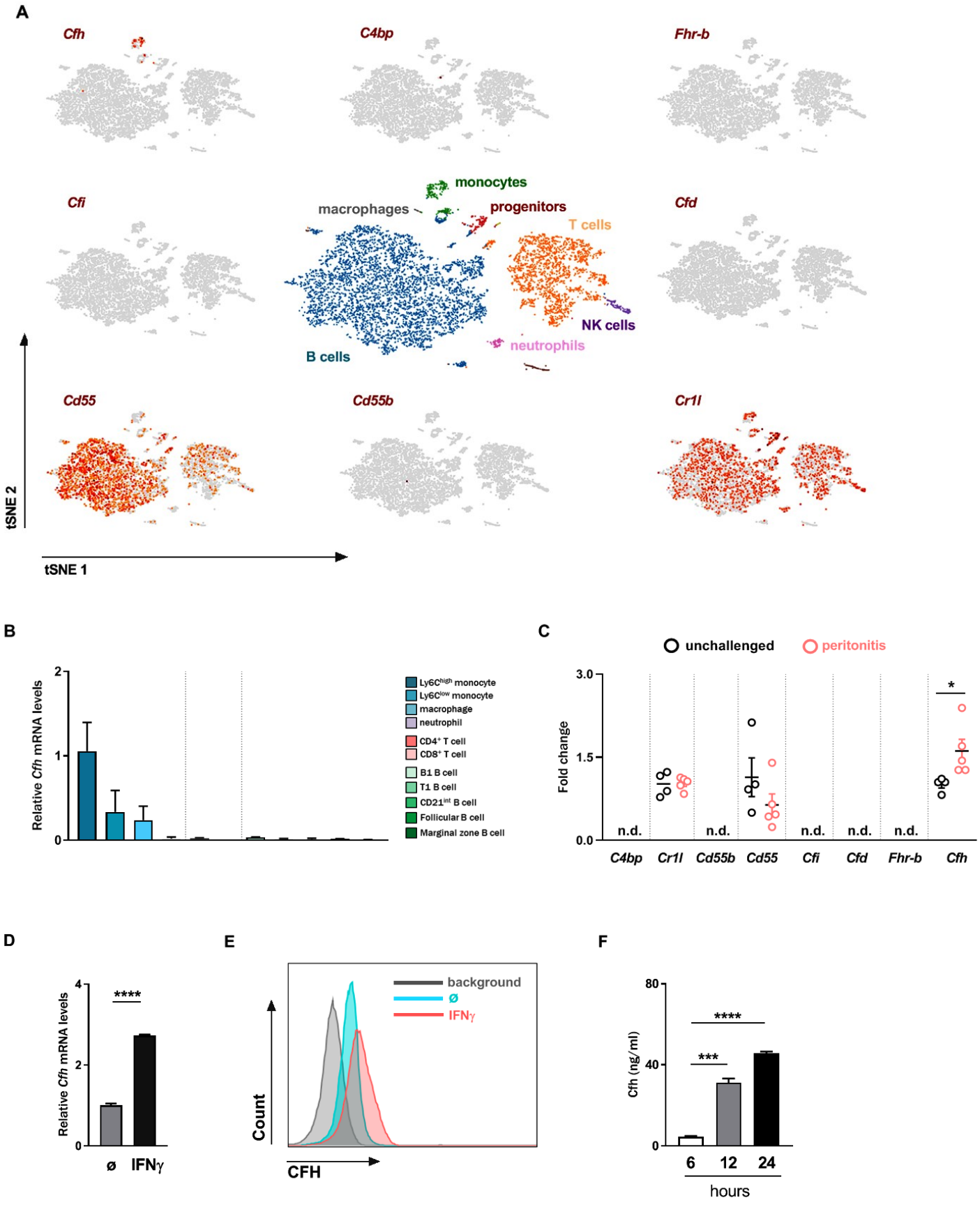
A
Cfh
C4bp
Fhr-b
Cfi
monocytes
macrophages
progenitors
T cells
Cfd
NK cells
neutrophils
B cells
Cd55
Cd55b
Cr1l
tSNE 2
tSNE 1
B
Relative Cfh mRNA levels
Ly6C^high monocyte
Ly6C^low monocyte
macrophage
neutrophil
CD4+ T cell
CD8+ T cell
B1 B cell
T1 B cell
CD21^int B cell
Follicular B cell
Marginal zone B cell
C
unchallenged
peritonitis
Fold change
n.d.
C4bp
Cr1l
Cd55b
Cd55
Cfi
Cfd
Fhr-b
Cfh
D
Relative Cfh mRNA levels
****
ø
IFNγ
E
background
ø
IFNγ
Count
CFH
F
Cfh (ng/ml)
****
***
6
12
24
hours

Figure 2

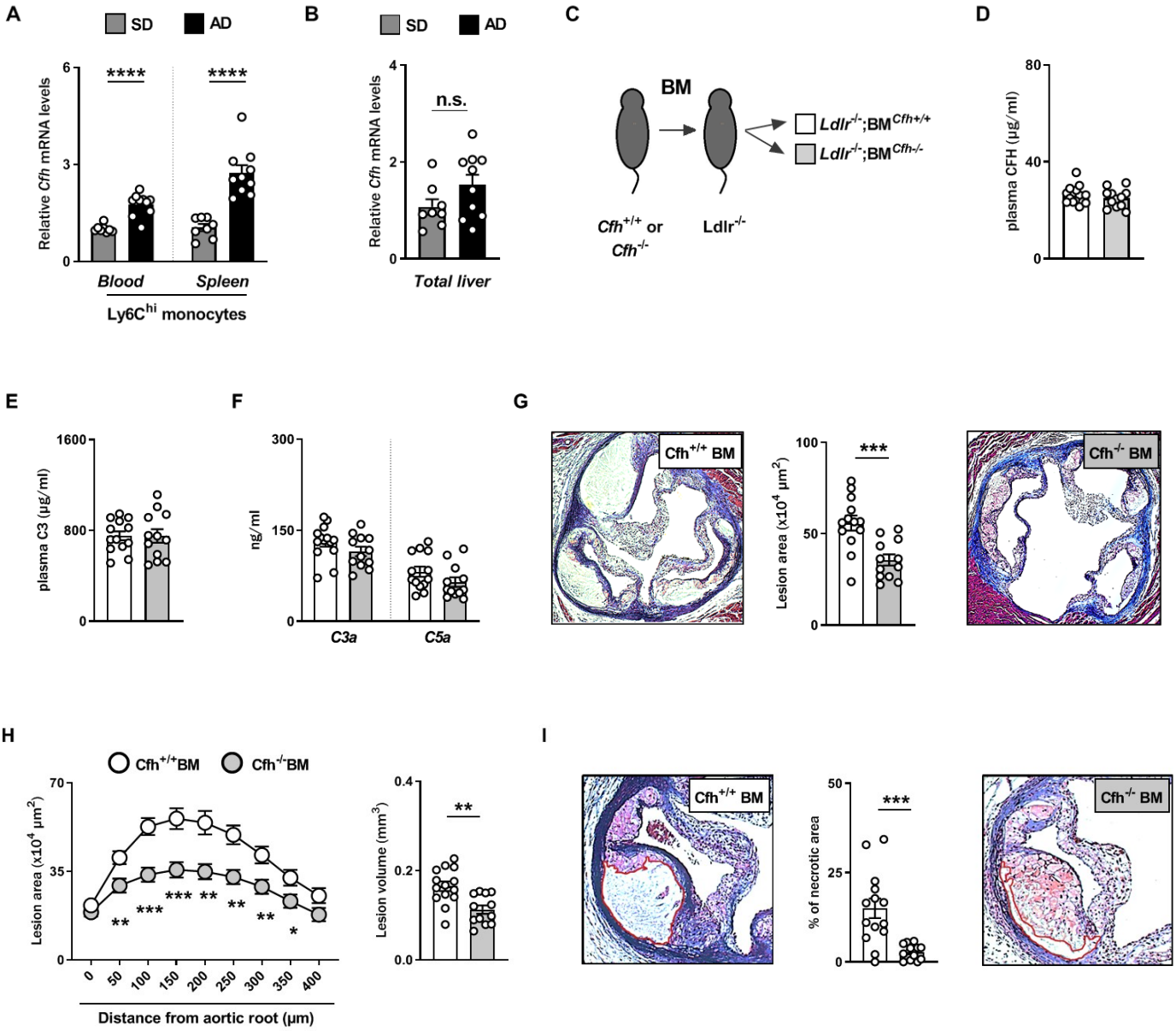
A
SD
AD
Relative Cfh mRNA levels
****
****
Blood
Spleen
Ly6C^hi monocytes
B
SD
AD
Relative Cfh mRNA levels
n.s.
Total liver
C
BM
Ldlr-/-;BM Cfh+/+
Ldlr-/-;BM Cfh-/-
Cfh+/+ or Cfh-/-
Ldlr-/-
D
plasma CFH (µg/ml)
E
plasma C3 (µg/ml)
F
ng/ml
C3a
C5a
G
Cfh+/+ BM
Lesion area (x10^4 µm^2)
***
Cfh-/- BM
H
Cfh+/+BM
Cfh-/-BM
Lesion area (x10^4 µm^2)
Distance from aortic root (µm)
Lesion volume (mm^3)
**
I
Cfh+/+ BM
% of necrotic area
***
Cfh-/- BM

Figure 3

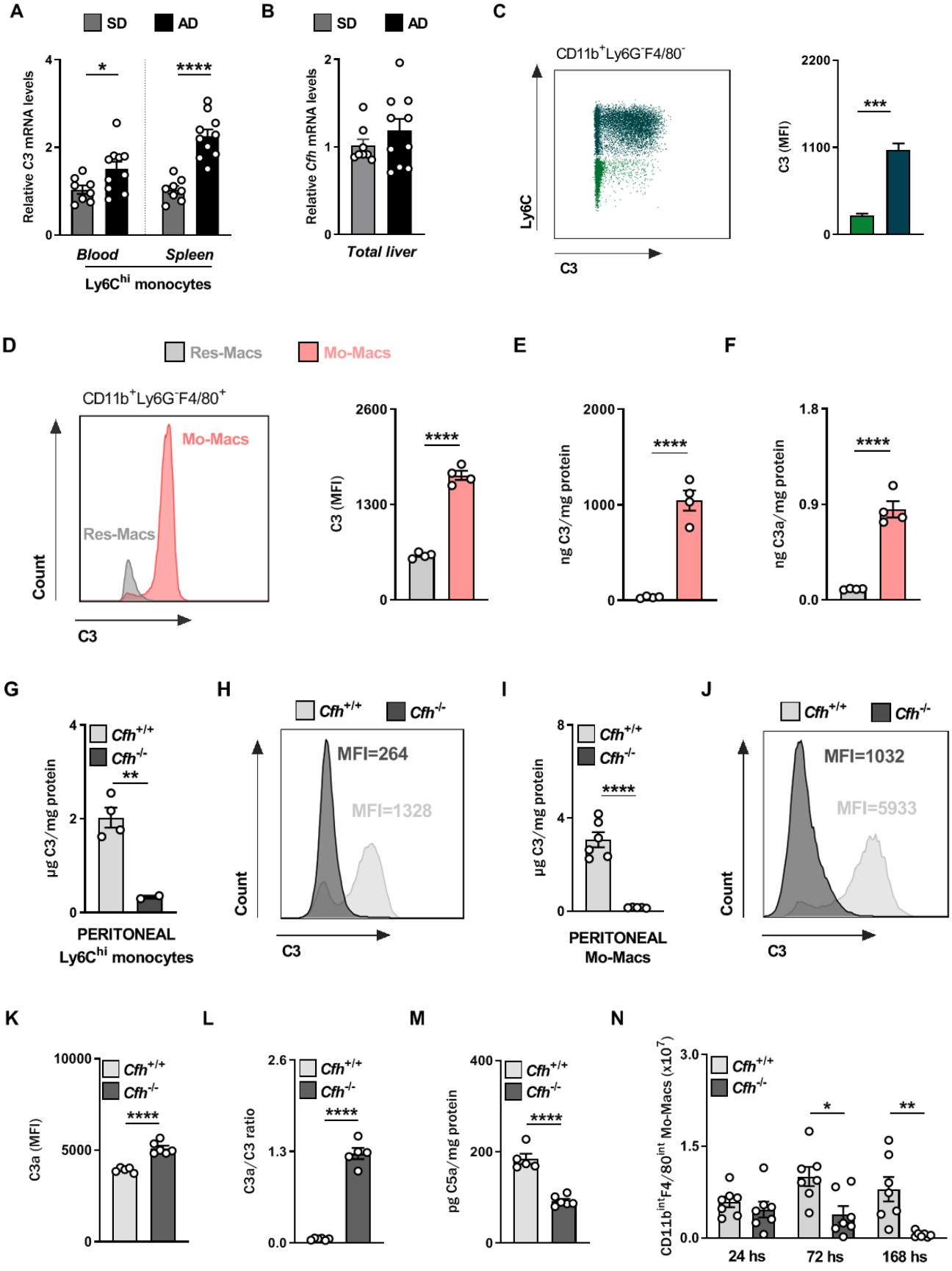
A
SD
AD
Relative C3 mRNA levels
*
****
Blood
Spleen
Ly6C^hi monocytes
B
SD
AD
Relative Cfh mRNA levels
Total liver
C
CD11b+Ly6G-F4/80-
Ly6C
C3
C3 (MFI)
***
D
Res-Macs
Mo-Macs
CD11b+Ly6G-F4/80+
Mo-Macs
Res-Macs
Count
C3
C3 (MFI)
****
E
ng C3/mg protein
****
F
ng C3a/mg protein
****
G
Cfh+/+
Cfh-/-
µg C3/mg protein
**
PERITONEAL
Ly6C^hi monocytes
H
Cfh+/+
Cfh-/-
MFI=264
MFI=1328
Count
C3
I
Cfh+/+
Cfh-/-
µg C3/mg protein
****
PERITONEAL
Mo-Macs
J
Cfh+/+
Cfh-/-
MFI=1032
MFI=5933
Count
C3
K
Cfh+/+
Cfh-/-
C3a (MFI)
****
L
Cfh+/+
Cfh-/-
C3a/C3 ratio
****
M
Cfh+/+
Cfh-/-
pg C5a/mg protein
****
N
Cfh+/+
Cfh-/-
CD11b^int F4/80^int Mo-Macs (x10^7)
*
**
24 hs
72 hs
168 hs

Figure 3 cont.

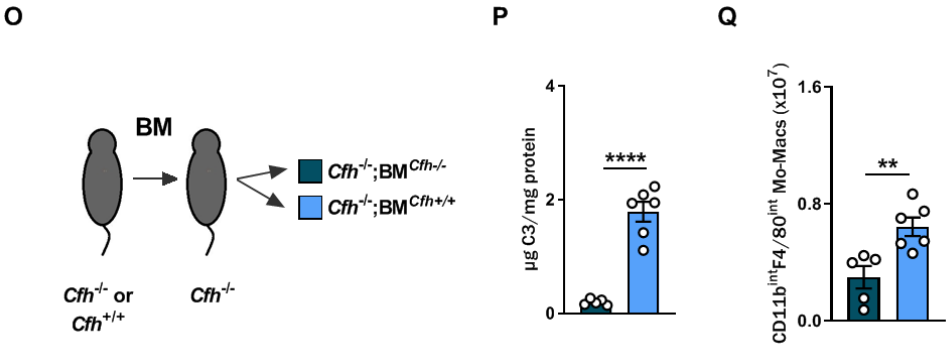

Figure 4

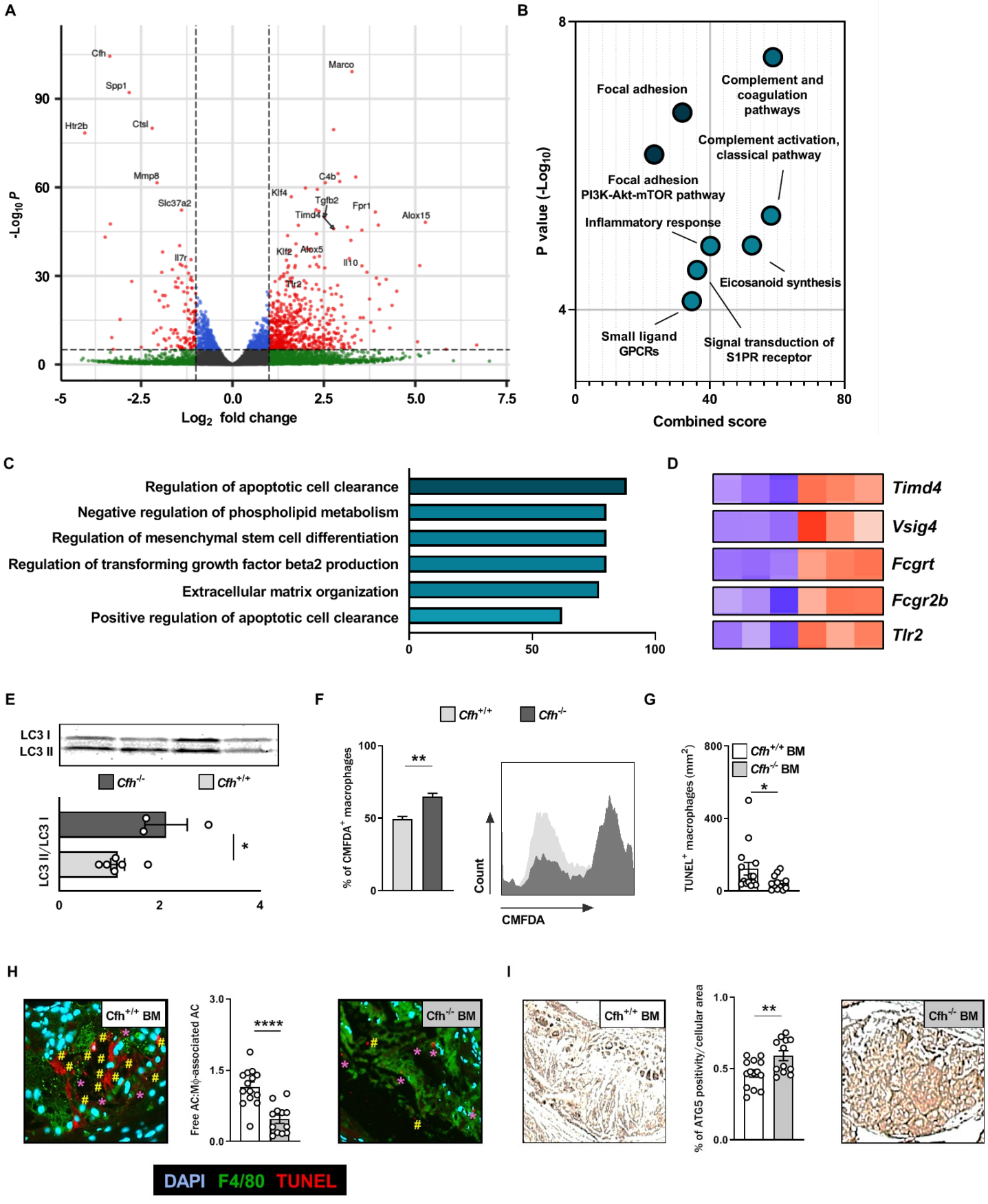
A
Cfh
Spp1
Htr2b
Ctsl
Mmp8
Slc37a2
Il7r
Marco
C4b
Klf4
Tgfb2
Timd4
Fpr1
Alox15
Klf2
Alox5
Il10
Tlr2
-Log10 P
Log2 fold change
B
Focal adhesion
Complement and coagulation pathways
Complement activation, classical pathway
Focal adhesion PI3K-Akt-mTOR pathway
Inflammatory response
Eicosanoid synthesis
Small ligand GPCRs
Signal transduction of S1PR receptor
P value (-Log10)
Combined score
C
Regulation of apoptotic cell clearance
Negative regulation of phospholipid metabolism
Regulation of mesenchymal stem cell differentiation
Regulation of transforming growth factor beta2 production
Extracellular matrix organization
Positive regulation of apoptotic cell clearance
D
Timd4
Vsig4
Fcgrt
Fcgr2b
Tlr2
E
LC3 I
LC3 II
Cfh-/-
Cfh+/+
LC3 II/LC3 I
F
Cfh+/+
Cfh-/-
% of CMFDA+ macrophages
Count
CMFDA
G
Cfh+/+ BM
Cfh-/- BM
TUNEL+ macrophages (mm2)
H
Cfh+/+ BM
Cfh-/- BM
Free AC:Mϕ-associated AC
DAPI F4/80 TUNEL
I
Cfh+/+ BM
Cfh-/- BM
% of ATG5 positivity/cellular area

Supplementary figure 1

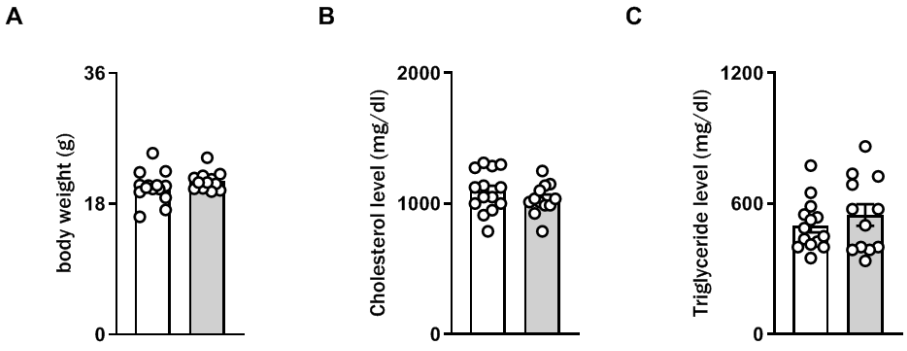

Supplementary figure 2

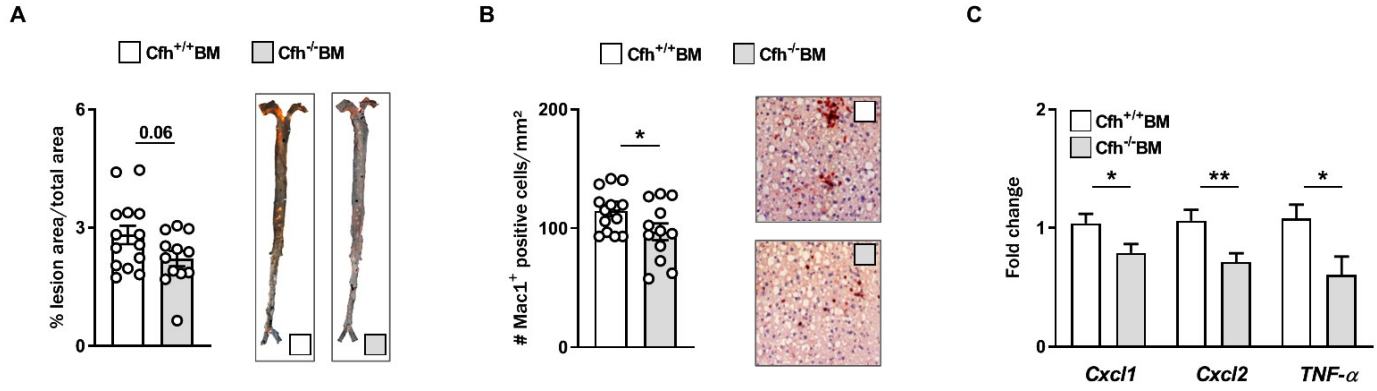

Supplementary figure 3

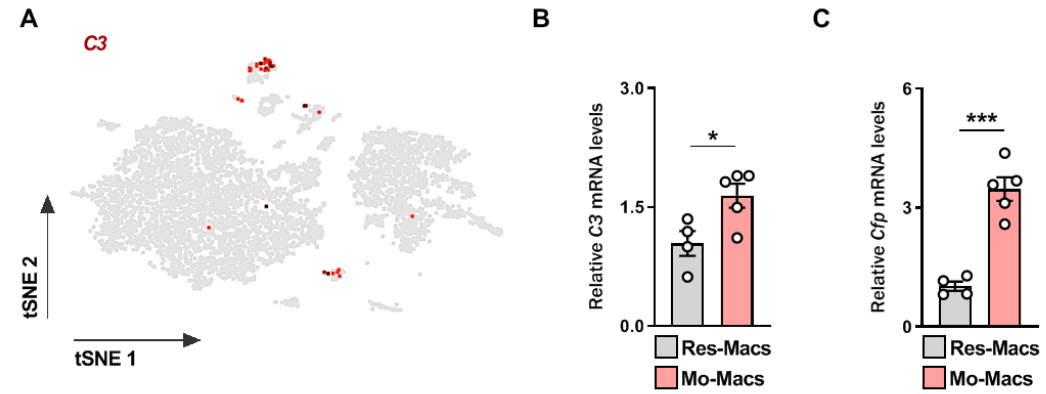

Supplementary figure 4

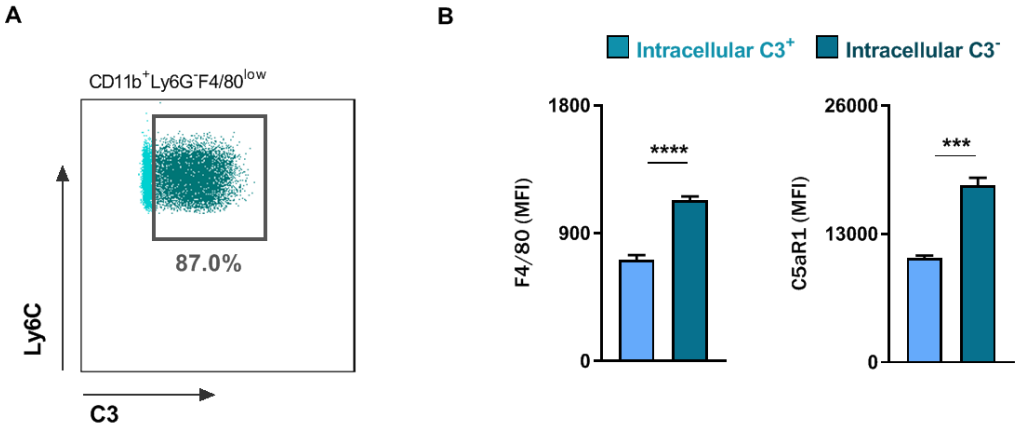

Supplementary figure 5

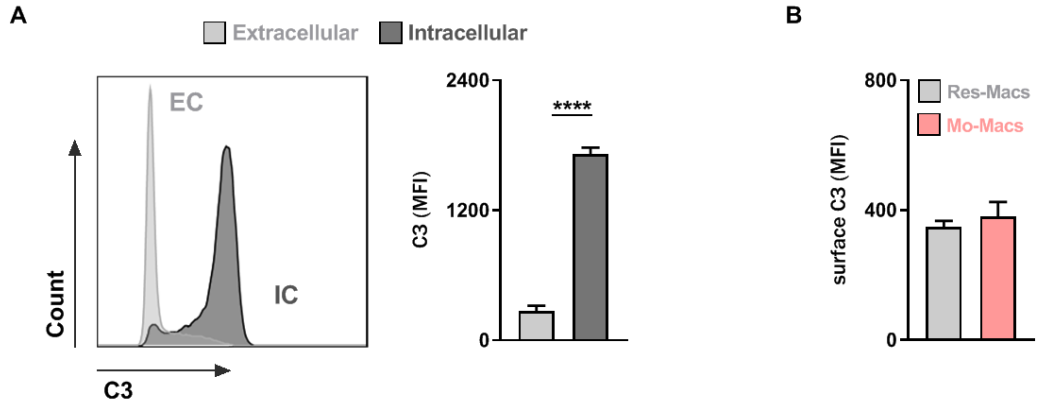

Supplementary figure 6

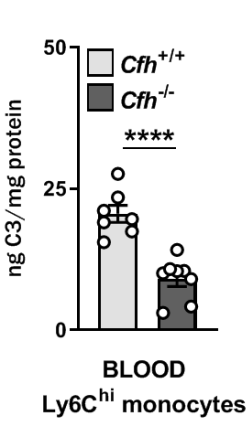

Supplementary figure 7

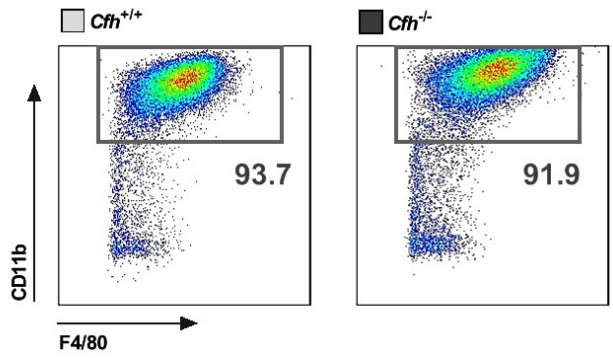

Supplementary Figure 8

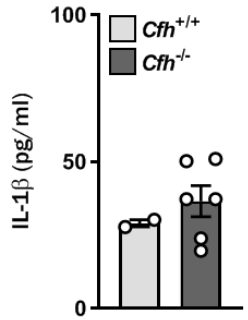

Supplementary Figure 9

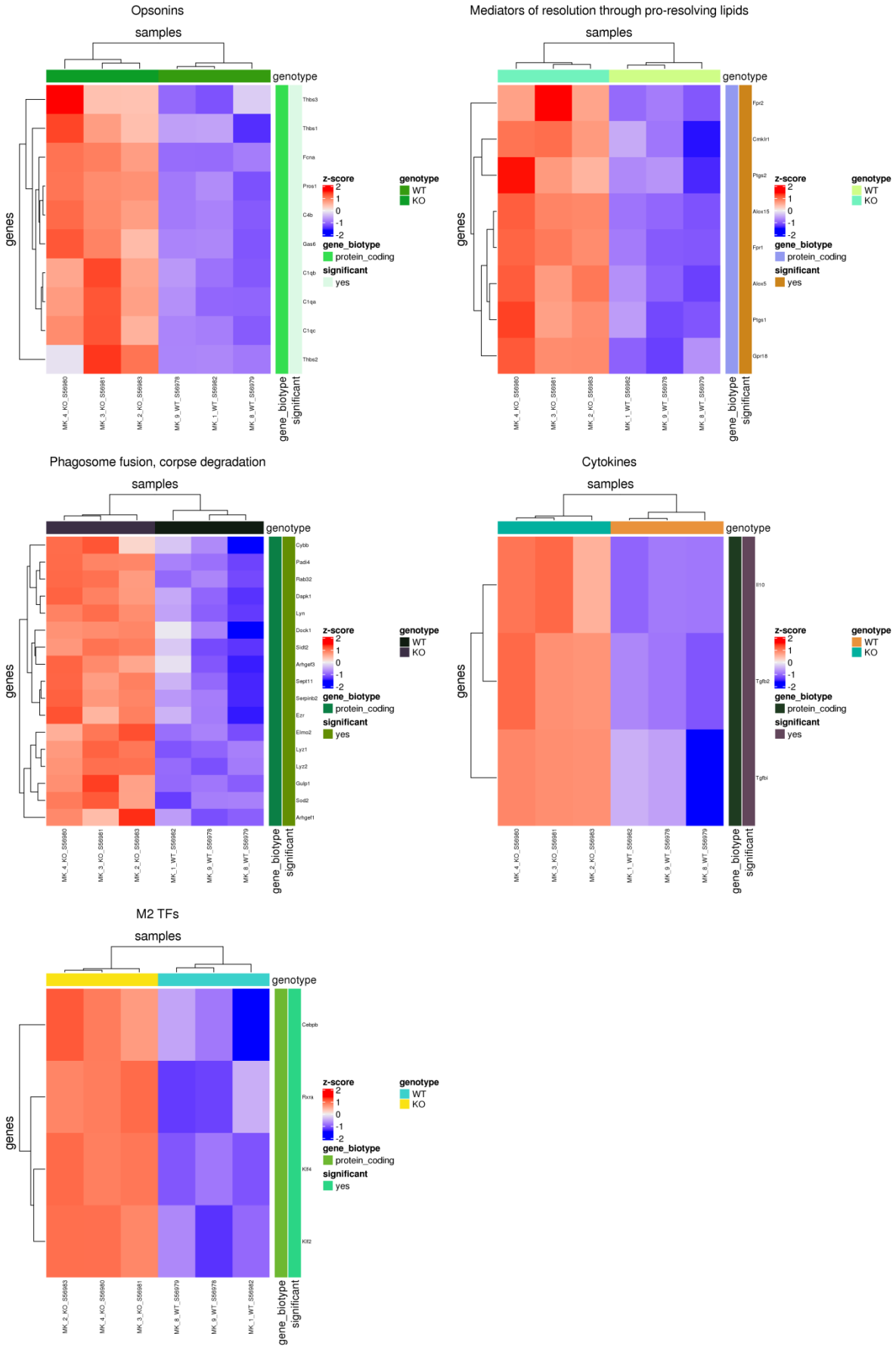

Supplementary Figure 10

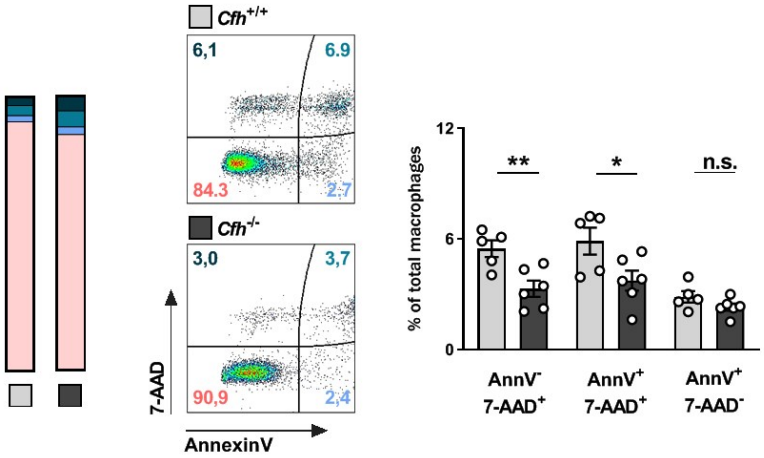

Supplementary FIgure 11

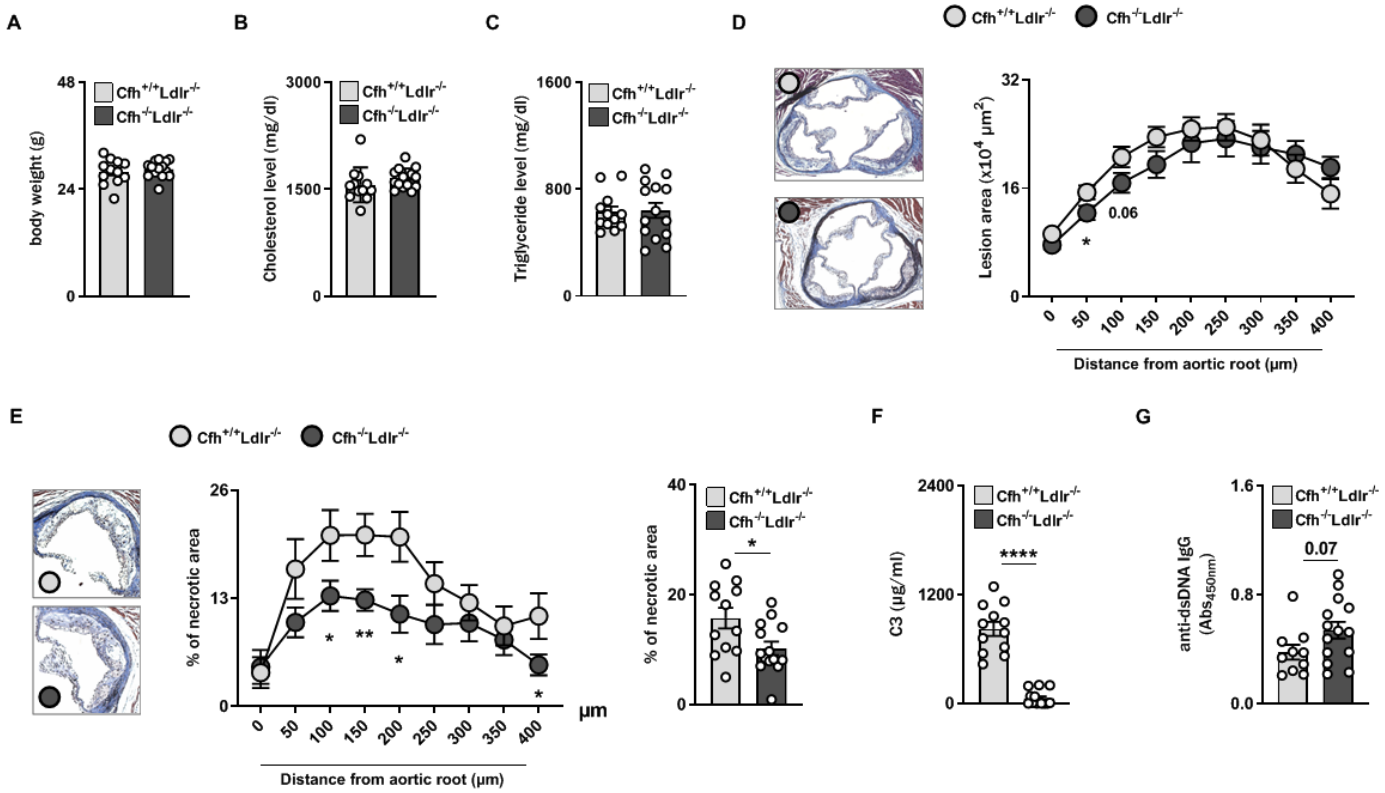

3 Discussion

3.1 General discussion

The field of complement research has been revolutionized by the discovery of intracellular complement activation. While complement protects from foreign intruders in the circulation and mediates paracrine and autocrine effector functions in nearby extracellular spaces, it is now evident that it simultaneously controls basic cellular processes within cells. The central complement components C3 and C5 have both been implicated in all layers of complement activation. However, it still remains unknown whether intracellular complement involves a distinct set of components (e.g. regulators) compared to the systemic cascade, or other canonical complement proteins are also functionally active inside cells, comprising an intracellular '*complosome*'.

Interestingly, long before describing the intracellular activity of complement, multiple studies reported intracellular expression and storage of factor D and properdin (Berger et al., 1991; Wirthmueller et al., 1997). Moreover, C3 and factor B are considered to be the first complement proteins to appear during evolution, even in species without a circulatory system (Kolev and Kemper, 2017). These observations strongly support that the alternative pathway of complement (that involves all the above-mentioned components) had originally evolved as an intracellular sensor system. Here, we provide evidence that Ly6C^{hi} monocytes are endowed with their own set of alternative complement proteins and their complement synthesis can be activated on-demand upon an inflammatory setting, particularly upon infiltration to the site of inflammation, where they differentiate into effector macrophages. This process likely endorses them to actively fine-tune complement activation both intracellularly as well as in the local microenvironment thereby modulating key cellular functions in host protection. Thus, our findings support a concept of local 'on-demand' complement activation during inflammation.

We could further demonstrate that complement factor H (CFH), the master repressor of alternative complement activation is expressed in inflammatory monocytes and macrophages and has the ability to control intracellular C3 levels thereby modulating cell-protective immune responses in atherosclerosis. In addition, our data suggest that CFH is the only

canonical complement regulator that is actively regulated upon an inflammatory challenge in Ly6C^{hi} monocytes. Therefore, CFH might have co-evolved with alternative complement components in order to control their intracellular activity.

Although the exact mechanism of action is still elusive, we can postulate several scenarios by which macrophage-derived CFH can affect intracellular C3 levels. CFH might exert its canonical complement-regulatory functions on an intracellular C3 convertase or might inhibit a cell-specific protease with C3-cleaving ability. Moreover, it is also unknown whether CFH readily acts on C3 inside the cell right after its synthesis. It is plausible that macrophages first need to secrete CFH and subsequently internalize it. This would be consistent with a previous report that CFH can be taken up by cells (Martin et al., 2016) and would allow multiple layers of modulation. As CFH has the ability to bind apoptotic cells in the microenvironment, exaggerated cell death and accumulation of dead cells could lead to enhanced tethering of CFH on apoptotic cell surfaces, which may simultaneously limit the re-uptake of CFH by macrophages thereby allowing more intracellular C3 cleavage. Ultimately, augmented intracellular complement activation would render macrophages more phagocytic thereby promoting the clearance of accumulating apoptotic cells. Conversely, clearance of dying cells could increase the availability of CFH to be re-internalized by macrophages to shut down the pro-efferocytotic program driven by intracellular complement activation. Thus, the concentration of free macrophage-derived CFH in the microenvironment may have an important role in modulating the resolution of inflammation.

It is still to be answered whether liver-derived, circulating CFH has the ability to regulate intracellular C3 cleavage and if so, whether it is equally potent in doing so compared to macrophage-derived CFH. Uptake of liver-derived CFH may increase the complexity of intracellular complement regulation and the contribution of cell autonomous complement regulation vis-à-vis systemic complement effects may differ depending on the anatomical site of inflammation. Importantly, accumulating evidence suggests that liver-derived, systemic C3 is qualitatively different from intracellular C3. Ancient C3 forms frequently contained additional protein domains that are characteristic of metabolically-active molecules (Kolev and Kemper, 2017). While some of them are still present in human C3, most of them have been lost during evolution. In line with this notion, different post-translational modifications seem to occur between intracellular and liver-derived C3 (West and Kemper, 2019) and in pancreatic beta cells C3 has been shown to be transcribed from an alternative ATG site resulting in an intracellular protein lacking the secretory signal peptide (King et al., 2019). Based on these observations, West and Kemper proposed, that while circulating C3 needs to be classically folded to be functionally active, intracellular C3 may be un-folded or even in a precursor C3 form and exert non-canonical effects based on single domain activities

triggered upon cell-specific proteolytic cleavage (West and Kemper, 2019). Therefore, other complement components of non-hepatic origin may also have a distinct nature compared to their liver-derived counterparts. Investigating the distinct forms of CFH in evolutionarily older organisms could shed light on potential functional differences in CFH of hepatic versus monocytic origin.

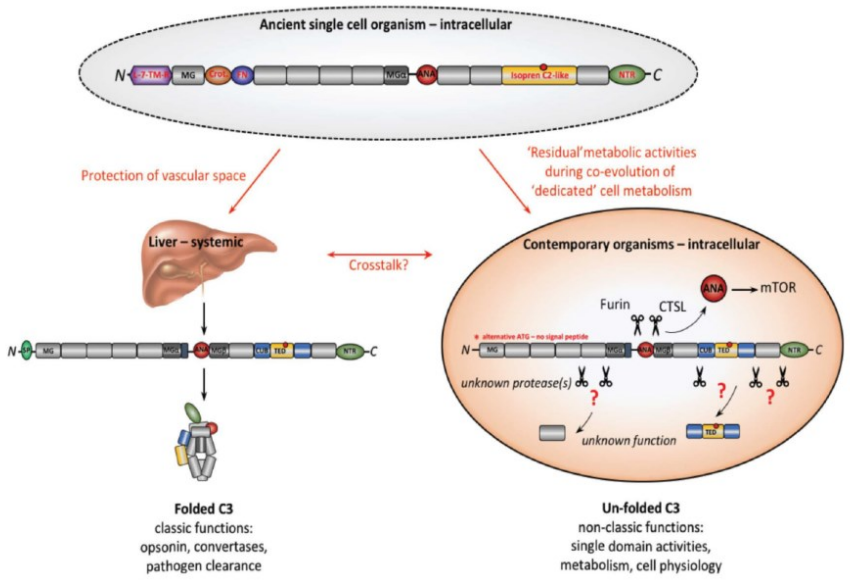

Figure 15 – Potential structural differences in systemic versus intracellular C3 – C3 might have diverged into two fundamental effector sites during evolution into multi-cellular organisms: liver-derived, systemic complement existing in a folded structure with canonical activities and intracellular C3 in an un-folded nature with key cellular homeostatic functions. Intracellular C3 might have lost certain metabolic domains of ancient C3 of evolutionary older organisms, but might still be activated upon the cleavage of its functional units by cell-specific proteases. *Adapted from (West and Kemper, 2019).*

The identification of on-demand complement activation as well as regulation might require the re-evaluation of studies discussing the effect of systemic complement on atherosclerosis with respect to intracellular complement activation in macrophages. One of the limitations of previous studies in experimental atherosclerosis is that they predominantly involve mice with global deficiency of certain complement factors, even though the majority of complement proteins have been reported to possess several sites of extrahepatic synthesis including atherosclerosis-relevant cell types, such as endothelial cells, smooth muscle cells or macrophages. These strategies do not allow distinguishing between the different layers of complement activation and might even disguise potential effects as a net result of

counteracting forces originating from systemic versus cell autonomous functions. In order to dissect these effects, models of selective deficiency are warranted.

Given our profound interest in CFH production by immune cells, we applied a bone marrow transplantation (BMT) strategy to distinguish between the systemic and local effects of CFH in complement regulation. In the first study, we identified a previously undefined mechanistic perspective on the function of CFH in protecting from autoimmunity via the modulation of splenic B cell differentiation and responsiveness. Our bone marrow transplantation study confirmed that the latter observation is not due to a cell intrinsic effect of CFH on B cells, but is clearly mediated by its systemic complement-regulatory function. In the second manuscript discussed in this thesis, we could show that CFH is expressed exclusively by monocytes among immune cells and is upregulated in monocyte-derived macrophages upon an inflammatory challenge. Here, selective deficiency of CFH in the hematopoietic compartment led to a robust decrease in lesion formation and necrotic area. Moreover, the role of hematopoietic (i.e. monocyte-derived) CFH in atherosclerosis appeared to be dominant over the effect of liver-derived CFH, as mice with global CFH deficiency still displayed a decrease in necrotic core formation, although having similar lesion size compared to controls. The lack of difference in lesion size between *Cfh*$^{+/+}$*Ldlr*$^{-/-}$ and *Cfh*$^{-/-}$*Ldlr*$^{-/-}$ mice may point towards a pro-atherogenic role for systemic CFH deficiency, possibly as a result of increased autoimmunity. Thus, dissecting the layers of CFH activity in a compartmentalized manner allowed us to identify opposing effects for this major complement repressor in atherosclerosis.

In light of our findings, it may also be worthwhile to reconsider recent studies investigating the inherited repertoire of polymorphisms in genes encoding complement components, termed the complotype (Harris et al., 2012), which indicated a role of alternative complement activity in significantly dictating certain disease risks. While individuals with a characteristic combination of common polymorphic variants in the alternative pathway components C3, CFB and CFH have been shown to exert insufficient complement activity with higher prevalence of infections, others carrying the opposite complotype are more prone to chronic inflammation and autoimmunity. Although these results were thought to be associated with systemic complement activation, it is tempting to speculate that the modulation of intracellular complement activation can also contribute to, or even drive the predisposition to inflammatory and infectious diseases.

In addition, certain genetic variants of CFH have been found to harbor altered binding capacity to ligands found on apoptotic cells. For example, we have previously shown that the Y402H polymorphism (rs1061170) in the CFH gene reduces the ability of CFH to bind the lipid peroxidation-derived malondlaldehyde (MDA) adducts, thereby limiting complement

regulation on modified host cell surfaces (Weismann et al., 2011). Importantly, Y402H variant confers a significantly increased risk to develop AMD (Edwards et al., 2005; Hageman et al., 2005; Haines et al., 2005; Klein et al., 2005) and has been recently shown to affect subretinal macrophage elimination (Calippe et al., 2017). Although previous investigations yielded conflicting results on the association of the Y402H variant with cardiovascular disease (CVD) risk (Buraczynska et al., 2009; Kardys et al., 2006; Pai et al., 2007; Stark et al., 2007; Volcik et al., 2008), it did show a two-fold decrease in susceptibility to CVD in a large cohort study of patients suffering from familial hypercholesterolemia (Koeijvoets et al., 2009). However, the impact of these genetic variants on intracellular complement activation remains yet entirely unknown and will need to be taken into consideration in future studies.

Besides mutations and genetic variants in the CFH gene, the availability of CFH-related proteins can also affect potent complement regulation by CFH. FHL-1 is an alternative splicing product of CFH and is composed of SCR1-7 with an additional four amino acid long residue (Zipfel and Skerka, 1999). Therefore, FHL-1 and CFH display overlapping complement-regulatory and co-factor functions. However, compared to FHL-1, CFH was found to have a 100-fold stronger decay accelerating activity on C3 convertases bound to sheep red blood cells and appears more potent to interact with C3b on non-activator surfaces (Kuhn and Zipfel, 1996). Thus, FHL-1 can modulate complement activation by occupying C3b for CFH binding.

CFHRs all consist of domains with varying degrees of similarity with SCRs in CFH (Figure 14). They do not have a regulatory region, but they possess high sequence homology with the anionic binding sites of CFH. In line with this, CFHRs have been shown to compete with the complement repressor activity of CFH on MDA-decorated surfaces (Weismann et al., 2011) and therefore, they can dampen anti-inflammatory iC3b generation on the surface of MDA-bearing surfaces, including apoptotic cells (Weismann and Binder, 2012). These findings can provide an explanation for the protective effect of the CFHR1 and CFHR3 deletion in AMD (Hughes et al., 2006). In our mouse model of CFH deficiency we could exclusively investigate the contribution of CFH to atherosclerosis development. However, FHL-1 and CFHRs likely influence the role of CFH in controlling intracellular C3 levels. Thus, CFH and its structurally related proteins may operate in a delicately orchestrated manner to modulate inflammatory responses via regulating intracellular complement activation in humans.

3.2 Conclusion and future prospects

In light of the results from the Canakinumab Anti-inflammatory Thrombosis Outcomes Study (CANTOS) trial - in which antibody-targeted inhibition of the proinflammatory cytokine interleukin-1beta (IL-1β) could reduce cardiovascular events in patients with previous myocardial infarction (Ridker et al., 2017) - now we have evidence that targeting inflammation independently of lipid levels holds promise for lowering the risk of atherosclerotic vascular diseases. However, anti-inflammatory drug therapies can potentially suppress host defense and lead to fatal infections, which calls for alternative strategies such as inducing resolution. Defective efferocytosis is the culprit of impaired resolution of inflammation in atherosclerosis (Yurdagul et al., 2017). Here, we identify a novel mechanism by which uncontrolled intracellular C3 activation resulting from CFH deficiency induces cyto-protective autophagy in macrophages, promotes lesional efferocytosis and mitigates atherosclerosis development.

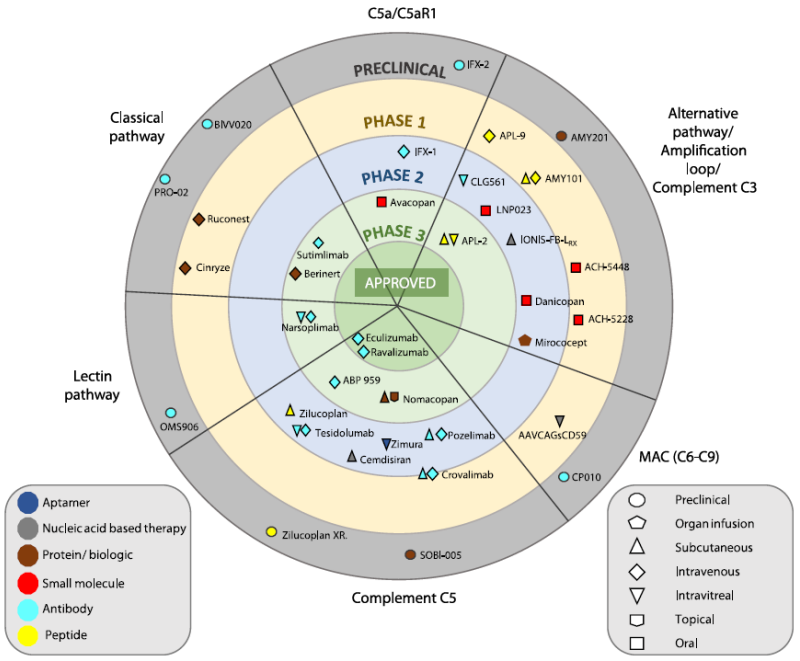

Figure 16 – Complement-targeting therapeutic agents in clinical development – Of note, preclinical as well as first-time-in-human drugs are included if target molecules are disclosed. *Adapted from (Zelek et al., 2019)*.

In 2007, the clinical approval of eculizumab (under the trade name *Soliris* by Alexion) for the treatment of the rare haemolytic disease paroxysmal nocturnal heamoglobinuria (PNH) gave a proof of efficacy for the therapeutic modulation of complement activation in human disease (Hillmen et al., 2006). Eculizumab is a humanized monoclonal antibody against C5 that inhibits C5 cleavage by the C5 convertase into C5a and C5b and its application was since broadened to patients with aHUS and refractory myasthenia gravis. Although the success of eculizumab propelled a rapid progress in complement drug discovery, to date no therapeutics against alternative targets of the complement cascade have reached the market accompanied by some unexpected failure of drug candidates in translating into clinical effects (Mastellos et al., 2019). As such, a recombinant form of soluble CR1 (TP10/CDX-1135) was assessed in a phase II trial as a therapeutic strategy to prevent myocardial infarction via inhibiting C3 and C5 convertase activity (Lazar et al., 2004). Albeit the treatment led to a reduction in cardiovascular events in male patients undergoing cardiopulmonary bypass, the development of the drug was discontinued due to its limited and gender-specific effect (Lazar et al., 2007).

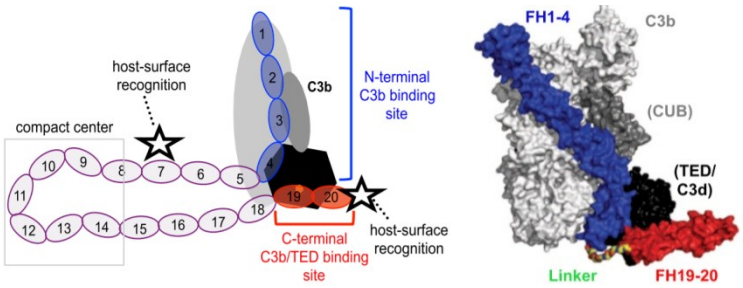

Figure 17 – The design of mini-FH – Schematic representation (*left*) of the interaction of CFH with C3b (*in gray*) via its complement-regulatory domains (*in blue*), as well as with anionic molecules through its surface recognition or thioester-containing domains (TED; *in red*) on host surfaces. Superimposed co-crystal structure *(right*) of the same interactions is shown for mini FH, which is composed of only SCR1-4 and SCR19-20, combined with a polyglycine linker (*in yellow*). *Adapted from (Schmidt et al., 2013).*

Currently, over 20 therapeutic agents targeting the complement cascade are at various stages of clinical development (**Figure 17**). Among them, increasing number of drugs against alternative pathway activation can be observed, including two C3-targeting agents (*AMY-101*, Amyndas and *APL-2*, Apellis) with the ability to bind native C3 and prevent C3 convertase activity. In addition, a truncated, engineered form of CFH with superior efficacy for surface recognition (*AMY-201* or *mini-FH*, Amyndas) has entered preclinical development

for the treatment of AMD (**Figure 18**; (Harris et al., 2018; Schmidt et al., 2013). However, the accumulating evidence highlighting the homeostatic functions of intracellular complement activation raises awareness about the potential implications of complement-targeting strategies. Furthermore, our findings suggest that enhanced cell autonomous complement activation associated with CFH deficiency promotes macrophage efferocytosis, which argues against the application of *mini-FH* in inflammatory diseases. Nevertheless, future studies are warranted to investigate whether these agents have the ability to interfere with intracellular complement activation.

Besides the expense of production, the way of administration and the duration of action, possibly the major challenge of complement drug development is to engineer agents that can modulate rather than shut down complement activation in a tissue-specific manner (Zelek et al., 2019). Therefore, we envision an era of next generation therapeutics with the potential to localize therapy to the site of pathology using homing agents, gene therapy or nanoimmunotherapy with a well-defined time window. The findings of the thesis presented here indicate that targeting intracellular complement regulation may provide novel opportunities against chronic inflammatory diseases without tempering host defense mechanisms.

References

Ait-Oufella, H., Kinugawa, K., Zoll, J., Simon, T., Boddaert, J., Heeneman, S., Blanc-Brude, O., Barateau, V., Potteaux, S., Merval, R.*, et al.* (2007). Lactadherin deficiency leads to apoptotic cell accumulation and accelerated atherosclerosis in mice. Circulation *115*, 2168-2177.

Ait-Oufella, H., Pouresmail, V., Simon, T., Blanc-Brude, O., Kinugawa, K., Merval, R., Offenstadt, G., Leseche, G., Cohen, P.L., Tedgui, A.*, et al.* (2008). Defective mer receptor tyrosine kinase signaling in bone marrow cells promotes apoptotic cell accumulation and accelerates atherosclerosis. Arterioscler Thromb Vasc Biol *28*, 1429-1431.

Alexander, J.J., and Quigg, R.J. (2007). The simple design of complement factor H: Looks can be deceiving. Mol Immunol *44*, 123-132.

An, G., Li, B., Liu, X., Zhang, M., Gao, F., Zhao, Y., An, F., Zhang, Y., and Zhang, C. (2016). Overexpression of complement component C5a accelerates the development of atherosclerosis in ApoE-knockout mice. Oncotarget *7*, 56060-56070.

An, G., Miwa, T., Song, W.L., Lawson, J.A., Rader, D.J., Zhang, Y., and Song, W.C. (2009). CD59 but not DAF deficiency accelerates atherosclerosis in female ApoE knockout mice. Mol Immunol *46*, 1702-1709.

Aprahamian, T., Rifkin, I., Bonegio, R., Hugel, B., Freyssinet, J.M., Sato, K., Castellot, J.J., Jr., and Walsh, K. (2004). Impaired clearance of apoptotic cells promotes synergy between atherogenesis and autoimmune disease. J Exp Med *199*, 1121-1131.

Arbore, G., Kemper, C., and Kolev, M. (2017). Intracellular complement - the complosome - in immune cell regulation. Mol Immunol *89*, 2-9.

Arbore, G., West, E.E., Spolski, R., Robertson, A.A.B., Klos, A., Rheinheimer, C., Dutow, P., Woodruff, T.M., Yu, Z.X., O'Neill, L.A.*, et al.* (2016). T helper 1 immunity requires complement-driven NLRP3 inflammasome activity in CD4(+) T cells. Science *352*, aad1210.

Back, M., Yurdagul, A., Jr., Tabas, I., Oorni, K., and Kovanen, P.T. (2019). Inflammation and its resolution in atherosclerosis: mediators and therapeutic opportunities. Nat Rev Cardiol *16*, 389-406.

Baudino, L., Sardini, A., Ruseva, M.M., Fossati-Jimack, L., Cook, H.T., Scott, D., Simpson, E., and Botto, M. (2014). C3 opsonization regulates endocytic handling of apoptotic cells resulting in enhanced T-cell responses to cargo-derived antigens. Proc Natl Acad Sci U S A *111*, 1503-1508.

Berger, M., Wetzler, E.M., Welter, E., Turner, J.R., and Tartakoff, A.M. (1991). Intracellular sites for storage and recycling of C3b receptors in human neutrophils. Proc Natl Acad Sci U S A *88*, 3019-3023.

Bhatia, V.K., Yun, S., Leung, V., Grimsditch, D.C., Benson, G.M., Botto, M.B., Boyle, J.J., and Haskard, D.O. (2007). Complement C1q reduces early atherosclerosis in low-density lipoprotein receptor-deficient mice. Am J Pathol *170*, 416-426.

Binder, C.J. (2010). Natural IgM antibodies against oxidation-specific epitopes. J Clin Immunol *30 Suppl 1*, S56-60.

Binder, C.J., Papac-Milicevic, N., and Witztum, J.L. (2016). Innate sensing of oxidation-specific epitopes in health and disease. Nat Rev Immunol *16*, 485-497.

Boisvert, W.A., Rose, D.M., Boullier, A., Quehenberger, O., Sydlaske, A., Johnson, K.A., Curtiss, L.K., and Terkeltaub, R. (2006). Leukocyte transglutaminase 2 expression limits atherosclerotic lesion size. Arterioscler Thromb Vasc Biol *26*, 563-569.

Borras, C., Canonica, J., Jorieux, S., Abache, T., El Sanharawi, M., Klein, C., Delaunay, K., Jonet, L., Salvodelli, M., Naud, M.C*., et al.* (2019). CFH exerts anti-oxidant effects on retinal pigment epithelial cells independently from protecting against membrane attack complex. Sci Rep *9*, 13873.

Brown, M.S., Ho, Y.K., and Goldstein, J.L. (1980). The cholesteryl ester cycle in macrophage foam cells. Continual hydrolysis and re-esterification of cytoplasmic cholesteryl esters. J Biol Chem *255*, 9344-9352.

Brown, S., Heinisch, I., Ross, E., Shaw, K., Buckley, C.D., and Savill, J. (2002). Apoptosis disables CD31-mediated cell detachment from phagocytes promoting binding and engulfment. Nature *418*, 200-203.

Buono, C., Binder, C.J., Stavrakis, G., Witztum, J.L., Glimcher, L.H., and Lichtman, A.H. (2005). T-bet deficiency reduces atherosclerosis and alters plaque antigen-specific immune responses. Proc Natl Acad Sci U S A *102*, 1596-1601.

Buono, C., Come, C.E., Witztum, J.L., Maguire, G.F., Connelly, P.W., Carroll, M., and Lichtman, A.H. (2002). Influence of C3 deficiency on atherosclerosis. Circulation *105*, 3025-3031.

Buraczynska, M., Ksiazek, P., Zukowski, P., Benedyk-Lorens, E., and Orlowska-Kowalik, G. (2009). Complement factor H gene polymorphism and risk of cardiovascular disease in end-stage renal disease patients. Clin Immunol *132*, 285-290.

Cai, B., Thorp, E.B., Doran, A.C., Sansbury, B.E., Daemen, M.J., Dorweiler, B., Spite, M., Fredman, G., and Tabas, I. (2017). MerTK receptor cleavage promotes plaque necrosis and defective resolution in atherosclerosis. J Clin Invest *127*, 564-568.

Calippe, B., Augustin, S., Beguier, F., Charles-Messance, H., Poupel, L., Conart, J.B., Hu, S.J., Lavalette, S., Fauvet, A., Rayes, J.*, et al.* (2017). Complement Factor H Inhibits CD47-Mediated Resolution of Inflammation. Immunity *46*, 261-272.

Campbell, L.A., and Kuo, C.C. (2003). Chlamydia pneumoniae and atherosclerosis. Semin Respir Infect *18*, 48-54.

Carroll, M.C. (2004). The complement system in B cell regulation. Mol Immunol *41*, 141-146.

Carroll, M.C., and Isenman, D.E. (2012). Regulation of humoral immunity by complement. Immunity *37*, 199-207.

Castellano, F., Montcourrier, P., and Chavrier, P. (2000). Membrane recruitment of Rac1 triggers phagocytosis. J Cell Sci *113 (Pt 17)*, 2955-2961.

Centa, M., Jin, H., Hofste, L., Hellberg, S., Busch, A., Baumgartner, R., Verzaal, N.J., Lind Enoksson, S., Perisic Matic, L., Boddul, S.V.*, et al.* (2019). Germinal Center-Derived Antibodies Promote Atherosclerosis Plaque Size and Stability. Circulation *139*, 2466-2482.

Chou, M.Y., Fogelstrand, L., Hartvigsen, K., Hansen, L.F., Woelkers, D., Shaw, P.X., Choi, J., Perkmann, T., Backhed, F., Miller, Y.I.*, et al.* (2009). Oxidation-specific epitopes are dominant targets of innate natural antibodies in mice and humans. J Clin Invest *119*, 1335-1349.

Chou, M.Y., Hartvigsen, K., Hansen, L.F., Fogelstrand, L., Shaw, P.X., Boullier, A., Binder, C.J., and Witztum, J.L. (2008). Oxidation-specific epitopes are important targets of innate immunity. J Intern Med *263*, 479-488.

Clark, S.J., Ridge, L.A., Herbert, A.P., Hakobyan, S., Mulloy, B., Lennon, R., Wurzner, R., Morgan, B.P., Uhrin, D., Bishop, P.N.*, et al.* (2013). Tissue-specific host recognition by complement factor H is mediated by differential activities of its glycosaminoglycan-binding regions. J Immunol *190*, 2049-2057.

Cochain, C., Vafadarnejad, E., Arampatzi, P., Pelisek, J., Winkels, H., Ley, K., Wolf, D., Saliba, A.E., and Zernecke, A. (2018). Single-Cell RNA-Seq Reveals the Transcriptional Landscape and Heterogeneity of Aortic Macrophages in Murine Atherosclerosis. Circ Res *122*, 1661-1674.

Costales, P., Castellano, J., Revuelta-Lopez, E., Cal, R., Aledo, R., Llampayas, O., Nasarre, L., Juarez, C., Badimon, L., and Llorente-Cortes, V. (2013). Lipopolysaccharide downregulates CD91/low-density lipoprotein receptor-related protein 1 expression through SREBP-1 overexpression in human macrophages. Atherosclerosis *227*, 79-88.

de Cordoba, S.R., and de Jorge, E.G. (2008). Translational mini-review series on complement factor H: genetics and disease associations of human complement factor H. Clin Exp Immunol *151*, 1-13.

Delves, P.J., and Roitt, I.M. (2000a). The immune system. First of two parts. N Engl J Med *343*, 37-49.

Delves, P.J., and Roitt, I.M. (2000b). The immune system. Second of two parts. N Engl J Med *343*, 108-117.

Drechsler, M., Megens, R.T., van Zandvoort, M., Weber, C., and Soehnlein, O. (2010). Hyperlipidemia-triggered neutrophilia promotes early atherosclerosis. Circulation *122*, 1837-1845.

Duewell, P., Kono, H., Rayner, K.J., Sirois, C.M., Vladimer, G., Bauernfeind, F.G., Abela, G.S., Franchi, L., Nunez, G., Schnurr, M.*, et al.* (2010). NLRP3 inflammasomes are required for atherogenesis and activated by cholesterol crystals. Nature *464*, 1357-1361.

Edwards, A.O., Ritter, R., 3rd, Abel, K.J., Manning, A., Panhuysen, C., and Farrer, L.A. (2005). Complement factor H polymorphism and age-related macular degeneration. Science *308*, 421-424.

Feng, X., Li, H., Rumbin, A.A., Wang, X., La Cava, A., Brechtelsbauer, K., Castellani, L.W., Witztum, J.L., Lusis, A.J., and Tsao, B.P. (2007). ApoE-/-Fas-/- C57BL/6 mice: a novel murine model simultaneously exhibits lupus nephritis, atherosclerosis, and osteopenia. J Lipid Res *48*, 794-805.

Fernandez, D.M., Rahman, A.H., Fernandez, N.F., Chudnovskiy, A., Amir, E.D., Amadori, L., Khan, N.S., Wong, C.K., Shamailova, R., Hill, C.A.*, et al.* (2019). Single-cell immune landscape of human atherosclerotic plaques. Nat Med.

Ferreira, V.P., Pangburn, M.K., and Cortes, C. (2010). Complement control protein factor H: the good, the bad, and the inadequate. Mol Immunol *47*, 2187-2197.

Foks, A.C., Engelbertsen, D., Kuperwaser, F., Alberts-Grill, N., Gonen, A., Witztum, J.L., Lederer, J., Jarolim, P., DeKruyff, R.H., Freeman, G.J.*, et al.* (2016). Blockade of Tim-1 and Tim-4 Enhances Atherosclerosis in Low-Density Lipoprotein Receptor-Deficient Mice. Arterioscler Thromb Vasc Biol *36*, 456-465.

Fujita, T. (2002). Evolution of the lectin-complement pathway and its role in innate immunity. Nat Rev Immunol *2*, 346-353.

Gadjeva, M., Verschoor, A., Brockman, M.A., Jezak, H., Shen, L.M., Knipe, D.M., and Carroll, M.C. (2002). Macrophage-derived complement component C4 can restore humoral immunity in C4-deficient mice. J Immunol *169*, 5489-5495.

Gal, P., Barna, L., Kocsis, A., and Zavodszky, P. (2007). Serine proteases of the classical and lectin pathways: similarities and differences. Immunobiology *212*, 267-277.

Geertinger, P., and Sorensen, H. (1970). Complement as a factor in arteriosclerosis. Acta Pathol Microbiol Scand A *78*, 284-288.

Glass, C.K., and Witztum, J.L. (2001). Atherosclerosis. the road ahead. Cell *104*, 503-516.

Gorovoy, M., Gaultier, A., Campana, W.M., Firestein, G.S., and Gonias, S.L. (2010). Inflammatory mediators promote production of shed LRP1/CD91, which regulates cell signaling and cytokine expression by macrophages. J Leukoc Biol *88*, 769-778.

Hageman, G.S., Anderson, D.H., Johnson, L.V., Hancox, L.S., Taiber, A.J., Hardisty, L.I., Hageman, J.L., Stockman, H.A., Borchardt, J.D., Gehrs, K.M.*, et al.* (2005). A common haplotype in the complement regulatory gene factor H (HF1/CFH) predisposes individuals to age-related macular degeneration. Proc Natl Acad Sci U S A *102*, 7227-7232.

Haines, J.L., Hauser, M.A., Schmidt, S., Scott, W.K., Olson, L.M., Gallins, P., Spencer, K.L., Kwan, S.Y., Noureddine, M., Gilbert, J.R.*, et al.* (2005). Complement factor H variant increases the risk of age-related macular degeneration. Science *308*, 419-421.

Harris, C.L., Heurich, M., Rodriguez de Cordoba, S., and Morgan, B.P. (2012). The complotype: dictating risk for inflammation and infection. Trends Immunol *33*, 513-521.

Harris, C.L., Pouw, R.B., Kavanagh, D., Sun, R., and Ricklin, D. (2018). Developments in anti-complement therapy; from disease to clinical trial. Mol Immunol *102*, 89-119.

Hellwage, J., Eberle, F., Babuke, T., Seeberger, H., Richter, H., Kunert, A., Hartl, A., Zipfel, P.F., Jokiranta, T.S., and Jozsi, M. (2006). Two factor H-related proteins from the mouse: expression analysis and functional characterization. Immunogenetics *58*, 883-893.

Henson, P.M., Bratton, D.L., and Fadok, V.A. (2001). Apoptotic cell removal. Curr Biol *11*, R795-805.

Hess, C., and Kemper, C. (2016). Complement-Mediated Regulation of Metabolism and Basic Cellular Processes. Immunity *45*, 240-254.

Hilgendorf, I., and Swirski, F.K. (2012). Making a difference: monocyte heterogeneity in cardiovascular disease. Curr Atheroscler Rep *14*, 450-459.

Hilgendorf, I., Theurl, I., Gerhardt, L.M., Robbins, C.S., Weber, G.F., Gonen, A., Iwamoto, Y., Degousee, N., Holderried, T.A., Winter, C.*, et al.* (2014). Innate response activator B cells aggravate atherosclerosis by stimulating T helper-1 adaptive immunity. Circulation *129*, 1677-1687.

Hillmen, P., Young, N.S., Schubert, J., Brodsky, R.A., Socie, G., Muus, P., Roth, A., Szer, J., Elebute, M.O., Nakamura, R.*, et al.* (2006). The complement inhibitor eculizumab in paroxysmal nocturnal hemoglobinuria. N Engl J Med *355*, 1233-1243.

Holers, V.M. (2014). Complement and its receptors: new insights into human disease. Annu Rev Immunol *32*, 433-459.

Huan, T., Zhang, B., Wang, Z., Joehanes, R., Zhu, J., Johnson, A.D., Ying, S., Munson, P.J., Raghavachari, N., Wang, R.*, et al.* (2013). A systems biology framework identifies molecular underpinnings of coronary heart disease. Arterioscler Thromb Vasc Biol *33*, 1427-1434.

Hughes, A.E., Orr, N., Esfandiary, H., Diaz-Torres, M., Goodship, T., and Chakravarthy, U. (2006). A common CFH haplotype, with deletion of CFHR1 and CFHR3, is associated with lower risk of age-related macular degeneration. Nat Genet *38*, 1173-1177.

Jozsi, M., Schneider, A.E., Karpati, E., and Sandor, N. (2019). Complement factor H family proteins in their non-canonical role as modulators of cellular functions. Semin Cell Dev Biol *85*, 122-131.

Jozsi, M., and Zipfel, P.F. (2008). Factor H family proteins and human diseases. Trends Immunol *29*, 380-387.

Kardys, I., Klaver, C.C., Despriet, D.D., Bergen, A.A., Uitterlinden, A.G., Hofman, A., Oostra, B.A., Van Duijn, C.M., de Jong, P.T., and Witteman, J.C. (2006). A common polymorphism in the complement factor H gene is associated with increased risk of myocardial infarction: the Rotterdam Study. J Am Coll Cardiol *47*, 1568-1575.

Kasikara, C., Doran, A.C., Cai, B., and Tabas, I. (2018). The role of non-resolving inflammation in atherosclerosis. J Clin Invest *128*, 2713-2723.

Kim, D.D., and Song, W.C. (2006). Membrane complement regulatory proteins. Clin Immunol *118*, 127-136.

Kim, K., Shim, D., Lee, J.S., Zaitsev, K., Williams, J.W., Kim, K.W., Jang, M.Y., Seok Jang, H., Yun, T.J., Lee, S.H.*, et al.* (2018). Transcriptome Analysis Reveals Nonfoamy Rather Than Foamy Plaque Macrophages Are Proinflammatory in Atherosclerotic Murine Models. Circ Res *123*, 1127-1142.

Kim, K.H., Choi, B.K., Kim, Y.H., Han, C., Oh, H.S., Lee, D.G., and Kwon, B.S. (2016). Extracellular stimulation of VSIG4/complement receptor Ig suppresses intracellular bacterial infection by inducing autophagy. Autophagy *12*, 1647-1659.

King, B.C., Kulak, K., Krus, U., Rosberg, R., Golec, E., Wozniak, K., Gomez, M.F., Zhang, E., O'Connell, D.J., Renstrom, E.*, et al.* (2019). Complement Component C3 Is Highly Expressed in Human Pancreatic Islets and Prevents beta Cell Death via ATG16L1 Interaction and Autophagy Regulation. Cell Metab *29*, 202-210 e206.

Klein, R.J., Zeiss, C., Chew, E.Y., Tsai, J.Y., Sackler, R.S., Haynes, C., Henning, A.K., SanGiovanni, J.P., Mane, S.M., Mayne, S.T.*, et al.* (2005). Complement factor H polymorphism in age-related macular degeneration. Science *308*, 385-389.

Koeijvoets, K.C., Mooijaart, S.P., Dallinga-Thie, G.M., Defesche, J.C., Steyerberg, E.W., Westendorp, R.G., Kastelein, J.J., van Hagen, P.M., and Sijbrands, E.J. (2009). Complement factor H Y402H decreases cardiovascular disease risk in patients with familial hypercholesterolaemia. Eur Heart J *30*, 618-623.

Kojima, Y., Downing, K., Kundu, R., Miller, C., Dewey, F., Lancero, H., Raaz, U., Perisic, L., Hedin, U., Schadt, E.*, et al.* (2014). Cyclin-dependent kinase inhibitor 2B regulates efferocytosis and atherosclerosis. J Clin Invest *124*, 1083-1097.

Kojima, Y., Volkmer, J.P., McKenna, K., Civelek, M., Lusis, A.J., Miller, C.L., Direnzo, D., Nanda, V., Ye, J., Connolly, A.J.*, et al.* (2016). CD47-blocking antibodies restore phagocytosis and prevent atherosclerosis. Nature *536*, 86-90.

Kolev, M., Dimeloe, S., Le Friec, G., Navarini, A., Arbore, G., Povoleri, G.A., Fischer, M., Belle, R., Loeliger, J., Develioglu, L.*, et al.* (2015). Complement Regulates Nutrient Influx and Metabolic Reprogramming during Th1 Cell Responses. Immunity *42*, 1033-1047.

Kolev, M., and Kemper, C. (2017). Keeping It All Going-Complement Meets Metabolism. Front Immunol *8*, 1.

Kolev, M., Le Friec, G., and Kemper, C. (2014). Complement--tapping into new sites and effector systems. Nat Rev Immunol *14*, 811-820.

Kuhn, S., and Zipfel, P.F. (1996). Mapping of the domains required for decay acceleration activity of the human factor H-like protein 1 and factor H. Eur J Immunol *26*, 2383-2387.

Kyaw, T., Tay, C., Krishnamurthi, S., Kanellakis, P., Agrotis, A., Tipping, P., Bobik, A., and Toh, B.H. (2011). B1a B lymphocytes are atheroprotective by secreting natural IgM that increases IgM deposits and reduces necrotic cores in atherosclerotic lesions. Circ Res *109*, 830-840.

Lalli, P.N., Strainic, M.G., Yang, M., Lin, F., Medof, M.E., and Heeger, P.S. (2008). Locally produced C5a binds to T cell-expressed C5aR to enhance effector T-cell expansion by limiting antigen-induced apoptosis. Blood *112*, 1759-1766.

Lazar, H.L., Bokesch, P.M., van Lenta, F., Fitzgerald, C., Emmett, C., Marsh, H.C., Jr., Ryan, U., Obe, and the, T.P.C.S.S.G. (2004). Soluble human complement receptor 1 limits ischemic damage in cardiac surgery patients at high risk requiring cardiopulmonary bypass. Circulation *110*, II274-279.

Lazar, H.L., Keilani, T., Fitzgerald, C.A., Shapira, O.M., Hunter, C.T., Shemin, R.J., Marsh, H.C., Jr., Ryan, U.S., and Group, T.P.C.S.S. (2007). Beneficial effects of complement inhibition with soluble complement receptor 1 (TP10) during cardiac surgery: is there a gender difference? Circulation *116*, I83-88.

Leffler, J., Herbert, A.P., Norstrom, E., Schmidt, C.Q., Barlow, P.N., Blom, A.M., and Martin, M. (2010). Annexin-II, DNA, and histones serve as factor H ligands on the surface of apoptotic cells. J Biol Chem *285*, 3766-3776.

Leung, V.W., Yun, S., Botto, M., Mason, J.C., Malik, T.H., Song, W., Paixao-Cavalcante, D., Pickering, M.C., Boyle, J.J., and Haskard, D.O. (2009). Decay-accelerating factor suppresses complement C3 activation and retards atherosclerosis in low-density lipoprotein receptor-deficient mice. Am J Pathol *175*, 1757-1767.

Lewis, M.J., Malik, T.H., Ehrenstein, M.R., Boyle, J.J., Botto, M., and Haskard, D.O. (2009). Immunoglobulin M is required for protection against atherosclerosis in low-density lipoprotein receptor-deficient mice. Circulation *120*, 417-426.

Lewis, R.D., Jackson, C.L., Morgan, B.P., and Hughes, T.R. (2010). The membrane attack complex of complement drives the progression of atherosclerosis in apolipoprotein E knockout mice. Mol Immunol *47*, 1098-1105.

Lewis, R.D., Perry, M.J., Guschina, I.A., Jackson, C.L., Morgan, B.P., and Hughes, T.R. (2011). CD55 deficiency protects against atherosclerosis in ApoE-deficient mice via C3a modulation of lipid metabolism. Am J Pathol *179*, 1601-1607.

Li, W. (2012). Eat-me signals: keys to molecular phagocyte biology and "appetite" control. J Cell Physiol *227*, 1291-1297.

Libby, P., Lichtman, A.H., and Hansson, G.K. (2013). Immune effector mechanisms implicated in atherosclerosis: from mice to humans. Immunity *38*, 1092-1104.

Libby, P., Ridker, P.M., and Hansson, G.K. (2011). Progress and challenges in translating the biology of atherosclerosis. Nature *473*, 317-325.

Liszewski, M.K., Kolev, M., Le Friec, G., Leung, M., Bertram, P.G., Fara, A.F., Subias, M., Pickering, M.C., Drouet, C., Meri, S.*, et al.* (2013). Intracellular complement activation sustains T cell homeostasis and mediates effector differentiation. Immunity *39*, 1143-1157.

Liu, F., Wu, L., Wu, G., Wang, C., Zhang, L., Tomlinson, S., and Qin, X. (2014). Targeted mouse complement inhibitor CR2-Crry protects against the development of atherosclerosis in mice. Atherosclerosis *234*, 237-243.

Lutgens, E., Tjwa, M., Garcia de Frutos, P., Wijnands, E., Beckers, L., Dahlback, B., Daemen, M.J., Carmeliet, P., and Moons, L. (2008). Genetic loss of Gas6 induces plaque stability in experimental atherosclerosis. J Pathol *216*, 55-63.

Malik, T.H., Cortini, A., Carassiti, D., Boyle, J.J., Haskard, D.O., and Botto, M. (2010). The alternative pathway is critical for pathogenic complement activation in endotoxin- and diet-induced atherosclerosis in low-density lipoprotein receptor-deficient mice. Circulation *122*, 1948-1956.

Manthey, H.D., Thomas, A.C., Shiels, I.A., Zernecke, A., Woodruff, T.M., Rolfe, B., and Taylor, S.M. (2011). Complement C5a inhibition reduces atherosclerosis in ApoE-/- mice. FASEB J *25*, 2447-2455.

Martin, M., Leffler, J., Smolag, K.I., Mytych, J., Bjork, A., Chaves, L.D., Alexander, J.J., Quigg, R.J., and Blom, A.M. (2016). Factor H uptake regulates intracellular C3 activation during apoptosis and decreases the inflammatory potential of nucleosomes. Cell Death Differ *23*, 903-911.

Martinez, J., Almendinger, J., Oberst, A., Ness, R., Dillon, C.P., Fitzgerald, P., Hengartner, M.O., and Green, D.R. (2011). Microtubule-associated protein 1 light chain 3 alpha (LC3)-associated phagocytosis is required for the efficient clearance of dead cells. Proc Natl Acad Sci U S A *108*, 17396-17401.

Martinez, J., Cunha, L.D., Park, S., Yang, M., Lu, Q., Orchard, R., Li, Q.Z., Yan, M., Janke, L., Guy, C.*, et al.* (2016). Noncanonical autophagy inhibits the autoinflammatory, lupus-like response to dying cells. Nature *533*, 115-119.

Martinez, J., Malireddi, R.K., Lu, Q., Cunha, L.D., Pelletier, S., Gingras, S., Orchard, R., Guan, J.L., Tan, H., Peng, J.*, et al.* (2015). Molecular characterization of LC3-associated phagocytosis reveals distinct roles for Rubicon, NOX2 and autophagy proteins. Nat Cell Biol *17*, 893-906.

Mastellos, D.C., Ricklin, D., and Lambris, J.D. (2019). Clinical promise of next-generation complement therapeutics. Nat Rev Drug Discov *18*, 707-729.

Matthijsen, R.A., de Winther, M.P., Kuipers, D., van der Made, I., Weber, C., Herias, M.V., Gijbels, M.J., and Buurman, W.A. (2009). Macrophage-specific expression of mannose-binding lectin controls atherosclerosis in low-density lipoprotein receptor-deficient mice. Circulation *119*, 2188-2195.

Mihlan, M., Stippa, S., Jozsi, M., and Zipfel, P.F. (2009). Monomeric CRP contributes to complement control in fluid phase and on cellular surfaces and increases phagocytosis by recruiting factor H. Cell Death Differ *16*, 1630-1640.

Miller, Y.I., Choi, S.H., Wiesner, P., Fang, L., Harkewicz, R., Hartvigsen, K., Boullier, A., Gonen, A., Diehl, C.J., Que, X.*, et al.* (2011). Oxidation-specific epitopes are danger-

associated molecular patterns recognized by pattern recognition receptors of innate immunity. Circ Res *108*, 235-248.

Moore, K.J., Sheedy, F.J., and Fisher, E.A. (2013). Macrophages in atherosclerosis: a dynamic balance. Nat Rev Immunol *13*, 709-721.

Moore, K.J., and Tabas, I. (2011). Macrophages in the pathogenesis of atherosclerosis. Cell *145*, 341-355.

Mortensen, S.A., Sander, B., Jensen, R.K., Pedersen, J.S., Golas, M.M., Thiel, S., and Andersen, G.R. (2018). Models of the complement C1 complex. Proc Natl Acad Sci U S A *115*, E3866.

Nahrendorf, M., and Swirski, F.K. (2015). Lifestyle effects on hematopoiesis and atherosclerosis. Circ Res *116*, 884-894.

Nordahl, E.A., Rydengard, V., Nyberg, P., Nitsche, D.P., Morgelin, M., Malmsten, M., Bjorck, L., and Schmidtchen, A. (2004). Activation of the complement system generates antibacterial peptides. Proc Natl Acad Sci U S A *101*, 16879-16884.

Noris, M., and Remuzzi, G. (2008). Translational mini-review series on complement factor H: therapies of renal diseases associated with complement factor H abnormalities: atypical haemolytic uraemic syndrome and membranoproliferative glomerulonephritis. Clin Exp Immunol *151*, 199-209.

Noris, M., and Remuzzi, G. (2013). Overview of complement activation and regulation. Semin Nephrol *33*, 479-492.

Nus, M., Sage, A.P., Lu, Y., Masters, L., Lam, B.Y.H., Newland, S., Weller, S., Tsiantoulas, D., Raffort, J., Marcus, D.*, et al.* (2017). Marginal zone B cells control the response of follicular helper T cells to a high-cholesterol diet. Nat Med *23*, 601-610.

Oksjoki, R., Kovanen, P.T., and Pentikainen, M.O. (2003). Role of complement activation in atherosclerosis. Curr Opin Lipidol *14*, 477-482.

Overton, C.D., Yancey, P.G., Major, A.S., Linton, M.F., and Fazio, S. (2007). Deletion of macrophage LDL receptor-related protein increases atherogenesis in the mouse. Circ Res *100*, 670-677.

Paffen, E., and DeMaat, M.P. (2006). C-reactive protein in atherosclerosis: A causal factor? Cardiovasc Res *71*, 30-39.

Pai, J.K., Manson, J.E., Rexrode, K.M., Albert, C.M., Hunter, D.J., and Rimm, E.B. (2007). Complement factor H (Y402H) polymorphism and risk of coronary heart disease in US men and women. Eur Heart J *28*, 1297-1303.

Papayannopoulos, V., and Zychlinsky, A. (2009). NETs: a new strategy for using old weapons. Trends Immunol *30*, 513-521.

Park, Y.M. (2014). CD36, a scavenger receptor implicated in atherosclerosis. Exp Mol Med *46*, e99.

Patel, S., Thelander, E.M., Hernandez, M., Montenegro, J., Hassing, H., Burton, C., Mundt, S., Hermanowski-Vosatka, A., Wright, S.D., Chao, Y.S.*, et al.* (2001). ApoE(-/-) mice develop atherosclerosis in the absence of complement component C5. Biochem Biophys Res Commun *286*, 164-170.

Persson, L., Boren, J., Robertson, A.K., Wallenius, V., Hansson, G.K., and Pekna, M. (2004). Lack of complement factor C3, but not factor B, increases hyperlipidemia and atherosclerosis in apolipoprotein E-/- low-density lipoprotein receptor-/- mice. Arterioscler Thromb Vasc Biol *24*, 1062-1067.

Pickering, M.C., and Cook, H.T. (2008). Translational mini-review series on complement factor H: renal diseases associated with complement factor H: novel insights from humans and animals. Clin Exp Immunol *151*, 210-230.

Pickering, M.C., Cook, H.T., Warren, J., Bygrave, A.E., Moss, J., Walport, M.J., and Botto, M. (2002). Uncontrolled C3 activation causes membranoproliferative glomerulonephritis in mice deficient in complement factor H. Nat Genet *31*, 424-428.

Pratt, J.R., Basheer, S.A., and Sacks, S.H. (2002). Local synthesis of complement component C3 regulates acute renal transplant rejection. Nat Med *8*, 582-587.

Pulanco, M.C., Cosman, J., Ho, M.M., Huynh, J., Fing, K., Turcu, J., and Fraser, D.A. (2017). Complement Protein C1q Enhances Macrophage Foam Cell Survival and Efferocytosis. J Immunol *198*, 472-480.

Reis, E.S., Mastellos, D.C., Hajishengallis, G., and Lambris, J.D. (2019). New insights into the immune functions of complement. Nat Rev Immunol *19*, 503-516.

Ricklin, D., Reis, E.S., and Lambris, J.D. (2016). Complement in disease: a defence system turning offensive. Nat Rev Nephrol *12*, 383-401.

Ridker, P.M., Everett, B.M., Thuren, T., MacFadyen, J.G., Chang, W.H., Ballantyne, C., Fonseca, F., Nicolau, J., Koenig, W., Anker, S.D.*, et al.* (2017). Antiinflammatory Therapy with Canakinumab for Atherosclerotic Disease. N Engl J Med *377*, 1119-1131.

Rodriguez de Cordoba, S., Esparza-Gordillo, J., Goicoechea de Jorge, E., Lopez-Trascasa, M., and Sanchez-Corral, P. (2004). The human complement factor H: functional roles, genetic variations and disease associations. Mol Immunol *41*, 355-367.

Rosen, B.S., Cook, K.S., Yaglom, J., Groves, D.L., Volanakis, J.E., Damm, D., White, T., and Spiegelman, B.M. (1989). Adipsin and complement factor D activity: an immune-related defect in obesity. Science *244*, 1483-1487.

Rothblat, G.H., and Phillips, M.C. (2010). High-density lipoprotein heterogeneity and function in reverse cholesterol transport. Curr Opin Lipidol *21*, 229-238.

Sage, A.P., Nus, M., Bagchi Chakraborty, J., Tsiantoulas, D., Newland, S.A., Finigan, A.J., Masters, L., Binder, C.J., and Mallat, Z. (2017). X-Box Binding Protein-1 Dependent Plasma Cell Responses Limit the Development of Atherosclerosis. Circ Res *121*, 270-281.

Samstad, E.O., Niyonzima, N., Nymo, S., Aune, M.H., Ryan, L., Bakke, S.S., Lappegard, K.T., Brekke, O.L., Lambris, J.D., Damas, J.K.*, et al.* (2014). Cholesterol crystals induce complement-dependent inflammasome activation and cytokine release. J Immunol *192*, 2837-2845.

Schmidt, C.Q., Bai, H., Lin, Z., Risitano, A.M., Barlow, P.N., Ricklin, D., and Lambris, J.D. (2013). Rational engineering of a minimized immune inhibitor with unique triple-targeting properties. J Immunol *190*, 5712-5721.

Schmidt, C.Q., Herbert, A.P., Hocking, H.G., Uhrin, D., and Barlow, P.N. (2008). Translational mini-review series on complement factor H: structural and functional correlations for factor H. Clin Exp Immunol *151*, 14-24.

Schmiedt, W., Kinscherf, R., Deigner, H.P., Kamencic, H., Nauen, O., Kilo, J., Oelert, H., Metz, J., and Bhakdi, S. (1998). Complement C6 deficiency protects against diet-induced atherosclerosis in rabbits. Arterioscler Thromb Vasc Biol *18*, 1790-1795.

Seifert, P.S., Hugo, F., Hansson, G.K., and Bhakdi, S. (1989). Prelesional complement activation in experimental atherosclerosis. Terminal C5b-9 complement deposition coincides with cholesterol accumulation in the aortic intima of hypercholesterolemic rabbits. Lab Invest *60*, 747-754.

Seifert, P.S., Hugo, F., Tranum-Jensen, J., Zahringer, U., Muhly, M., and Bhakdi, S. (1990). Isolation and characterization of a complement-activating lipid extracted from human atherosclerotic lesions. J Exp Med *172*, 547-557.

Selle, J., Asare, Y., Kohncke, J., Alampour-Rajabi, S., Shagdarsuren, G., Klos, A., Weber, C., Jankowski, J., and Shagdarsuren, E. (2015). Atheroprotective role of C5ar2 deficiency in apolipoprotein E-deficient mice. Thromb Haemost *114*, 848-858.

Serhan, C.N. (2014). Pro-resolving lipid mediators are leads for resolution physiology. Nature *510*, 92-101.

Shagdarsuren, E., Bidzhekov, K., Mause, S.F., Simsekyilmaz, S., Polakowski, T., Hawlisch, H., Gessner, J.E., Zernecke, A., and Weber, C. (2010). C5a receptor targeting in neointima formation after arterial injury in atherosclerosis-prone mice. Circulation *122*, 1026-1036.

Shishido, S.N., Varahan, S., Yuan, K., Li, X., and Fleming, S.D. (2012). Humoral innate immune response and disease. Clin Immunol *144*, 142-158.

Sorbara, M.T., Foerster, E.G., Tsalikis, J., Abdel-Nour, M., Mangiapane, J., Sirluck-Schroeder, I., Tattoli, I., van Dalen, R., Isenman, D.E., Rohde, J.R.*, et al.* (2018). Complement C3 Drives Autophagy-Dependent Restriction of Cyto-invasive Bacteria. Cell Host Microbe *23*, 644-652 e645.

Speidl, W.S., Kastl, S.P., Huber, K., and Wojta, J. (2011a). Complement in atherosclerosis: friend or foe? J Thromb Haemost *9*, 428-440.

Speidl, W.S., Kastl, S.P., Hutter, R., Katsaros, K.M., Kaun, C., Bauriedel, G., Maurer, G., Huber, K., Badimon, J.J., and Wojta, J. (2011b). The complement component C5a is present in human coronary lesions in vivo and induces the expression of MMP-1 and MMP-9 in human macrophages in vitro. FASEB J *25*, 35-44.

Stark, K., Neureuther, K., Sedlacek, K., Hengstenberg, W., Fischer, M., Baessler, A., Wiedmann, S., Jeron, A., Holmer, S., Erdmann, J.*, et al.* (2007). The common Y402H variant in complement factor H gene is not associated with susceptibility to myocardial infarction and its related risk factors. Clin Sci (Lond) *113*, 213-218.

Steiner, T., Francescut, L., Byrne, S., Hughes, T., Jayanthi, A., Guschina, I., Harwood, J., Cianflone, K., Stover, C., and Francis, S. (2014). Protective role for properdin in progression of experimental murine atherosclerosis. PLoS One *9*, e92404.

Strainic, M.G., Liu, J., Huang, D., An, F., Lalli, P.N., Muqim, N., Shapiro, V.S., Dubyak, G.R., Heeger, P.S., and Medof, M.E. (2008). Locally produced complement fragments C5a and C3a provide both costimulatory and survival signals to naive CD4+ T cells. Immunity *28*, 425-435.

Subramanian, M., Proto, J.D., Matsushima, G.K., and Tabas, I. (2016). Deficiency of AXL in Bone Marrow-Derived Cells Does Not Affect Advanced Atherosclerotic Lesion Progression. Sci Rep *6*, 39111.

Swirski, F.K., and Nahrendorf, M. (2013). Leukocyte behavior in atherosclerosis, myocardial infarction, and heart failure. Science *339*, 161-166.

Tabas, I. (2010). Macrophage death and defective inflammation resolution in atherosclerosis. Nat Rev Immunol *10*, 36-46.

Tabas, I. (2011). Pulling down the plug on atherosclerosis: finding the culprit in your heart. Nat Med *17*, 791-793.

Tabas, I., and Lichtman, A.H. (2017). Monocyte-Macrophages and T Cells in Atherosclerosis. Immunity *47*, 621-634.

Tall, A.R., Yvan-Charvet, L., Terasaka, N., Pagler, T., and Wang, N. (2008). HDL, ABC transporters, and cholesterol efflux: implications for the treatment of atherosclerosis. Cell Metab *7*, 365-375.

Tam, J.C., Bidgood, S.R., McEwan, W.A., and James, L.C. (2014). Intracellular sensing of complement C3 activates cell autonomous immunity. Science *345*, 1256070.

Tao, H., Yancey, P.G., Babaev, V.R., Blakemore, J.L., Zhang, Y., Ding, L., Fazio, S., and Linton, M.F. (2015). Macrophage SR-BI mediates efferocytosis via Src/PI3K/Rac1 signaling and reduces atherosclerotic lesion necrosis. J Lipid Res *56*, 1449-1460.

Tay, C., Liu, Y.H., Kanellakis, P., Kallies, A., Li, Y., Cao, A., Hosseini, H., Tipping, P., Toh, B.H., Bobik, A.*, et al.* (2018). Follicular B Cells Promote Atherosclerosis via T Cell-Mediated Differentiation Into Plasma Cells and Secreting Pathogenic Immunoglobulin G. Arterioscler Thromb Vasc Biol *38*, e71-e84.

Teupser, D., Pavlides, S., Tan, M., Gutierrez-Ramos, J.C., Kolbeck, R., and Breslow, J.L. (2004). Major reduction of atherosclerosis in fractalkine (CX3CL1)-deficient mice is at the brachiocephalic artery, not the aortic root. Proc Natl Acad Sci U S A *101*, 17795-17800.

Thorp, E., Cui, D., Schrijvers, D.M., Kuriakose, G., and Tabas, I. (2008). Mertk receptor mutation reduces efferocytosis efficiency and promotes apoptotic cell accumulation and plaque necrosis in atherosclerotic lesions of apoe-/- mice. Arterioscler Thromb Vasc Biol *28*, 1421-1428.

Torzewski, J., Torzewski, M., Bowyer, D.E., Frohlich, M., Koenig, W., Waltenberger, J., Fitzsimmons, C., and Hombach, V. (1998). C-reactive protein frequently colocalizes with the terminal complement complex in the intima of early atherosclerotic lesions of human coronary arteries. Arterioscler Thromb Vasc Biol *18*, 1386-1392.

Trouw, L.A., Nilsson, S.C., Goncalves, I., Landberg, G., and Blom, A.M. (2005). C4b-binding protein binds to necrotic cells and DNA, limiting DNA release and inhibiting complement activation. J Exp Med *201*, 1937-1948.

Tsai, R.K., and Discher, D.E. (2008). Inhibition of "self" engulfment through deactivation of myosin-II at the phagocytic synapse between human cells. J Cell Biol *180*, 989-1003.

Tse, K., Tse, H., Sidney, J., Sette, A., and Ley, K. (2013). T cells in atherosclerosis. Int Immunol *25*, 615-622.

Tsiantoulas, D., Diehl, C.J., Witztum, J.L., and Binder, C.J. (2014). B cells and humoral immunity in atherosclerosis. Circ Res *114*, 1743-1756.

Tsiantoulas, D., Sage, A.P., Mallat, Z., and Binder, C.J. (2015). Targeting B cells in atherosclerosis: closing the gap from bench to bedside. Arterioscler Thromb Vasc Biol *35*, 296-302.

Ugurlar, D., Howes, S.C., de Kreuk, B.J., Koning, R.I., de Jong, R.N., Beurskens, F.J., Schuurman, J., Koster, A.J., Sharp, T.H., Parren, P.*, et al.* (2018). Structures of C1-IgG1 provide insights into how danger pattern recognition activates complement. Science *359*, 794-797.

Van Vre, E.A., Ait-Oufella, H., Tedgui, A., and Mallat, Z. (2012). Apoptotic cell death and efferocytosis in atherosclerosis. Arterioscler Thromb Vasc Biol *32*, 887-893.

Virmani, R., Burke, A.P., Kolodgie, F.D., and Farb, A. (2002). Vulnerable plaque: the pathology of unstable coronary lesions. J Interv Cardiol *15*, 439-446.

Volcik, K.A., Ballantyne, C.M., Braun, M.C., Coresh, J., Mosley, T.H., and Boerwinkle, E. (2008). Association of the complement factor H Y402H polymorphism with cardiovascular disease is dependent upon hypertension status: The ARIC study. Am J Hypertens *21*, 533-538.

Walport, M.J. (2001a). Complement. First of two parts. N Engl J Med *344*, 1058-1066.

Walport, M.J. (2001b). Complement. Second of two parts. N Engl J Med *344*, 1140-1144.

Wang, Y., Subramanian, M., Yurdagul, A., Jr., Barbosa-Lorenzi, V.C., Cai, B., de Juan-Sanz, J., Ryan, T.A., Nomura, M., Maxfield, F.R., and Tabas, I. (2017). Mitochondrial Fission Promotes the Continued Clearance of Apoptotic Cells by Macrophages. Cell *171*, 331-345 e322.

Warnatsch, A., Ioannou, M., Wang, Q., and Papayannopoulos, V. (2015). Inflammation. Neutrophil extracellular traps license macrophages for cytokine production in atherosclerosis. Science *349*, 316-320.

Weber, C., and Noels, H. (2011). Atherosclerosis: current pathogenesis and therapeutic options. Nat Med *17*, 1410-1422.

Weismann, D., and Binder, C.J. (2012). The innate immune response to products of phospholipid peroxidation. Biochim Biophys Acta *1818*, 2465-2475.

Weismann, D., Hartvigsen, K., Lauer, N., Bennett, K.L., Scholl, H.P., Charbel Issa, P., Cano, M., Brandstatter, H., Tsimikas, S., Skerka, C.*, et al.* (2011). Complement factor H binds malondialdehyde epitopes and protects from oxidative stress. Nature *478*, 76-81.

West, E.E., and Kemper, C. (2019). Complement and T Cell Metabolism: Food for Thought. Immunometabolism *1*, e190006.

Wezel, A., de Vries, M.R., Lagraauw, H.M., Foks, A.C., Kuiper, J., Quax, P.H., and Bot, I. (2014). Complement factor C5a induces atherosclerotic plaque disruptions. J Cell Mol Med *18*, 2020-2030.

Wilensky, R.L., and Macphee, C.H. (2009). Lipoprotein-associated phospholipase A(2) and atherosclerosis. Curr Opin Lipidol *20*, 415-420.

Winkels, H., Ehinger, E., Vassallo, M., Buscher, K., Dinh, H.Q., Kobiyama, K., Hamers, A.A.J., Cochain, C., Vafadarnejad, E., Saliba, A.E.*, et al.* (2018). Atlas of the Immune Cell Repertoire in Mouse Atherosclerosis Defined by Single-Cell RNA-Sequencing and Mass Cytometry. Circ Res *122*, 1675-1688.

Wirthmueller, U., Dewald, B., Thelen, M., Schafer, M.K., Stover, C., Whaley, K., North, J., Eggleton, P., Reid, K.B., and Schwaeble, W.J. (1997). Properdin, a positive regulator of complement activation, is released from secondary granules of stimulated peripheral blood neutrophils. J Immunol *158*, 4444-4451.

Wu, G., Hu, W., Shahsafaei, A., Song, W., Dobarro, M., Sukhova, G.K., Bronson, R.R., Shi, G.P., Rother, R.P., Halperin, J.A.*, et al.* (2009). Complement regulator CD59 protects against

atherosclerosis by restricting the formation of complement membrane attack complex. Circ Res *104*, 550-558.

Yan, Z.Q., and Hansson, G.K. (2007). Innate immunity, macrophage activation, and atherosclerosis. Immunol Rev *219*, 187-203.

Yancey, P.G., Blakemore, J., Ding, L., Fan, D., Overton, C.D., Zhang, Y., Linton, M.F., and Fazio, S. (2010). Macrophage LRP-1 controls plaque cellularity by regulating efferocytosis and Akt activation. Arterioscler Thromb Vasc Biol *30*, 787-795.

Yancey, P.G., Ding, Y., Fan, D., Blakemore, J.L., Zhang, Y., Ding, L., Zhang, J., Linton, M.F., and Fazio, S. (2011). Low-density lipoprotein receptor-related protein 1 prevents early atherosclerosis by limiting lesional apoptosis and inflammatory Ly-6Chigh monocytosis: evidence that the effects are not apolipoprotein E dependent. Circulation *124*, 454-464.

Yang, X., Peterson, L., Thieringer, R., Deignan, J.L., Wang, X., Zhu, J., Wang, S., Zhong, H., Stepaniants, S., Beaulaurier, J.*, et al.* (2010). Identification and validation of genes affecting aortic lesions in mice. J Clin Invest *120*, 2414-2422.

Yasojima, K., Schwab, C., McGeer, E.G., and McGeer, P.L. (2001). Complement components, but not complement inhibitors, are upregulated in atherosclerotic plaques. Arterioscler Thromb Vasc Biol *21*, 1214-1219.

Yin, C., Ackermann, S., Ma, Z., Mohanta, S.K., Zhang, C., Li, Y., Nietzsche, S., Westermann, M., Peng, L., Hu, D.*, et al.* (2019). ApoE attenuates unresolvable inflammation by complex formation with activated C1q. Nat Med *25*, 496-506.

Yun, S., Leung, V.W., Botto, M., Boyle, J.J., and Haskard, D.O. (2008). Brief report: accelerated atherosclerosis in low-density lipoprotein receptor-deficient mice lacking the membrane-bound complement regulator CD59. Arterioscler Thromb Vasc Biol *28*, 1714-1716.

Yurdagul, A., Jr., Doran, A.C., Cai, B., Fredman, G., and Tabas, I.A. (2017). Mechanisms and Consequences of Defective Efferocytosis in Atherosclerosis. Front Cardiovasc Med *4*, 86.

Yvan-Charvet, L., Pagler, T., Gautier, E.L., Avagyan, S., Siry, R.L., Han, S., Welch, C.L., Wang, N., Randolph, G.J., Snoeck, H.W*., et al.* (2010a). ATP-binding cassette transporters and HDL suppress hematopoietic stem cell proliferation. Science *328*, 1689-1693.

Yvan-Charvet, L., Ranalletta, M., Wang, N., Han, S., Terasaka, N., Li, R., Welch, C., and Tall, A.R. (2007). Combined deficiency of ABCA1 and ABCG1 promotes foam cell accumulation and accelerates atherosclerosis in mice. J Clin Invest *117*, 3900-3908.

Yvan-Charvet, L., Wang, N., and Tall, A.R. (2010b). Role of HDL, ABCA1, and ABCG1 transporters in cholesterol efflux and immune responses. Arterioscler Thromb Vasc Biol *30*, 139-143.

Yvan-Charvet, L., Welch, C., Pagler, T.A., Ranalletta, M., Lamkanfi, M., Han, S., Ishibashi, M., Li, R., Wang, N., and Tall, A.R. (2008). Increased inflammatory gene expression in ABC transporter-deficient macrophages: free cholesterol accumulation, increased signaling via toll-like receptors, and neutrophil infiltration of atherosclerotic lesions. Circulation *118*, 1837-1847.

Zelcer, N., and Tontonoz, P. (2006). Liver X receptors as integrators of metabolic and inflammatory signaling. J Clin Invest *116*, 607-614.

Zelek, W.M., Xie, L., Morgan, B.P., and Harris, C.L. (2019). Compendium of current complement therapeutics. Mol Immunol *114*, 341-352.

Zernecke, A., Bot, I., Djalali-Talab, Y., Shagdarsuren, E., Bidzhekov, K., Meiler, S., Krohn, R., Schober, A., Sperandio, M., Soehnlein, O*., et al.* (2008). Protective role of CXC receptor 4/CXC ligand 12 unveils the importance of neutrophils in atherosclerosis. Circ Res *102*, 209-217.

Zhu, X., Owen, J.S., Wilson, M.D., Li, H., Griffiths, G.L., Thomas, M.J., Hiltbold, E.M., Fessler, M.B., and Parks, J.S. (2010). Macrophage ABCA1 reduces MyD88-dependent Toll-like receptor trafficking to lipid rafts by reduction of lipid raft cholesterol. J Lipid Res *51*, 3196-3206.

Zipfel, P.F. (2001). Complement factor H: physiology and pathophysiology. Semin Thromb Hemost *27*, 191-199.

Zipfel, P.F., Mihlan, M., and Skerka, C. (2007). The alternative pathway of complement: a pattern recognition system. Adv Exp Med Biol *598*, 80-92.

Zipfel, P.F., and Skerka, C. (1999). FHL-1/reconectin: a human complement and immune regulator with cell-adhesive function. Immunol Today *20*, 135-140.

Zipfel, P.F., and Skerka, C. (2009). Complement regulators and inhibitory proteins. Nat Rev Immunol *9*, 729-740.

Curriculum Vitae

Full name: Máté Kiss

Nationality: Hungarian

Date of birth: 24.06.1990

Place of birth: Pécs, Hungary

Current position

Graduate student at the Medical University of Vienna under the supervision of Prof. Christoph J. Binder

Laboratory of Immunity and Atherosclerosis, CeMM Research Center for Molecular Medicine of the Austrian Academy of Sciences

Working address

Department of Laboratory Medicine, Medical University of Vienna

& CeMM Research Center for Molecular Medicine of the Austrian Academy of Sciences

Lazarettgasse 14, Bauteil 25.2/6, 1090 Vienna, Austria

Tel: + 43 1 40400 73762, Mobile: + 43 650 454 1918

Fax: + 43 1 40400 73588

e-mail: mkiss@cemm.oeaw.ac.at

Education

09/2013 to date	Medical University of Vienna & CeMM Research Center for Molecular Medicine of the Austrian Academy of Sciences - Vienna, Austria Predoctoral training in progress Title: *"Novel functions of complement factor H in regulating extracellular vis-à-vis intracellular complement activation during chronic inflammation"*
06/2016 – 12/2016	Center for Systems Biology, Massachusetts General Hospital & Harvard Medical School, Boston, Massachusetts, United States Predoctoral internship in Dr. Filip K. Swirski's laboratory Title: *"The effect of sleep on atherosclerosis"*
09/2011 – 06/2013	University of Pécs, Medical School (UPMS) - Pécs, Hungary

	Master‘s degree in Medical Biotechnology (in English); graduated as top of the class with first class honours (5.0)
	Thesis: *“Development of a short, functional, tissue-specific FoxN1 promoter for studying thymic epithelial cell aging”*
09/2008 – 07/2011	University of Pécs, Science School (UPSS) - Pécs, Hungary
	Bachelor‘s degree in Biology
	Thesis: *“Comparative assay of the mycotoxin Zearalenone and its derivatives, alpha-Zearalenol and beta-Zearalenol”*
09/2000 – 06/2008	Saint Maurus Catholic Secondary School - Pécs, Hungary
	General certificate of secondary education

Scholarships, honours and awards

02/2019	Travel grant to participate and present at the 87th Congress of the European Atherosclerosis Society EAS 2019, Maastricht, The Netherlands
03/2018	Travel grant to participate and present at the XVIIIth International Symposium on Atherosclerosis ISA 2018, Toronto, Canad
02/2018	Travel grant to participate and present at the 86th Congress of the European Atherosclerosis Society EAS 2018, Lisbon, Portugal
05/2017	AAS Best Presentation Award 2017 at the 24th Annual Meeting of the Austrian Atherosclerosis Society, St. Gilgen, Austria
04/2017	Poster Award at the 85th Congress of the European Atherosclerosis Society EAS 2017, Prague, Czech Republic
03/2017	Second Place Poster Award at the Immuno-Metabolic Mechanisms of Atherosclerosis Conference at the Fiesta Americana Condesa, Cancun, Mexico
02/2017	Travel grant to participate and present at the 85th Congress of the European Atherosclerosis Society EAS 2017, Prague, Czech Republic
10/2013	Cell Communication in Health and Disease (CCHD) PhD Scholarship – Medical University of Vienna
10/2013	*Outstanding Achievement Award* – University of Pécs, Medical School
10/2012	Fellowship granted by the Republic of Hungary by the Ministry of Human Resources *‚for outstanding academic and eminent professional achievement‘* in term 2012/13
10/2012	*Outstanding Achievement Award* – University of Pécs, Medical School

06/2011	Best oral presentation of public thesis defense – University of Pécs, Science School

Teaching experience

06/2018	Co-supervision of visiting student Ananya Dewan at the Medical University of Vienna

Publications

1. **M.G. Kiss**, M. Ozsvár-Kozma, F. Porsch, L. Göderle, N. Papac-Miličević, B. Bartolini-Gritti, D. Tsiantoulas, M.C. Pickering, C.J. Binder (2019). Complement factor H modulates splenic B cell development and limits autoantibody production. *Front Immunol* 2019 Jul 11;10:1607. doi: 10.3389/fimmu.2019.01607.
2. H. Douna, J. Amersfoort, F.H. Schaftenaar, M.J. Kröner, **M.B. Kiss**, B. Slütter, M.A.C. Depuydt, M.N.A.B. Kleijn, A. Wezel, H. Smeets, H. Yagita, C.J. Binder, I. Bot, G.H.M van Puijvelde, J. Kuiper, A.C. Foks (2019). BTLA stimulation protects against atherosclerosis by regulating follicular B cells. *Cardiovasc Res*. 2019 May 31. pii: cvz129. doi: 10.1093/cvr/cvz129.
3. C.S. McAlpine, **M.G. Kiss**, S. Rattik, S. He, A. Vassalli, C. Valet, A. Anzai, C.T. Chan, J.E. Mindur, F. Kahles, W.C. Poller, V. Frodermann, A.M. Fenn, A.F. Gregory, L. Halle, Y. Iwamoto, F.F. Hoyer, C.J. Binder, P. Libby, M. Tafti, T.E. Scammell, M. Nahrendorf, F.K. Swirski (2019). Sleep modulates haematopoiesis and protects against atherosclerosis. *Nature.* 2019 Feb;566(7744):383-387. doi: 10.1038/s41586-019-0948-2.
4. D. Tsiantoulas, **M. Kiss**, B. Bartolini-Gritti, A. Bergthaler, Z. Mallat, H. Jumaa, C.J. Binder (2017). Secreted IgM deficiency leads to increased BCR signaling that results in abnormal splenic B cell development. *Sci Rep*. 2017 Jun 14;7(1):3540. doi: 10.1038/s41598-017-03688-8.

Language certificates

11/2010	complex B2 Italian exam (TELC)
07/2009	complex B2 German exam (ÖSD)
06/2008	complex B2 English exam (ECL)
+	fluent in Hungarian (mother tongue) and basic skills in French.

Work experience and social skills

12/2013 – 12/2014	Student representative at CeMM Research Center for Molecular Medicine of the Austrian Academy of Sciences

01/2012 – 06/2013	Student representative of the Medical Biotechnology Master Program, University of Pécs, Medical School
08/2012	Student demonstrator at the Department of Immunology and Biotechnology, University of Pécs, Medical School
from 2012	Volunteer of *Hungarian League Against Cancer*

Other skills and competences

Computer literacy:	Proficient in Microsoft Office, Adobe, GraphPad Prism, BLASTs
Driving license:	Category *B* (2010)

Activities and interest

Huge fan of sports (U19 Football Champion of Baranya County in 2007/08), film arts, languages and coin collection